CNWRA 2005-04

SUMMARY AND ANALYSIS OF SUBSURFACE FRACTURE DATA FROM THE TOPOPAH SPRING TUFF UPPER LITHOPHYSAL, MIDDLE NONLITHOPHYSAL, LOWER LITHOPHYSAL, AND LOWER NONLITHOPHYSAL ZONES AT YUCCA MOUNTAIN, NEVADA

Prepared for

U.S. Nuclear Regulatory Commission
Contract NRC–02–02–012

Prepared by

Kevin J. Smart
Danielle Y. Wyrick
Paul S. Landis
Deborah J. Waiting

Center for Nuclear Waste Regulatory Analyses
Geosciences and Engineering Division
Southwest Research Institute®
San Antonio, Texas

February 2006

ABSTRACT

Fractures are among the most abundant deformation structures found in rocks. Although individual fractures are rarely of great importance, the number of fractures makes them a key component of many geologic and engineering-related processes. Fractures are direct contributors to geotechnical processes for the stability of underground openings and indirectly influence processes such as thermal stress accommodation, near-surface water infiltration and flow, and unsaturated zone radionuclide transport. The purpose of this report is to provide an up-to-date synthesis of subsurface fracture data collected at Yucca Mountain, Nevada, for use by staff at the U.S. Nuclear Regulatory Commission (NRC) and Center for Nuclear Waste Regulatory Analyses (CNWRA) during the evaluation of a potential license application for a high-level waste repository. Analyses in this report are restricted to data collected by the U.S. Department of Energy (DOE) and its contractors from the Exploratory Studies Facility (ESF)[1] and the Enhanced Characterization of the Repository Block (ECRB)[2] Cross-Drift at Yucca Mountain. Furthermore, analyses are focused on data collected from the Topopah Spring Tuff Upper Lithophysal, Middle Nonlithophysal, Lower Lithophysal, and Lower Nonlithophysal zones. The primary goals are to (i) summarize fracture data collected by both detailed line survey and full-periphery geologic mapping techniques; (ii) analyze these data and determine primary fracture sets and average fracture properties, such as fracture spacing (i.e., density) and fracture size (i.e., trace length); and (iii) replicate DOE synthetic fracture generation analyses performed with the commercial code FracMan®.

Definitive cooling joints and vapor phase partings are present in all zones within the Topopah Spring Tuff, but are not abundant and represent only 5–11 percent of all recorded fractures. Fractures with measurable displacement are present, but account for only 3–4 percent of the total population and are predominantly subvertical with either a northwest or northeast strike. Regardless of lithostratigraphic interval, distinctive orientation-based fracture sets are present. This observation holds for analyses of long (trace length >1 m [3.3 ft]) and short (trace length <1 m [3.3 ft]) fractures. The overall distribution of fracture size, based on observed curvilinear trace length measured along tunnel walls, is strongly skewed, with short fractures being significantly more abundant than long fractures. The most abundant fracture set throughout the Middle Nonlithophysal, Lower Lithophysal, and Lower Nonlithophysal zones is a northwest-striking subvertical set. This apparent dominance of northwest-striking subvertical fractures reflects in part the orientation bias introduced by the ESF and ECRB Cross-Drift tunnels. A subhorizontal fracture set and a northeast-striking subvertical set are also present. A north-south-striking subvertical set is dominant in the Upper Lithophysal zone, although the northwest-striking subvertical set is also present along with a weakly developed subhorizontal set. Overall linear and areal fracture intensities are highest in the nonlithophysal zones. The subhorizontal fracture set has a higher intensity than indicated in previous DOE reports because the bias introduced by the tunnel orientation has been partially corrected in this report. In the Upper and Lower Lithophysal zones, the subhorizontal fracture intensity is nearly the same as that for the northwest-striking subvertical fractures. Orientation and intensity data derived from full-periphery geologic mapping in the cross-drift confirm observations made from detailed line

[1]It should be noted that the Exploratory Studies Facility is often known by researchers as ESF; consequently, the term ESF will be used throughout this report.

[2]It should be noted that Enhanced Characterization of the Repository Block is often known by researchers as ECRB; consequently, the term ECRB will be used throughout this report.

survey data. FracMan synthetic fracture populations generated for the Middle Nonlithophysal zone contain the prominent northwest-striking subvertical set along with a northeast-striking subvertical set. A northwest striking, moderately northeast dipping set is present in the synthetic population, but an equivalent set is not present in the natural fracture population. The subhorizontal fracture set is not well developed in the synthetic fracture population. Synthetic fracture populations generated for the Lower Lithophysal zone also contain the prominent northwest-striking subvertical set. The north-south-striking subvertical and the subhorizontal fracture sets are well represented in the synthetic fracture populations.

References:

Golder Associates, Inc. "FracMan Interactive Discrete Feature Data Analysis, Geometric Modeling, and Exploration Simulation User Documentation, Version 2.6." Seattle, Washington: Golder Associates, Inc. 1998.

_____. "FracWorksXP Module User Documentation." Seattle, Washington: Golder Associates, Inc. 2002.

CONTENTS

FIGURES

FIGURES (continued)

TABLES

ACKNOWLEDGMENTS

This report was prepared to document work performed by the Center for Nuclear Waste Regulatory Analyses (CNWRA) and its contractors for the U.S. Nuclear Regulatory Commission (NRC) under Contract No. NRC–02–02–012. The activities reported here were performed on behalf of the NRC Office of Nuclear Material Safety and Safeguards, Division of High-Level Waste Repository Safety. The report is an independent product of CNWRA and does not necessarily reflect the views or regulatory position of NRC.

The authors thank Alan P. Morris, David A. Ferrill, and Phillip S. Justus for their reviews of this report. The authors are grateful to Sharon Odam for assisting with the word processing and preparation of the final report and to Erika Hanson for editorial review.

QUALITY OF DATA, ANALYSES, AND CODE DEVELOPMENT

DATA: All CNWRA-original data contained in this report were collected and analyzed to meet quality assurance requirements as described in the CNWRA Quality Assurance Manual and documented in Scientific Notebooks 606E and 685E. Sources for all other data should be consulted to determine the level of quality for these data.

ANALYSES AND CODES: No CNWRA-developed codes were used to analyze data for this report. The following commercial-off-the-shelf software packages were used for analysis: Microsoft® Excel 2002, RockWare StereoStat® Version 1.3, TurboCAD Deluxe Version 10.2, ESRI® ArcGIS Version 9, and FracMan® Version 2.6. Figures were produced using Adobe® Illustrator® Version 10 and Adobe® Photoshop® Version 7. All commercial-off-the-shelf software packages used in this report are under Technical Operating Procedure (TOP)–018 control.

References:

Adobe Systems, Inc. “Adobe Illustrator Version 10.” San Jose, California. 2002.

Adobe Systems, Inc. “Adobe Photoshop Version 7.” San Jose, California. 2002.

ESRI, Inc. “ArcGIS Version 9.” Redlands, California. 2004.

Golder Associates, Inc. “FracWorksXP Module User Documentation.” Seattle, Washington: Golder Associates, Inc. 2002.

_____. “FracMan Interactive Discrete Feature Data Analysis, Geometric Modeling, and Exploration Simulation User Documentation, Version 2.6.” Seattle, Washington: Golder Associates, Inc. 1998.

IMSI, Inc. “TurboCAD Deluxe Version 10.2.” Novato, California. 2004.

Microsoft Corporation, Inc. “Microsoft Excel 2002.” Redmond, Washington: Microsoft Corporation. 2002.

Rockware, Inc. “StereoStat Version 1.3.” Golden, Colorado. 2004.

1 INTRODUCTION

Fractures are among the most abundant deformation structures found in rocks (Nelson, 2001). Although individual fractures are rarely of great importance—unlike a large fault that may be capable of producing damaging earthquakes—the number of fractures makes them an important component of many different geologic or engineering-related processes. Fractures are direct contributors to most geotechnical processes, for the stability of underground openings, including rock fall and drift degradation. In particular, fracture orientation and spacing control the size and shape of rock blocks that can form, which in turn influences the assessments of the distribution and size of rubble piles that accumulate on waste packages or drip shields (Ahola, et al., 1996; Gute, et al., 2003). Fracture characteristics indirectly influence related processes such as thermal stress accommodation (Bechtel SAIC Company, LLC, 2004a,b; Ofoegbu, 2000), in-drift heat transfer (Manepally, et al., 2004), and waste retrievability (Chen, 2000). Near-surface infiltration (Bechtel SAIC Company, LLC, 2004c), seepage (Bechtel SAIC Company, LLC, 2003; Liu, et al., 1998), flow (Hinds, et al., 2003; Fedors, et al., 2002), and radionuclide transport (Pearcy, et al., 1995; Pearcy, 1994) in the unsaturated zone are additional processes that fractures influence at drift- and mountain-scales.

The purpose of this report is to provide an up-to-date synthesis of subsurface fracture data collected at Yucca Mountain, Nevada for use by staff at the U.S. Nuclear Regulatory Commission (NRC) and Center for Nuclear Waste Regulatory Analyses (CNWRA) during the evaluation of a potential license application for a high-level waste repository. This report is designed to evaluate existing U.S. Department of Energy (DOE) documents (e.g., Nieder-Westermann, 2000; Sweetkind and Williams-Stroud, 1996) that have summarized fracture data and interpretations for surface exposures, boreholes, and portions of the subsurface. This report is restricted to data collected by DOE and its contractors from the Exploratory Studies Facility (ESF)[1] and the Enhanced Characterization of the Repository Block (ECRB)[2] Cross-Drift at Yucca Mountain, Nevada. In addition, analyses are further focused on data collected from only the Topopah Spring Tuff Upper Lithophysal, Middle Nonlithophysal, Lower Lithophysal, and Lower Nonlithophysal zones, which currently define the planned repository host horizon interval (Bechtel SAIC Company, LLC, 2002; Nieder-Westermann, 2000; CRWMS M&O, 1997, 2000).

The specific goals of this report are to

- Summarize fracture data collected by both detailed line survey and full-periphery geologic mapping techniques
- Analyze these data and determine primary fracture sets and average fracture properties, such as fracture spacing (i.e., density) and fracture size (i.e., trace length)
- Replicate the DOE synthetic fracture generation analyses performed with FracMan®

[1]It should be noted that the Exploratory Studies Facility is often known by researchers as ESF; consequently, the term ESF will be used throughout this report.

[2]It should be noted that Enhanced Characterization of the Repository Block is often known by researchers as ECRB; consequently, the term ECRB will be used throughout this report.

2 SUBSURFACE FRACTURE DATA COLLECTION BY DOE

2.1 DOE Data Collection Methods

Fracture data collected in support of the DOE characterization analyses of Yucca Mountain are numerous and varied. Data have been collected on surface exposures (e.g., Sweetkind and Williams-Stroud, 1996; Sweetkind, et al., 1995a,b; Throckmorton and Verbeek, 1995; Barton, et al., 1993), in exploratory boreholes, and in tunnels and alcoves of the ESF and the ECRB Cross-Drift. This report, however, is restricted to analysis of fracture data collected in the ESF and ECRB Cross-Drift from the Topopah Spring Tuff Upper Lithophysal, Middle Nonlithophysal, Lower Lithophysal, and Lower Nonlithophysal zones. These four zones are part of the moderately to densely welded, crystal-poor member of the Topopah Spring Tuff (Potter, et al., 2004; Buesch and Spengler, 1998; Day, et al., 1998; Buesch, et al., 1996a,b; Geslin and Moyer, 1995; Geslin, et al., 1995; Moyer, et al., 1995). These references should be consulted for detailed stratigraphic information, including thickness distributions, and spatial variations in composition, texture, and lithophysal characteristics. The primary data sources for fractures are Mongano, et al. (1999), Albin, et al. (1997), Eatman, et al. (1997), Kicker, et al. (1997), Barr, et al. (1996), Beason, et al. (1996), Brechtel, et al. (1995), and numerous digital data sets (Table 2-1). This report also makes use of several DOE documents that partially synthesize the primary data (Board, 2003; CRWMS M&O, 2000; Nieder-Westermann, 2000; Sweetkind and Williams-Stroud, 1996).

Two different, but complementary techniques were employed by DOE and its contractors to collect fracture data from the ESF and the ECRB Cross-Drift. The first approach is referred to as a detailed line survey, which is a traditional one-dimensional scanline method for collecting discontinuity data (e.g., Priest, 1993; Priest and Hudson, 1981; International Society for Rock Mechanics, 1978). The primary advantage of this technique is rapid data acquisition because data are recorded only for fractures that intersect the scanline. The scanline in the ESF was located 0.9 m [3.0 ft] below the right wall spring-line, whereas the scanline in the ECRB Cross-Drift was located 0.9 m [3.0 ft] below the left wall spring-line. Data collection focused on a position along the tunnel (intersection of discontinuity with scanline) and included characteristics such as orientation, curvilinear trace length above and below the scanline, discontinuity type (i.e., fracture, vapor phase parting, cooling joint, shear, fault), minimum and maximum aperture along the discontinuity, magnitude and sense of displacement if visible, planarity, and termination type (U.S. Bureau of Reclamation and U.S. Geological Survey, 1997). The disadvantage of the detailed line survey approach is that it does not provide information on the two- or three-dimensional fracture characteristics. Scanlines are also more susceptible to orientation bias problems than are other techniques (Priest, 1993), although some corrections can be made during postprocessing.

The second approach employed by DOE and its contractors was the construction of full-periphery geologic maps. This technique was conducted behind the tunnel boring machine and resulted in 1:125-scale maps that depict fractures (and engineering features such as supports and rock bolts) on the tunnel walls and ceilings. Although this technique is referred to as full-periphery, the invert on the tunnel floor obscures approximately 17 percent of the tunnel circumference. Unlike the detailed line survey, only fracture location and orientation were directly recorded during the full-periphery geologic mapping. Although the full-periphery mapping is still subject to certain sampling biases (i.e., the tunnels can be envisioned as large

boreholes), it does provide a somewhat less biased methodology because it captures fractures beyond those that intersect the scanline.

Because lithologic character (i.e., the degree of welding and the presence or absence of lithophysal cavities) was expected to be a significant control on fracturing, DOE analyses have generally considered fracture characteristics in the context of the host stratigraphic units (Mongano, et al., 1999; Albin, et al., 1997; Eatman, et al.,1997; Barr, et al., 1996; Beason, et al.,1996). The primary northeast-southwest orientation for the ECRB Cross-Drift (Figure 2-1) provides data for all four of the Topopah Spring Tuff zones (Mongano, et al., 1999). The ESF is dominated by measurements from the Middle Nonlithophysal zone with this stratigraphic interval exposed for 47 percent of the 7.8-km [4.8-mi]-long tunnel and did not provide measurements from the Lower Nonlithophysal zone (Albin, et al., 1997; Eatman, et al.,1997; Barr, et al., 1996; Beason, et al.,1996). The 2.7-km [1.7-mi]-long north-south-trending main drift (Figure 2-1) exposes only the Middle Nonlithophysal zone and a short section of the Lower Lithophysal zone (Albin, et al., 1997).

During the course of data collection, DOE and its contractors employed different minimum size thresholds (i.e., trace length cut-offs) for fracture measurement and inclusion in data sets (Albin, et al., 1997; Barr, et al., 1996; Beason, et al., 1996). Initially, all fractures with trace lengths greater than or equal to 30 cm [12 in] were measured during the detailed line survey. Beginning with station 37+80 in the ESF, the minimum trace length was increased to 1 m [3.3 ft]. However, DOE switched back to a 30-cm [12-in] cut-off for selected 50-m [164-ft]-long drift segments between stations 45+00 to 45+50 and 50+00 to 50+50 (Albin, et al., 1997). The full-periphery geologic mapping in both the ESF and the ECRB Cross-Drift employed a minimum tracelength cut-off of 1 m [3.3 ft]. Fracture measurements in the ECRB Cross-Drift were conducted with a 1-m [3.3-ft] trace length cut-off, with the exception of a separate small-scale fracture study. For the small-scale fracture study, DOE re-occupied selected locations in the ECRB Cross-Drift and used short horizontal 6-m [19.7-ft]-long and vertical 2-m [6.6-ft]-high (i.e., along the curved tunnel wall) scanlines to document fractures up to 1 m [3.3 ft] in length. Two horizontal and six vertical scanlines were conducted in the Middle Nonlithophysal zone. Three horizontal and nine vertical scanlines were used in the Lower Lithophysal zone. One horizontal and three vertical scanlines were used in the Lower Nonlithophysal zone. The Upper Lithophysal zone was not sampled during the small-scale fracture study. Some fractures that were measured during the initial detailed line survey were also recorded in the small-scale data files, resulting in data duplication.

Table 2-1. Summary of Digital Data Sets for Fracture Data Collected by the U.S. Department of Energy (DOE) in the Exploratory Studies Facility (ESF) and the Enhanced Characterization of the Repository Block (ECRB) Cross-Drift

Data Tracking Number	Description
GS960708314224.010	Provisional results: Geotechnical Data for Station 40+00 to Station 45+00, Main Drift of the ESF.
GS960908314224.014	Fracture Type data from the ESF North Ramp, and Yucca Mountain Project Detailed Line Survey-Data Collected from Station 50+00 to 55+00.
GS970208314224.003	Geotechnical Data for Station 60+00 to Station 65+00, South Ramp of the ESF.
GS970808314224.010	Provisional Results: Geotechnical Data for Station 70+00 to Station 75+00, South Ramp of the ESF.
GS970808314224.012	Provisional Results: Geotechnical Data for Station 75+00 to Station 78+77, South Ramp of the ESF.
GS971108314224.020	Revision 1 of Detailed Line Survey Data, Station 0+60 to Station 4+00, North Ramp Starter Tunnel, Exploratory Studies Facility.
GS971108314224.021	Revision 1 of Detailed Line Survey Data, Station 4+00 to Station 8+00, North Ramp, Exploratory Studies Facility.
GS971108314224.022	Revision 1 of Detailed Line Survey Data, Station 8+00 to Station 10+00, North Ramp, Exploratory Studies Facility.
GS971108314224.023	Revision 1 of Detailed Line Survey Data, Station 10+00 to Station 18+00, North Ramp, Exploratory Studies Facility.
GS971108314224.024	Revision 1 of Detailed Line Survey Data, Station 18+00 to Station 26+00, North Ramp, Exploratory Studies Facility.
GS971108314224.025	Revision 1 of Detailed Line Survey Data, Station 26+00 to Station 30+00, North Ramp, Exploratory Studies Facility.
GS971108314224.026	Revision 1 of Detailed Line Survey Data, Station 45+00 to Station 50+00, Main Drift, Exploratory Studies Facility.
GS971108314224.028	Fracture Type data (Revision 1 of Detailed Line Survey data) South Ramp, ESF, collected from stations 55+00.18 to 59+99.95.
GS000608314224.004	Fracture Type data from the Main Drift of the ESF, and Yucca Mountain Project Detailed Line Survey-Data collected from Station 35+00 to 40+00.
GS990408314224.001	Detailed Line Survey Data for Stations 00+00.89 to 14+95.18, ECRB Cross-Drift.
GS990408314224.002	Detailed Line Survey Data for Stations 15+00.85 to 26+63.8, ECRB Cross-Drift.
GS990408314224.003	Full-Periphery Geologic Maps for Station 0+10 to 10+00, ECRB Cross-Drift.
GS990408314224.004	Full-Periphery Geologic Maps for Station 10+00 to 15+00, ECRB Cross-Drift.
GS990408314224.005	Full-Periphery Geologic Maps for Station 15+00 to 20+00, ECRB Cross-Drift.
GS990408314224.006	Full-Periphery Geologic Maps for Station 20+00 to 26+81, ECRB Cross-Drift.
GS990908314224.009	Detailed line survey data for horizontal and vertical traverses, ECRB.
MO9904MWDFPG16.000	Fracture Attitude data for full periphery geotechnical mapping of strike and dip data entry correction analysis.

2.2 Limitations of DOE Fracture Data

Scientific data collection is almost always subject to sampling limitations and biases. DOE has acknowledged some of these limitations, which can be placed into one of three categories: (i) stratigraphic, (ii) orientation, and (iii) size.

A key stratigraphic limitation is that the ESF provided exposures primarily of the Middle Nonlithophysal zone (Figure 2-1). Fracture observations have a further stratigraphic limitation in that measurements did not consider stratigraphic subzones that reflect variations in degree of welding and vitric intervals within the four main lithostratigraphic intervals. In addition to this stratigraphic bias, the long stretches of uniform orientation {e.g., north ramp trends 299° for 2.2 km [1.4 mi], main drift trends 183° for 3.2 km [2.0 mi], south ramp trends 091° for 1.4 km [0.9 mi]} lead to orientation bias because the scanline technique cannot adequately sample fractures with strikes that are nearly parallel to the scanline orientation (Terzaghi, 1965). For example, the main drift portion leads to severe undersampling of steeply dipping fractures with strikes in the range of 173 to 193° (or 353 to 013°). Additional orientation sampling bias is introduced by the nearly horizontal plunge (typically within 3°) of the drift. Fractures that dip less than 10° are necessarily strongly undersampled by the nearly horizontal detailed line survey. As DOE has acknowledged (e.g., Nieder-Westermann, 2000; Mongano, et al., 1999), a size bias exists for the fracture data collected in the ESF because a minimum trace length cut-off was used during data collection. This cut-off results in a bias towards larger fractures in the data set because no sampling of fractures below the minimum size threshold occurred. As a further complication, fractures that are nearly parallel to the tunnel orientation (either steeply dipping or subhorizontal) will show apparent trace lengths that are larger than fractures oriented at a high angle to the tunnel.

The ECRB Cross-Drift was designed, in part, to remedy the ESF stratigraphic bias problem because it was constructed to intersect each of the four repository host horizon intervals (Mongano, et al., 1999). The ECRB Cross-Drift, however, still suffers from orientation bias. Except for the beginning (stations 0+00 to 3+00) and western end of the tunnel (stations 23+20 to 26+64), the 2.6-km [1.6-mi]-long Cross-Drift trends 229° (Figure 2-1). Because of this 229° trend, nearly parallel northeast-southwest striking fractures (strike azimuths of approximately 039 to 059°) are undersampled. The ECRB Cross-Drift is also nearly horizontal; therefore, shallowly dipping fractures are undersampled, which adds to the orientation bias. Size bias was alleviated partially in the ECRB Cross-Drift by the small-scale fracture study that was conducted after the primary detailed line survey data collection had been completed. However, it is difficult to merge the two data sets into a single coherent package because they were not collected at the same time under similar conditions. For example, although the smallest fractures from the detailed line survey should correlate with the largest fractures from the small-scale fracture study, DOE has not presented such an analysis.

Although the full-periphery geologic maps capture more fractures than the detailed line survey, some limitations still exist. The full-periphery geologic maps from the drift walls and ceiling are an effective means of sampling fractures whose spacings are small (i.e., less than approximately the tunnel diameter). In this situation, the full-periphery geologic maps of the tunnel walls and ceiling will show fractures of all orientations (i.e., a complete range of strike and dip), unlike the one-dimensional detailed line survey. DOE has suggested that the full-periphery maps eliminate the under-representation of low-angle fractures (e.g., Bechtel SAIC Company, LLC, 2004a,b; Board, 2003; Nieder-Westermann, 2000). Fractures whose

spacing is greater than the tunnel diameter, however, are still undersampled by the full-periphery geologic maps (Ferrill, et al., 2000). Size bias is also not eliminated because the full-periphery mapping was restricted to fractures that were greater than or equal to 1 m [3.3 ft] in trace length. Data collection during full-periphery mapping was restricted to fracture location (along the tunnel) and orientation (i.e., strike and dip). Finally, the full-periphery geologic maps do not cover the entire tunnel periphery since the invert obscures the lowermost portion (approximately 17 percent) of the tunnel circumference.

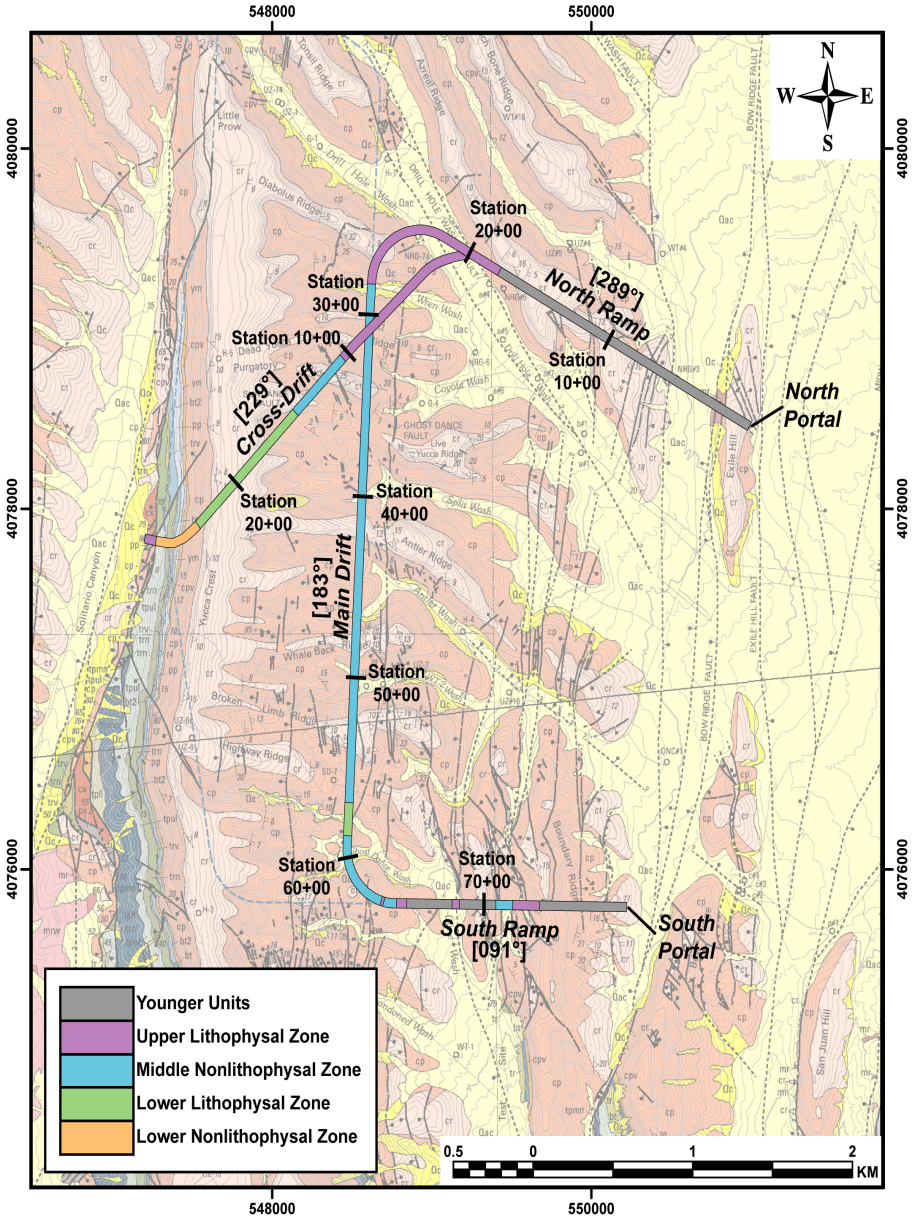

Figure 2-1. Location Map for the ESF and ECRB Cross-Drift Showing Intervals in Tunnels Where the Topopah Spring Tuff Zones Were Analyzed. Background Image Is a Portion of the 1:24,000-Scale Geologic Map of Day, et al. (1998). Note That Tunnel Locations Are Exact, But That Tunnel Width Has Been Exaggerated for Illustration Purposes.

3 SYNTHESIS OF FRACTURE CHARACTERISTICS

3.1 Detailed Line Survey Data

The detailed line survey data collection employed a classification scheme (Mongano, et al., 1999; Albin, et al., 1997; Eatman, et al., 1997; Kicker, et al., 1997; Barr, et al., 1996; Beason, et al., 1996) for discontinuity type that included vapor phase partings, cooling joints, shears {offset <0.1 m [0.3 ft] or offset indeterminate}, faults {offset >0.1 m [0.3 ft]}, and fractures (no apparent offset). Fracture is used in this report as a general term to encompass all types of discontinuities measured in the ESF and ECRB Cross-Drift.

Nearly 18,000 individual measurements were made in the ESF via the detailed line survey technique (data sets listed in Table 2-1; Albin, et al., 1997; Eatman, et al., 1997; Kicker, et al., 1997; Barr, et al., 1996; Beason, et al., 1996). Approximately 14,000 of the measurements were from the Topopah Spring Tuff Upper Lithophysal, Middle Nonlithophysal, and Lower Lithophysal zones, with nearly 90 percent from the Middle Nonlithophysal zone. When all three zones are considered together, approximately 90 percent of the discontinuities were classified as fractures (Figure 3-1). Cooling joints and vapor phase partings accounted for 5.3 percent, while shears and faults accounted for 4.5 percent. The breakdown is similar for both the Upper Lithophysal and Middle Nonlithophysal zones. The Lower Lithophysal zone shows nearly 40 percent shears and faults and no cooling joints or vapor phase partings, although this data set consists of only 38 measurements.

Only 418 of the 18,000 discontinuities (3 percent) in the ESF have recorded offsets, with a mean of 29 ± 251 cm [11.4 ± 98.8 in] and a maximum of 50 m [164 ft]. The offset distribution is positively skewed (Figure 3-2a), with a median displacement of 5 cm [2.0 in] and more than 97 percent of the 418 fractures having 1 m [3.3 ft] or less displacement. A comparison of total trace length versus offset displays a weak positive correlation for each lithostratigraphic zone (Figure 3-2b). At least three fracture sets are observed (Figures 3-2c and 3-2d). The most abundant fractures have a northwest-strike and steep southwest dip. In the Upper Lithophysal zone, a north-south striking, subvertical set is also present.

A total of 1,801 discontinuities were recorded by detailed line survey in the ECRB Cross-Drift (Mongano, et al., 1999) from each of the four zones in the Topopah Spring Tuff, although more than 50 percent are in the Middle Nonlithophysal. When all ECRB discontinuities are grouped together, approximately 81 percent are classified as fractures (Figure 3-1). Cooling joints and vapor phase partings accounted for 11 percent, while shears and faults accounted for the remaining 8 percent. The breakdowns, however, are dramatically different when each zone is considered separately (Figure 3-1). For example, cooling joints and vapor phase partings account for 21 percent of the discontinuities in the Upper Lithophysal. In the Lower Nonlithophysal, shears and faults account for 21 percent of the total fractures in that unit.

Measurable offset was recorded for 78 discontinuities in the ECRB Cross-Drift (4 percent), including the westernmost strand of the Solitario Canyon fault with 175 m [394 ft] offset. The mean and maximum offsets, excluding the Solitario Canyon fault measurement, are 47 ± 154 cm [18 ± 61 in] and 12 m [39 ft], respectively. The ECRB Cross-Drift offset distribution is positively skewed (Figure 3-3a) with a median value of 3 cm [1.2 in]. Only 10 of the 78 fractures (13 percent) have displacements of 1 m [3 ft] or greater. A comparison of total

trace length versus recorded offset shows little correlation (Figure 3-3b). A northwest-striking subvertical fracture set is present (Figures 3-3c and 3-3d).

3.1.1 Topopah Spring Tuff Upper Lithophysal Zone

Fracture data from the Topopah Spring Upper Lithophysal zone were obtained by detailed line survey in both the ESF and the ECRB Cross-Drift. More than 1,700 measurements were recorded with two-thirds having a north-south strike and steep west dip (set 2, Table 3-1, Figure 3-4). A second steeply dipping, northwest-striking set (set 1) and a shallowly dipping fracture set is also present. The apparent paucity of shallowly dipping fractures may reflect the orientation sampling bias discussed earlier.

The overall trace length distribution is positively skewed with a mean of 2.56 m [8.40 ft] and a median of 1.42 m [4.66 ft]. This pattern is repeated for each of the fractures sets, with the shallowly dipping fracture measuring approximately twice as long as the more steeply dipping fractures (Table 3-1). Fracture spacing [i.e., corrected for bias introduced by tunnel orientation (Terzaghi, 1965)] is positively skewed for all fracture sets with mean values that are greater than twice the median values. Given the highly skewed spacing distribution, the median provides a more appropriate measure of central tendency because it is less influenced by extreme values (e.g., Davis, 1986; Witte, 1985). Linear fracture intensity (Dershowitz and Herda, 1992), defined as the number of fractures per unit length or the inverse of median fracture spacing, was determined for each fracture set (Table 3-1). This parameter is one that is most requested by workers using fracture data for understanding related processes (e.g., drift degradation, unsaturated zone flow). For the Upper Lithophysal zone, median intensity values range from 0.77 to 1.53 m^{-1} [0.23 to 0.47 ft^{-1}].

3.1.2 Topopah Spring Tuff Middle Nonlithophysal Zone

As noted previously, nearly 50 percent of the ESF consists of exposures of the Topopah Spring Middle Nonlithophysal zone. More than 11,300 fractures were recorded for this interval by detailed line survey in the ESF and the ECRB Cross-Drift (Table 3-2, Figure 3-5). This data set includes a portion of the ESF main drift (stations 42+00 to 51+50) that has been referred to as the intensely fractured zone (Albin, et al., 1997). The most abundant fracture set has a northwest-southeast strike and steep southwest dip and comprises more than two-thirds of the fractures (Figure 3-5). A second subvertical, northeast-striking set is present, along with a shallowly dipping fracture set.

The Middle Nonlithophysal zone is characterized by a positively skewed overall size distribution with a mean trace length of 2.12 m [6.96 ft] and a median of 1.58 m [5.18 ft]. The pattern is repeated for each fracture set with median values that are 60–80 percent of the corresponding mean (Table 3-2). True fracture spacings are positively skewed with mean values that are 2 to 2.5 times greater than median values. Linear fracture intensity ranges from 1.92 to 5.20 m^{-1} [0.59 to 1.58 ft^{-1}], with the greatest intensity for the northwest striking subvertical fracture set.

Table 3-1. Summary of Fracture Data from the Topopah Spring Tuff Upper Lithophysal Zone Based on Detailed Line Surveys in the Enhanced Characterization of the Repository Block (ECRB) Cross-Drift and the Exploratory Studies Facility (ESF). This Data Set Was Collected With a Lower Trace Length Cut-Off of 1 m [3.3 ft] {i.e., Sampled Fractures with Trace Lengths >1 m [3.3 ft]}. True Spacing Reflects Correction of Orientation Bias Using a Truncated Terzaghi Approach.* Median Intensity Is the Inverse of Median Fracture Spacing (Equivalent to Number of Fractures Per Unit Length of Scanline). An Expanded Data Table That Includes Standard Deviations for Trace Length and Spacing is Provided in Appendix Table A–1.

Set	Number and Percentage	Mean Orientation (Strike/Dip)	Fisher Dispersion Coefficient†	Total Trace Length, m [ft]		True Spacing, m [ft]		Median Linear Fracture Intensity, m^{-1} [ft^{-1}]
				Mean	Median	Mean	Median	
All	1758, 100%	*n.a.*	*n.a.*	2.56 [8.40]	1.42 [4.66]	*n.a.*	*n.a.*	*n.a.*
1	538, 31%	116°/85°	7.462	2.09 [6.86]	1.44 [4.72]	2.82 [9.25]	0.75 [2.46]	1.34 [0.41]
2	1024, 58%	181°/85°	1.945	2.29 [7.51]	1.30 [4.66]	1.73 [5.68]	0.65 [2.13]	1.53 [0.47]
3	95, 5%	320°/19°	9.436	5.73 [18.80]	4.31 [14.14]	3.98 [13.06]	1.29 [4.23]	0.77 [0.23]
Random	101, 6%	*n.a.*	*n.a.*	4.87 [15.98]	2.10 [6.89]	*n.a.*	*n.a.*	*n.a.*

*Terzaghi, R.D. "Sources of Error in Joint Surveys." *Geotechnique*. Vol. 15. pp. 287–304. 1965.
†The Fisher dispersion coefficient (also referred to as the concentration parameter) is a measure of the degree to which spherical data are concentrated around the mean (Fisher, N.I, T. Lewis, and B.J.J. Embleton. *Statistical Analysis of Spherical Data*. Cambridge, United Kingdom: Cambridge University Press. 1993; Mardia, K.V. *Statistics of Directional Data*. New York, New York: Academic Press. 1972; Fisher, R.A. "Dispersion On a Sphere." Proceedings of the Royal Society of London. Vol. A217. pp. 295–305. 1953). Larger values of the Fisher dispersion coefficient indicate tighter clustering (i.e., less dispersion).

As noted above, the ESF main drift encountered a 950-m [3,117-ft]-long zone where fracture intensity was greater than the other portions of the tunnel (referred to as the intensely fractured zone). The data for the Middle Nonlithophysal zone were analyzed without the fractures from the intensely fractured zone to help better understand the effect of this anomalous zone. The intensely fractured zone contains more than 4,500 fractures (Figure 3-6), of which 85 percent are northwest striking and subvertical (Table 3-3, Figure 3-6). The trace length distributions for the intensely fractured zone are similar to those for the entire Middle Nonlithophysal zone. Fracture spacing for the northwest-striking subvertical fracture set, however, is smaller, with a correspondingly higher linear fracture intensity of 8.27 m^{-1} [2.52 ft^{-1}]. With the data from the intensely fractured zone removed, there are approximately 8,900 fractures remaining in the Middle Nonlithophysal zone (Table 3-4, Figure 3-7). As expected, the northwest-striking subvertical fracture set is less abundant (i.e., with the intensely fractured zone removed), but still present. Further, the linear intensity for this fracture set is reduced to 3.54 m^{-1} [1.08 ft^{-1}].

Table 3-2. Summary of Fracture Data from the Topopah Spring Tuff Middle Nonlithophysal Zone (Including Intensely Fractured Zone) Based on Detailed Line Surveys in the Exploratory Studies Facility (ESF) and the Enhanced Characterization of the Repository Block (ECRB) Cross-Drift . This Data Set Was Collected With a Lower Trace Length Cut-Off of 1 m [3.3 ft]. True Spacing Reflects Correction of Orientation Bias Using a Truncated Terzaghi Approach.* Median Intensity Is the Inverse of Median Fracture Spacing (Equivalent to Number of Fractures Per Unit Length of Scanline). An Expanded Data Table That Includes Standard Deviations for Trace Length and Spacing is Provided in Appendix Table A–2.

Set	Number and Percentage	Mean Orientation (Strike/Dip)	Fisher Dispersion Coefficient†	Total Trace Length, m [ft]		True Spacing, m [ft]		Median Linear Fracture Intensity, m^{-1} [ft^{-1}]
				Mean	Median	Mean	Median	
All	13493, 100%	*n.a.*	*n.a.*	2.12 [6.96]	1.58 [5.18]	*n.a.*	*n.a.*	*n.a.*
1	8919, 66%	126°/84°	17.670	2.18 [7.15]	1.70 [5.58]	0.42 [1.39]	0.19 [0.62]	5.20 [1.58]
2	2973, 22%	227°/86°	5.329	1.90 [6.23]	1.35 [4.43]	0.92 [3.02]	0.46 [1.51]	2.19 [0.67]
3	679, 5%	326°/08°	27.225	2.47 [8.10]	1.54 [5.05]	1.19 [3.90]	0.52 [1.71]	1.92 [0.59]
Random	922, 7%	*n.a.*	*n.a.*	2.02 [6.63]	1.27 [4.17]	*n.a.*	*n.a.*	*n.a.*

*Terzaghi, R.D. "Sources of Error in Joint Surveys." *Geotechnique*. Vol. 15. pp. 287–304. 1965.
†The Fisher dispersion coefficient (also referred to as the concentration parameter) is a measure of the degree to which spherical data are concentrated around the mean (Fisher, N.I, T. Lewis, and B.J.J. Embleton. *Statistical Analysis of Spherical Data*. Cambridge, United Kingdom: Cambridge University Press. 1993; Mardia, K.V. *Statistics of Directional Data*. New York, New York: Academic Press. 1972; Fisher, R.A. "Dispersion On a Sphere." Proceedings of the Royal Society of London. Vol. A217. pp. 295–305. 1953). Larger values of the Fisher dispersion coefficient indicate tighter clustering (i.e., less dispersion).

A total of 391 measurements of small-scale fractures {i.e., trace lengths <1 m [3.3 ft]} was recorded on two horizontal {6-m [20-ft]}-long and six vertical {2-m [7-ft]}-tall scanlines (i.e., along the curved tunnel wall) in the ECRB Cross-Drift (Table 3-5, Figure 3-8). Three sets are present in the small-scale fracture data (i.e., two steeply dipping sets and one subhorizontal set). The trace length and spacing distributions for the small fractures are highly positively skewed with mean values that are 1.5 to 3 times greater than the median values (Table 3-5). As expected, the absolute trace lengths for the small-scale fractures are smaller than for the regular detailed line survey data. Intensity values, in contrast, are 3 to 4 times greater for the small-scale fractures.

3.1.3 Topopah Spring Tuff Lower Lithophysal Zone

Fracture data from the Topopah Spring Lower Lithophysal zone were obtained by detailed line surveys in both the ESF and the ECRB Cross-Drift. Nearly 340 measurements were recorded (Table 3-6, Figure 3-9) with three-fourths of the fractures falling into a northwest-striking subvertical fracture set. An additional steeply dipping set and a shallowly dipping set are also present.

Table 3-3. Summary of Fracture Data from the Intensely Fractured Zone in the Topopah Spring Tuff Middle Nonlithophysal Zone Based on Detailed Line Surveys in the Exploratory Studies Facility (ESF). This Data Set Was Collected With a Lower Trace Length Cut-Off of 1 m [3.3 ft]. True Spacing Reflects Correction of Orientation Bias Using a Truncated Terzaghi Approach.* Median Intensity Is the Inverse of Median Fracture Spacing (Equivalent to Number of Fractures Per Unit Length of Scanline). An Expanded Data Table That Includes Standard Deviations for Trace Length and Spacing is Provided in Appendix Table A–3.

Set	Number and Percentage	Mean Orientation (Strike/Dip)	Fisher Dispersion Coefficient†	Total Trace Length, m [ft]		True Spacing, m [ft]		Median Linear Fracture Intensity, m^{-1} [ft^{-1}]
				Mean	Median	Mean	Median	
All	4566, 100%	*n.a.*	*n.a.*	2.18 [7.15]	1.80 [5.91]	*n.a.*	*n.a.*	*n.a.*
1	3875, 85%	129°/84°	29.093	2.23 [7.32]	1.85 [6.07]	0.20 [0.66]	0.12 [0.39]	8.27 [2.52]
2	525, 11%	231°/87°	7.943	2.04 [6.69]	1.57 [5.15]	1.34 [4.40]	0.74 [2.43]	1.35 [0.41]
3	54, 1%	340°/07°	20.711	1.21 [3.97]	0.96 [3.15]	2.08 [6.82]	0.43 [1.41]	2.32 [0.71]
Random	112, 2%	*n.a.*	*n.a.*	1.73 [5.68]	1.37 [4.49]	*n.a.*	*n.a.*	*n.a.*

*Terzaghi, R.D. "Sources of Error in Joint Surveys." *Geotechnique*. Vol. 15. pp. 287–304. 1965.
†The Fisher dispersion coefficient (also referred to as the concentration parameter) is a measure of the degree to which spherical data are concentrated around the mean (Fisher, N.I, T. Lewis, and B.J.J. Embleton. *Statistical Analysis of Spherical Data*. Cambridge, United Kingdom: Cambridge University Press. 1993; Mardia, K.V. *Statistics of Directional Data*. New York, New York: Academic Press. 1972; Fisher, R.A. "Dispersion On a Sphere." Proceedings of the Royal Society of London. Vol. A217. pp. 295–305. 1953). Larger values of the Fisher dispersion coefficient indicate tighter clustering (i.e., less dispersion).

The overall trace length distribution is highly skewed with a mean of 4.04 m [13.26 ft] and a median of 1.92 m [6.30 ft]. This pattern is repeated for each of the fracture sets with measured trace lengths of the shallowly dipping fractures being almost twice as long as the steep fractures (Table 3-6). True fracture spacing (corrected for orientation bias) is positively skewed for all fracture sets with mean values that are 1.5 to 3 times larger than the median values. The contrast is most extreme for the shallowly dipping fracture set. Linear fracture intensity values range from 0.16 to 0.72 m^{-1} [0.05 to 0.22 ft^{-1}] for all sets.

A total of 649 measurements of small-scale fractures {i.e., trace lengths <1 m [3.3 ft]} were recorded on three horizontal {6-m-long [20-ft-long]} and nine vertical {2-m-tall [7-ft-tall]} scanlines in the ECRB Cross-Drift (Table 3-7, Figure 3-10). The most abundant fracture sets are a northwest-striking steeply dipping set and a subhorizontal set. The trace length distributions for the small fractures are not as positively skewed, except for the shallowly dipping fractures where the mean trace length is more than three times larger than the median (Table 3-7). The true spacing distributions are also positively skewed with the mean spacing for the northwest-striking subvertical set being 36 times greater than the median (Table 3-7). Linear intensity values are much higher {8.39 to 27.56 m^{-1} [2.56 to 8.40 ft^{-1}]} for the small fractures in the Lower Lithophysal zone than the longer fractures.

Table 3-4. Summary of Fracture Data from the Topopah Spring Tuff Middle Nonlithophysal Zone (Excluding Intensely Fractured Zone) Based on Detailed Line Surveys in the Exploratory Studies Facility (ESF) and the Enhanced Characterization of the Repository Block (ECRB) Cross-Drift. This Data Set Was Collected with a Lower Trace Length Cut-Off of 1 m [3.3 ft]. True Spacing Reflects Correction of Orientation Bias Using a Truncated Terzaghi Approach.* Median Intensity Is the Inverse of Median Fracture Spacing (Equivalent to Number of Fractures Per Unit Length of Scanline). An Expanded Data Table That Includes Standard Deviations for Trace Length and Spacing is Provided in Appendix Table A–4.

Set	Number and Percentage	Mean Orientation (Strike/Dip)	Fisher Dispersion Coefficient†	Total Trace Length, m [ft]		True Spacing, m [ft]		Median Linear Fracture Intensity, m^{-1} [ft^{-1}]
				Mean	Median	Mean	Median	
All	8927, 100%	*n.a.*	*n.a.*	2.09 [6.86]	1.43 [4.69]	*n.a.*	*n.a.*	*n.a.*
1	5044, 57%	124°/85°	13.814	2.14 [7.02]	1.52 [4.99]	0.59 [1.94]	0.28 [0.92]	3.54 [1.08]
2	2448, 27%	226°/86°	4.994	1.87 [6.14]	1.30 [4.27]	0.84 [2.76]	0.41 [1.35]	2.41 [0.73]
3	625, 7%	326°/08°	27.979	2.58 [8.46]	1.61 [5.28]	1.09 [3.58]	0.53 [1.74]	1.89 [0.58]
Random	810, 9%	*n.a.*	*n.a.*	2.07 [6.79]	1.27 [4.17]	*n.a.*	*n.a.*	*n.a.*

*Terzaghi, R.D. "Sources of Error in Joint Surveys." *Geotechnique*. Vol. 15. pp. 287–304. 1965.
†The Fisher dispersion coefficient (also referred to as the concentration parameter) is a measure of the degree to which spherical data are concentrated around the mean (Fisher, N.I, T. Lewis, and B.J.J. Embleton. *Statistical Analysis of Spherical Data*. Cambridge, United Kingdom: Cambridge University Press. 1993; Mardia, K.V. *Statistics of Directional Data*. New York, New York: Academic Press. 1972; Fisher, R.A. "Dispersion On a Sphere." Proceedings of the Royal Society of London. Vol. A217. pp. 295–305. 1953). Larger values of the Fisher dispersion coefficient indicate tighter clustering (i.e., less dispersion).

3.1.4 Topopah Spring Tuff Lower Nonlithophysal Zone

Fracture data from the Topopah Spring Lower Nonlithophysal zone were obtained by detailed line survey in the ECRB Cross-Drift. Nearly 200 measurements were recorded (Table 3-8, Figure 3-11), with slightly fewer than two-thirds of the fractures falling into a northwest-striking subvertical fracture set. An additional steeply dipping set and a shallowly dipping set are also present.

The overall trace length distribution is positively skewed with a mean of 4.04 m [13.26 ft] and a median of 1.93 m [6.33 ft]. The positive skew is repeated for all fracture sets except the shallowly dipping fractures (Table 3-8). True fracture spacing is positively skewed for all fracture sets with mean values that are 1.5 to 2.5 times larger than the median values. Linear fracture intensity values range from 0.63 to 1.42 m^{-1} [0.19 to 0.43 ft^{-1}] for all sets.

Table 3-5. Summary of Small-Scale Fracture Data from the Topopah Spring Tuff Middle Nonlithophysal Zone Based on Two 6-m [20-ft] Horizontal and Six 2-m [7-ft] Vertical Scanlines in the Enhanced Characterization of the Repository Block (ECRB) Cross-Drift. This Data Set Was Collected With an Upper Trace Length Cut-Off of 1 m [3.3 ft]. True Spacing Reflects Correction of Orientation Bias Using a Truncated Terzaghi Approach.* Median Intensity Is the Inverse of Median Fracture Spacing (Equivalent to Number of Fractures Per Unit Length of Scanline). An Expanded Data Table That Includes Standard Deviations for Trace Length and Spacing is Provided in Appendix Table A–5.

Set	Number and Percentage	Mean Orientation (Strike/Dip)	Fisher Dispersion Coefficient†	Total Trace Length, m [ft]		True Spacing, m [ft]		Median Linear Fracture Intensity, m^{-1} [ft^{-1}]
				Mean	Median	Mean	Median	
All	391, 100%	*n.a.*	*n.a.*	0.63 [2.07]	0.20 [0.66]	*n.a.*	*n.a.*	*n.a.*
1	164, 42%	179°/88°	14.449	0.38 [1.25]	0.15 [0.49]	0.07 [0.23]	0.04 [0.13]	26.10 [7.95]
2	118, 30%	118°/86°	15.514	1.06 [3.48]	0.30 [0.98]	0.11 [0.36]	0.07 [0.23]	15.31 [4.67]
3	54, 14%	312°/05°	42.197	0.76 [2.49]	0.31 [1.02]	0.19 [0.62]	0.12 [0.39]	8.37 [2.55]
Random	55, 14%	*n.a.*	*n.a.*	0.33 [1.08]	0.17 [0.56]	*n.a.*	*n.a.*	*n.a.*

*Terzaghi, R.D. "Sources of Error in Joint Surveys." *Geotechnique*. Vol. 15. pp. 287–304. 1965.
†The Fisher dispersion coefficient (also referred to as the concentration parameter) is a measure of the degree to which spherical data are concentrated around the mean (Fisher, N.I, T. Lewis, and B.J.J. Embleton. *Statistical Analysis of Spherical Data*. Cambridge, United Kingdom: Cambridge University Press. 1993; Mardia, K.V. *Statistics of Directional Data*. New York, New York: Academic Press. 1972; Fisher, R.A. "Dispersion On a Sphere." Proceedings of the Royal Society of London. Vol. A217. pp. 295–305. 1953). Larger values of the Fisher dispersion coefficient indicate tighter clustering (i.e., less dispersion).

3.2 Full-Periphery Geologic Mapping Data

The full-periphery geologic mapping in the entire ESF resulted in nearly 31,000 fracture measurements (Figure 3-12). In all, 21,589 fractures were mapped over the interval where the Topopah Spring Tuff Upper Lithophysal, Middle Nonlithophysal, and Lower Lithophysal zones were measured. The full-periphery mapping shows fracture orientations (Figure 3-13) that are similar to those obtained by the detailed line survey. A northwest-striking, southwest-dipping set and a northeast-striking, northwest-dipping set are well developed . A subhorizontal fracture set also is present, although it accounts for only 6 percent of the total fracture population. Fractures from the Upper Lithophysal zone (11 percent of the total population) are dominated by a north-trending subvertical set (Figure 3-14). As with the detailed line survey data, the full-periphery geologic mapping data in the ESF are dominated by Middle Nonlithophysal zone fractures (87 percent) that are characterized by a well-developed northwest-striking subvertical set, a northeast-striking subvertical set, and a subhorizontal set (Figure 3-15). Lower Lithophysal zone fractures are a minor component (2 percent), but display a prominent northwest-striking subvertical set and a weakly developed northeast-striking subvertical set (Figure 3-16).

Table 3-6. Summary of Fracture Data from the Topopah Spring Tuff Lower Lithophysal Zone Based on Detailed Line Surveys in the Exploratory Studies Facility (ESF) and the Enhanced Characterization of the Repository Block (ECRB) Cross-Drift. This Data Set Was Collected With a Lower Trace Length Cut-Off of 1 m [3.3 ft]. True Spacing Reflects Correction of Orientation Bias Using a Truncated Terzaghi Approach.* Median Intensity Is the Inverse of Median Fracture Spacing (Equivalent to Number of Fractures Per Unit Length of Scanline). An Expanded Data Table That Includes Standard Deviations for Trace Length and Spacing is Provided in Appendix Table A–6.

Set	Number and Percentage	Mean Orientation (Strike/Dip)	Fisher Dispersion Coefficient†	Total Trace Length, m [ft]		True Spacing, m [ft]		Median Linear Fracture Intensity, m^{-1} [ft^{-1}]
				Mean	Median	Mean	Median	
All	338, 100%	*n.a.*	*n.a.*	4.04 [13.26]	1.92 [6.30]	*n.a.*	*n.a.*	*n.a.*
1	254, 75%	158°/81°	2.606	4.21 [13.81]	1.88 [6.19]	3.48 [11.42]	1.39 [4.56]	0.72 [0.22]
2	60, 18%	087°/85°	17.759	2.32 [7.61]	1.63 [5.35]	9.07 [29.76]	6.17 [20.24]	0.16 [0.05]
3	19, 6%	329°/05°	53.085	7.36 [24.15]	3.42 [11.22]	4.59 [15.06]	1.39 [4.56]	0.72 [0.22]
Random	5, 1%	*n.a.*	*n.a.*	3.16 [10.37]	3.55 [11.65]	*n.a.*	*n.a.*	*n.a.*

*Terzaghi, R.D. "Sources of Error in Joint Surveys." *Geotechnique*. Vol. 15. pp. 287–304. 1965.
†The Fisher dispersion coefficient (also referred to as the concentration parameter) is a measure of the degree to which spherical data are concentrated around the mean (Fisher, N.I, T. Lewis, and B.J.J. Embleton. *Statistical Analysis of Spherical Data*. Cambridge, United Kingdom: Cambridge University Press. 1993; Mardia, K.V. *Statistics of Directional Data*. New York, New York: Academic Press. 1972; Fisher, R.A. "Dispersion On a Sphere." Proceedings of the Royal Society of London. Vol. A217. pp. 295–305. 1953). Larger values of the Fisher dispersion coefficient indicate tighter clustering (i.e., less dispersion).

More than 5,200 fractures were recorded on the full-periphery geologic maps collected in the ECRB Cross-Drift (Figure 3-17). As with the fracture data obtained in the ESF, the full-periphery mapping in the ECRB Cross-Drift reveals three prominent fracture sets: (i) a northwest-striking subvertical set, (ii) a north-northeast-striking subvertical set, and (iii) a shallowly dipping or subhorizontal set. Fractures from the Upper Lithophysal zone (20 percent of the total population) are dominated by the north-northeast-trending subvertical set, but the northwest-striking subvertical and subhorizontal sets are also present (Figure 3-18). Approximately one-half of the full-periphery geologic mapping data collected in the ECRB comes from the Middle Nonlithophysal zone (Figure 3-19). Lower Lithophysal zone fractures, representing nearly one-quarter of the ECRB data, display a prominent north-northwest-striking subvertical set and a subhorizontal fracture set (Figure 3-20). Lower Nonlithophysal zone fractures account for less than 10 percent of the fractures mapped in the ECRB Cross-Drift, but display three prominent fracture sets (Figure 3-21).

Table 3-7. Summary of Small-Scale Fracture Data from the Topopah Spring Tuff Lower Lithophysal Zone Based on Three 6-m [20-ft] Horizontal and Nine 2-m [7-ft] Vertical Scanlines in the Enhanced Characterization of the Repository Block (ECRB) Cross-Drift. This Data Set Was Collected With an Upper Trace Length Cut-Off of 1 m [3.3 ft]. True Spacing Reflects Correction of Orientation Bias Using a Truncated Terzaghi Approach.* Median Intensity Is the Inverse of Median Fracture Spacing (Equivalent to Number of Fractures Per Unit Length of Scanline). An Expanded Data Table That Includes Standard Deviations for Trace Length and Spacing is Provided in Appendix Table A–1.

Set	Number and Percentage	Mean Orientation (Strike/Dip)	Fisher Dispersion Coefficient†	Total Trace Length, m [ft]		True Spacing, m [ft]		Median Linear Fracture Intensity, m^{-1} [ft^{-1}]
				Mean	Median	Mean	Median	
All	649, 100%	*n.a.*	*n.a.*	0.31 [1.02]	0.16 [0.52]	*n.a.*	*n.a.*	*n.a.*
1	421, 65%	134°/82°	3.344	0.25 [0.82]	0.17 [0.56]	1.08 [3.54]	0.03 [0.10]	27.56 [8.40]
2	49, 8%	079°/82°	14.633	0.19 [0.62]	0.14 [0.50]	0.24 [0.79]	0.12 [0.39]	8.39 [2.56]
3	125, 19%	313°/04°	47.359	0.63 [2.07]	0.19 [0.62]	0.10 [0.33]	0.06 [0.20]	16.71 [5.09]
Random	54, 8%	*n.a.*	*n.a.*	0.17 [0.56]	0.12 [0.39]	*n.a.*	*n.a.*	*n.a.*

*Terzaghi, R.D. "Sources of Error in Joint Surveys." *Geotechnique*. Vol. 15. pp. 287–304. 1965.
†The Fisher dispersion coefficient (also referred to as the concentration parameter) is a measure of the degree to which spherical data are concentrated around the mean (Fisher, N.I, T. Lewis, and B.J.J. Embleton. *Statistical Analysis of Spherical Data*. Cambridge, United Kingdom: Cambridge University Press. 1993; Mardia, K.V. *Statistics of Directional Data*. New York, New York: Academic Press. 1972; Fisher, R.A. "Dispersion On a Sphere." Proceedings of the Royal Society of London. Vol. A217. pp. 295–305. 1953). Larger values of the Fisher dispersion coefficient indicate tighter clustering (i.e., less dispersion).

Fracture trace length was not explicitly recorded during the full-periphery geologic mapping. However, it is possible to extract trace length information from each 100-m [328-ft]-long panel of the digitized full-periphery geologic maps from the ECRB Cross-Drift. Total trace length varies along the tunnel and correlates with stratigraphic position (Figure 3-22). Total trace length in the Middle Nonlithophysal zone is more than twice as large as total trace length in the Upper or Lower Lithophysal zones. Trace length data determined from the detailed line survey in the ECRB Cross-Drift are presented in Figure 3-23 for comparison purposes. For both sampling techniques, the largest trace lengths are found for the Middle Nonlithophysal zone.

Fracture spacing data were also not explicitly collected during the full-periphery mapping. Areal fracture density or trace length per unit area (Dershowitz and Herda, 1992), however, can be determined from the total trace length data (Figure 3-24). Whether the density is calculated over 10-m [33-ft] or 100-m [328-ft]-long panels, values are highest for the Middle Nonlithophysal zone. As a further comparison, areal fracture density was calculated with ESRI® ArcGIS for each 100-m [328-ft]-long full-periphery map panel (Figures 3-25 to 3-30).

Table 3-8. Summary of Fracture Data from the Topopah Spring Tuff Lower Nonlithophysal Zone Based on Detailed Line Survey in the Enhanced Characterization of the Repository Block (ECRB) Cross-Drift. This Data Set Was Collected With a Lower Trace Length Cut-Off of 1 m [3.3 ft]. True Spacing Reflects Correction of Orientation Bias Using a Truncated Terzaghi Approach.* Median Intensity Is the Inverse of Median Fracture Spacing (Equivalent to Number of Fractures Per Unit Length of Scanline). An Expanded Data Table That Includes Standard Deviations for Trace Length and Spacing is Provided in Appendix Table A–8.

Set	Number and Percentage	Mean Orientation (Strike/Dip)	Fisher Dispersion Coefficient†	Total Trace Length, m [ft]		True Spacing, m [ft]		Median Linear Fracture Intensity, m^{-1} [ft^{-1}]
				Mean	Median	Mean	Median	
All	199, 100%	*n.a.*	*n.a.*	4.04 [13.26]	1.93 [6.33]	*n.a.*	*n.a.*	*n.a.*
1	121, 61%	134°/80°	48.804	4.39 [14.40]	2.25 [7.38]	1.89 [6.20]	0.73 [2.40]	1.37 [0.42]
2	61, 31%	209°/85°	18.362	4.05 [13.29]	1.66 [5.45]	1.79 [5.87]	0.70 [2.30]	1.42 [0.43]
3	16, 8%	337°/15°	67.639	1.55 [5.09]	1.31 [4.30]	2.75 [9.02]	1.59 [5.22]	0.63 [0.19]
Random	1, <1%	*n.a.*	*n.a.*	1.85 [6.07]	1.85 [6.07]	*n.a.*	*n.a.*	*n.a.*

*Terzaghi, R.D. "Sources of Error in Joint Surveys." *Geotechnique*. Vol. 15. pp. 287–304. 1965.

†The Fisher dispersion coefficient (also referred to as the concentration parameter) is a measure of the degree to which spherical data are concentrated around the mean (Fisher, N.I, T. Lewis, and B.J.J. Embleton. *Statistical Analysis of Spherical Data*. Cambridge, United Kingdom: Cambridge University Press. 1993; Mardia, K.V. *Statistics of Directional Data*. New York, New York: Academic Press. 1972; Fisher, R.A. "Dispersion On a Sphere." Proceedings of the Royal Society of London. Vol. A217. pp. 295–305. 1953). Larger values of the Fisher dispersion coefficient indicate tighter clustering (i.e., less dispersion).

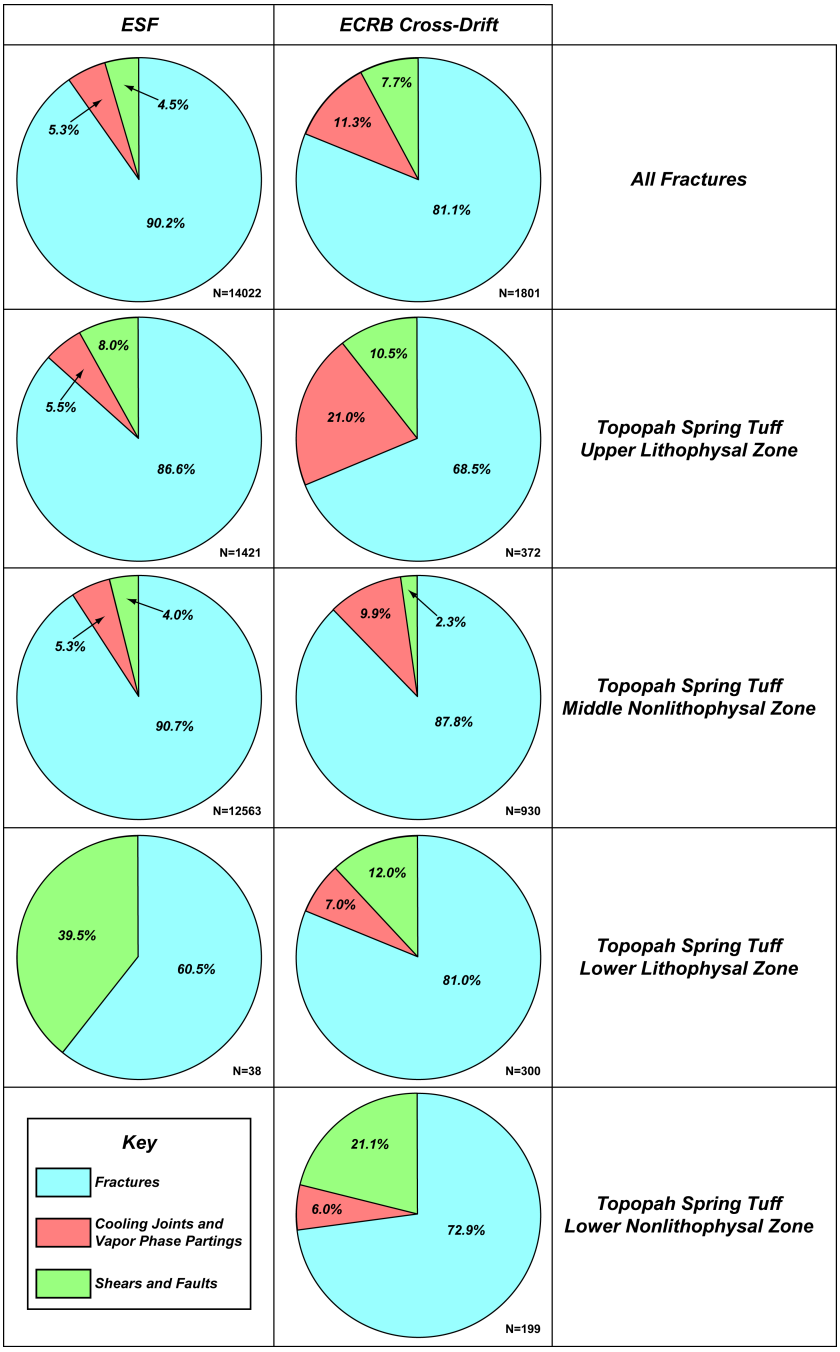

Figure 3-1. Distribution of Fractures By Type As Recorded By Detailed Line Survey. Fracture Type Reflects the Information Recorded In the Digital Data Sets As Determined During the Original Survey Work and Has Not Been Reinterpreted for This Report. Data Are Separated By Location (i.e., ESF Versus ECRB Cross-Drift) As Well As Lithostratigraphic Zone to Illustrate the Spatial and Stratigraphic Variability That Is Present In This Data Set. Note That the Topopah Spring Tuff Lower Nonlithophysal Zone Was Only Encountered In the ECRB Cross-Drift.

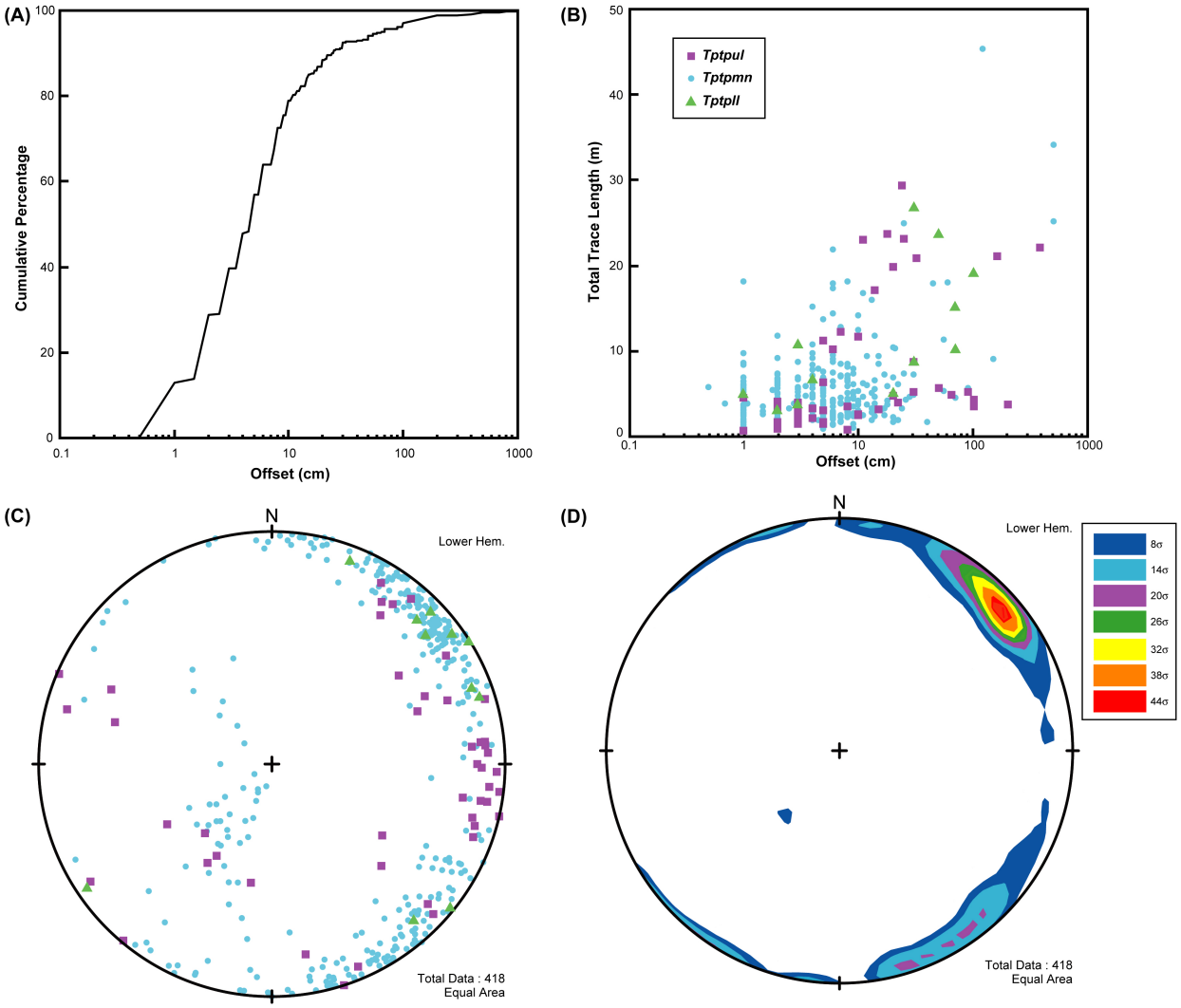

Figure 3-2. Summary of Fractures with Recorded Offset Based upon Detailed Line Survey in the ESF. (A) Offset Versus Cumulative Percentage. (B) Comparison of Total Trace Length Versus Recorded Offset. (C) Equal-Area Stereonet Plot of Fracture Poles. (D) Contours of Poles to All 418 Fracture Planes Calculated with the Kamb Method (Kamb, 1959). The Kamb Contouring Method Was Used Because the 1% Method Is Not Appropriate for Data Sets Smaller than Approximately 500 Data Points. Measurements Are Separated on the Basis of Lithostratigraphic Zone in (B) and (C) to Illustrate the Stratigraphic Variability in the Original Data.

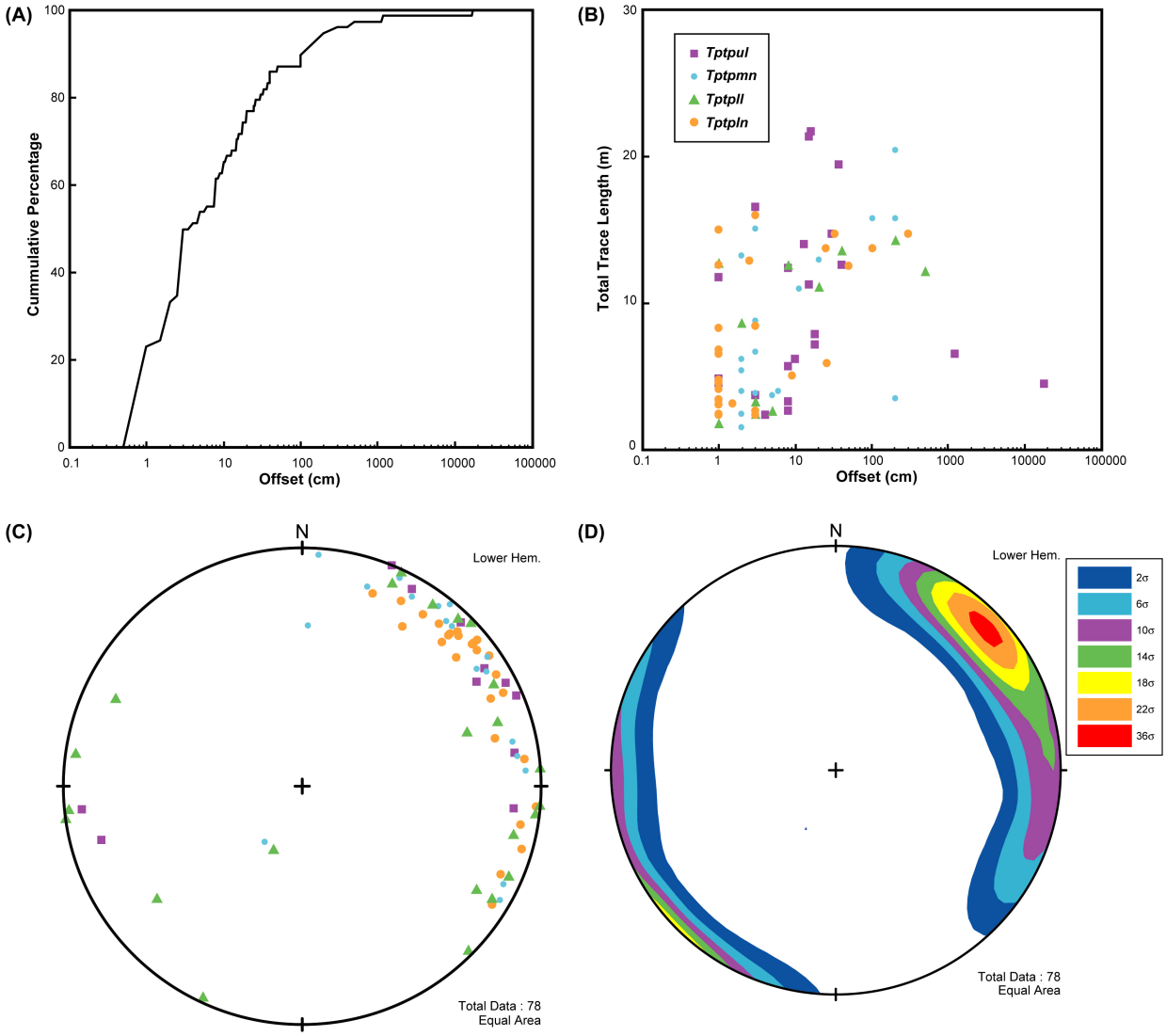

Figure 3-3. Summary of Fractures with Recorded Offset Based upon Detailed Line Survey in the ECRB Cross-Drift. (A) Offset Versus Cumulative Percentage. (B) Comparison of Total Trace Length Versus Recorded Offset. (C) Equal-Area Stereonet Plot of Fracture Poles. (D) Contours of Poles to All 78 Fracture Planes Calculated with the Kamb Method (Kamb, 1959). Measurements Are Separated on the Basis of Lithostratigraphic Zone in (B) and (C) to Illustrate the Stratigraphic Variability in the Original Data.

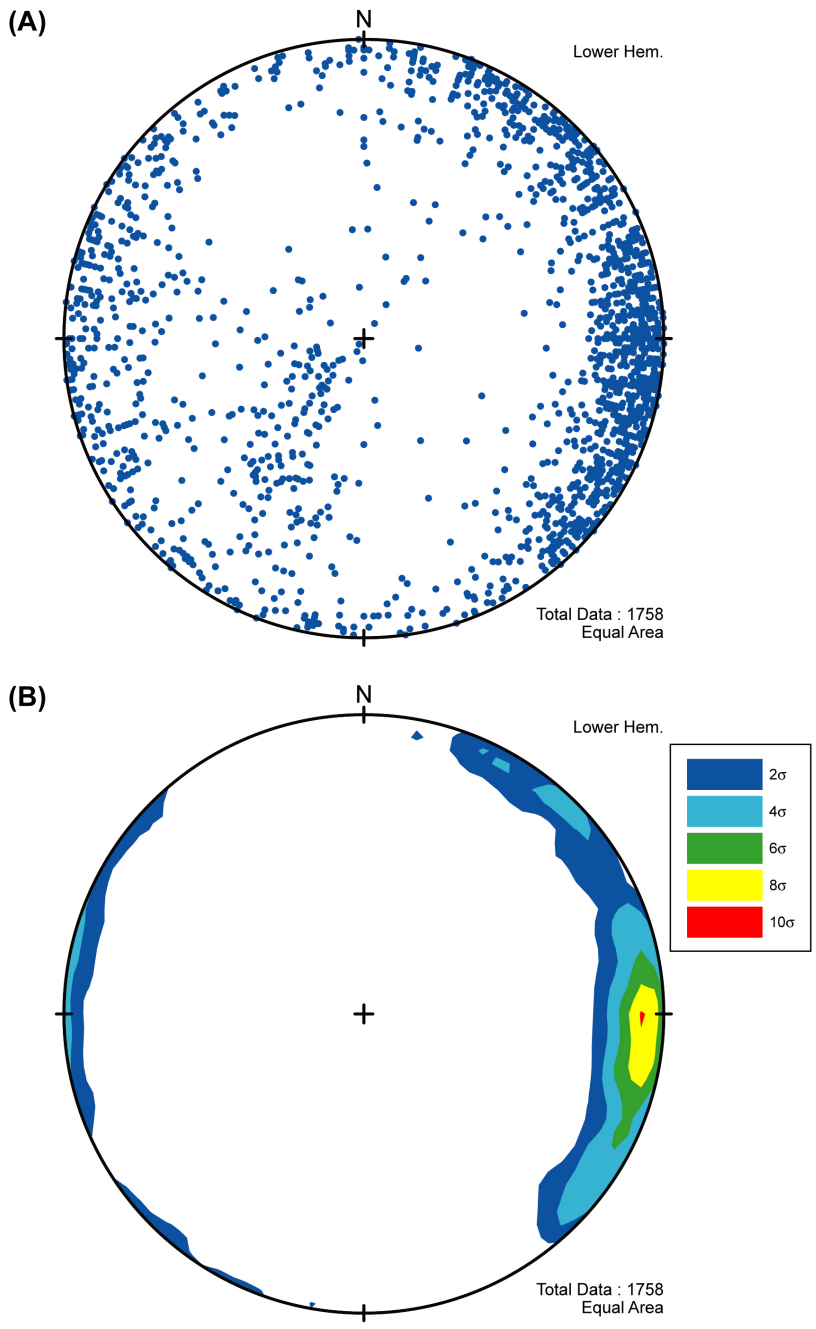

Figure 3-4. Orientation Summary for Fractures from the Topopah Spring Tuff Upper Lithophysal Zone Recorded by Detailed Line Survey in the ESF and the ECRB Cross-Drift. (A) Equal-Area Stereonet Plot of Poles to Fracture Planes. (B) Contours of Poles to Fracture Planes Calculated with 1% Area Method (Knopf and Ingerson, 1938; Turner and Weiss, 1963).

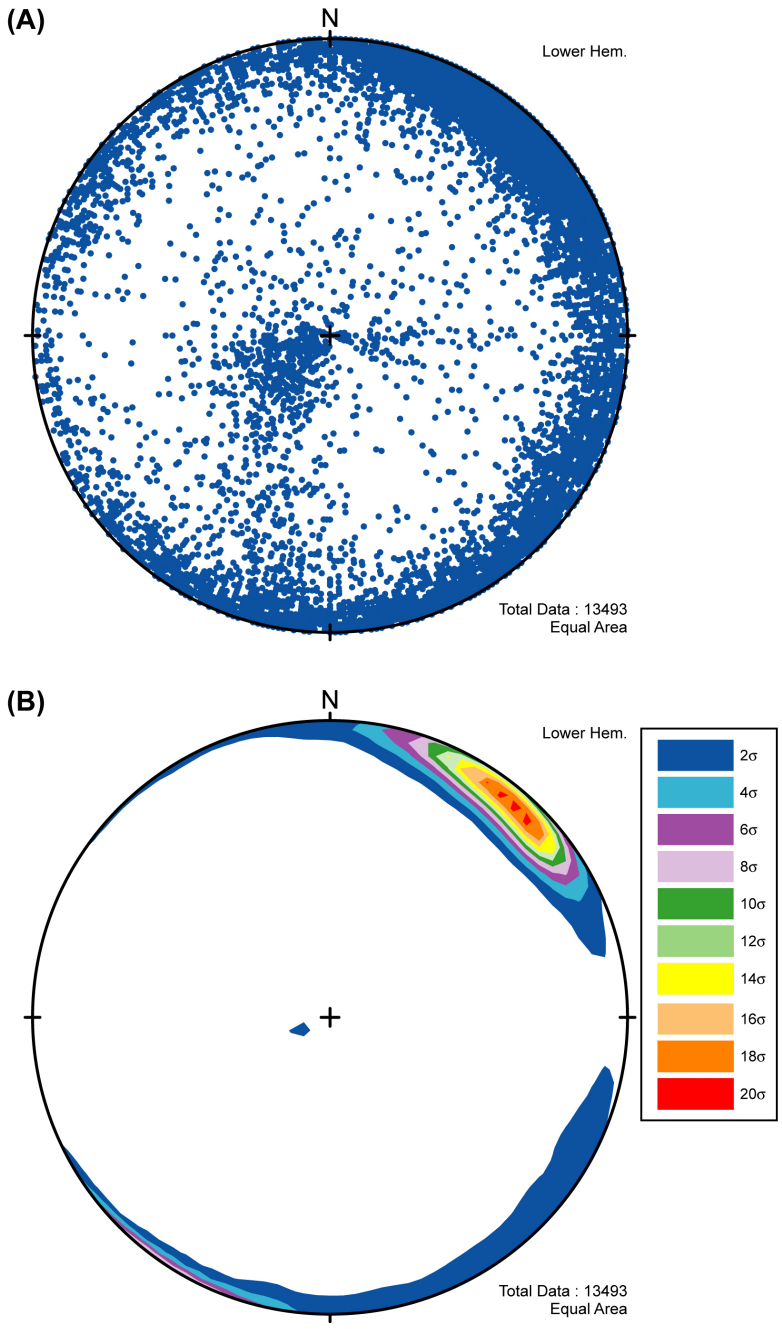

Figure 3-5. Orientation Summary for Fractures from the Topopah Spring Tuff Middle Nonlithophysal Zone (Including the Intensely Fractured Zone) Recorded by Detailed Line Survey in the ESF and the ECRB Cross-Drift. (A) Equal-Area Stereonet Plot of Poles to Fracture Planes. (B) Contours of Poles to Fracture Planes Calculated with 1% Area Method.

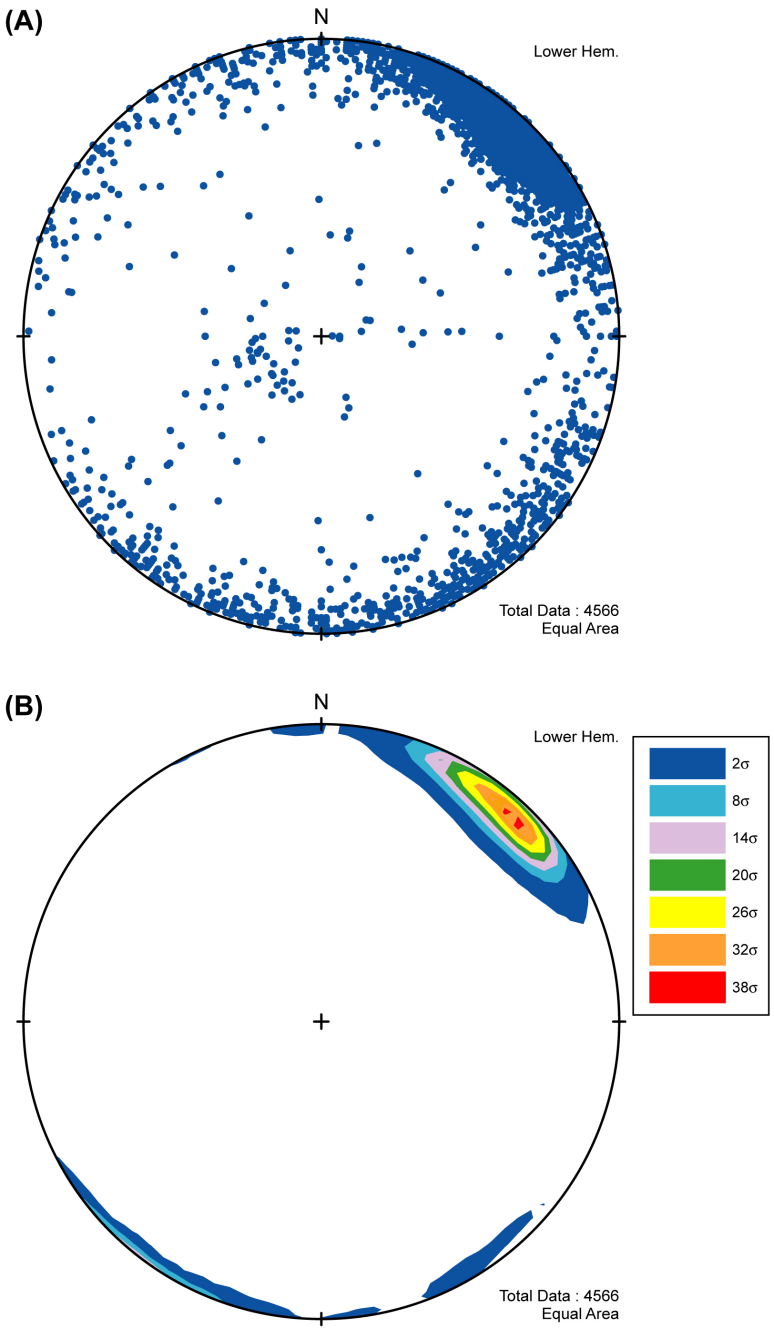

Figure 3-6. Orientation Summary for Fractures from the Intensely Fractured Zone Within the Topopah Spring Tuff Middle Nonlithophysal Zone Recorded by Detailed Line Survey in the ESF (Stations 42+00 to 51+50). (A) Equal-Area Stereonet Plot of Poles to Fracture Planes. (B) Contours of Poles to Fracture Planes Calculated with 1% Area Method.

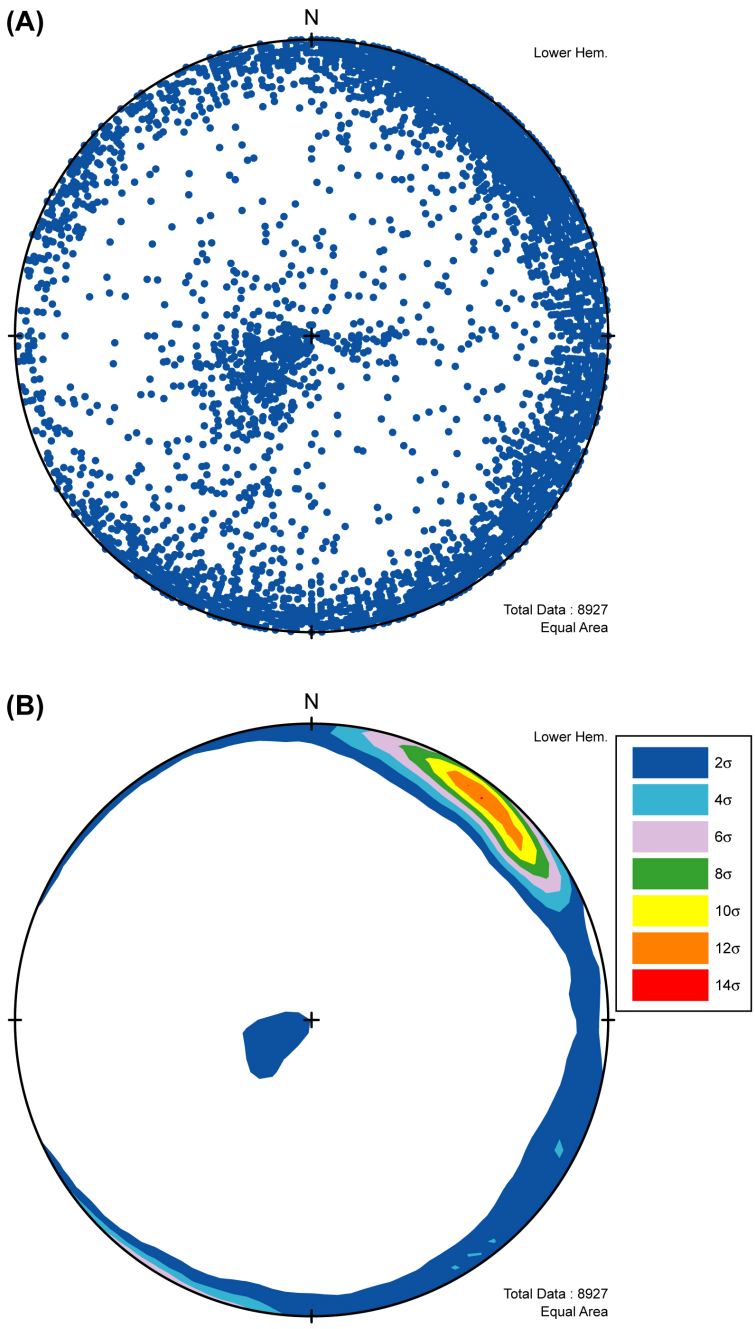

Figure 3-7. Orientation Summary for Fractures from the Topopah Spring Tuff Middle Nonlithophysal Zone (Excluding the Intensely Fractured Zone) Recorded by Detailed Line Survey in the ESF and the ECRB Cross-Drift. (A) Equal-Area Stereonet Plot of Poles to Fracture Planes. (B) Contours of Poles to Fracture Planes Calculated with 1% Area Method.

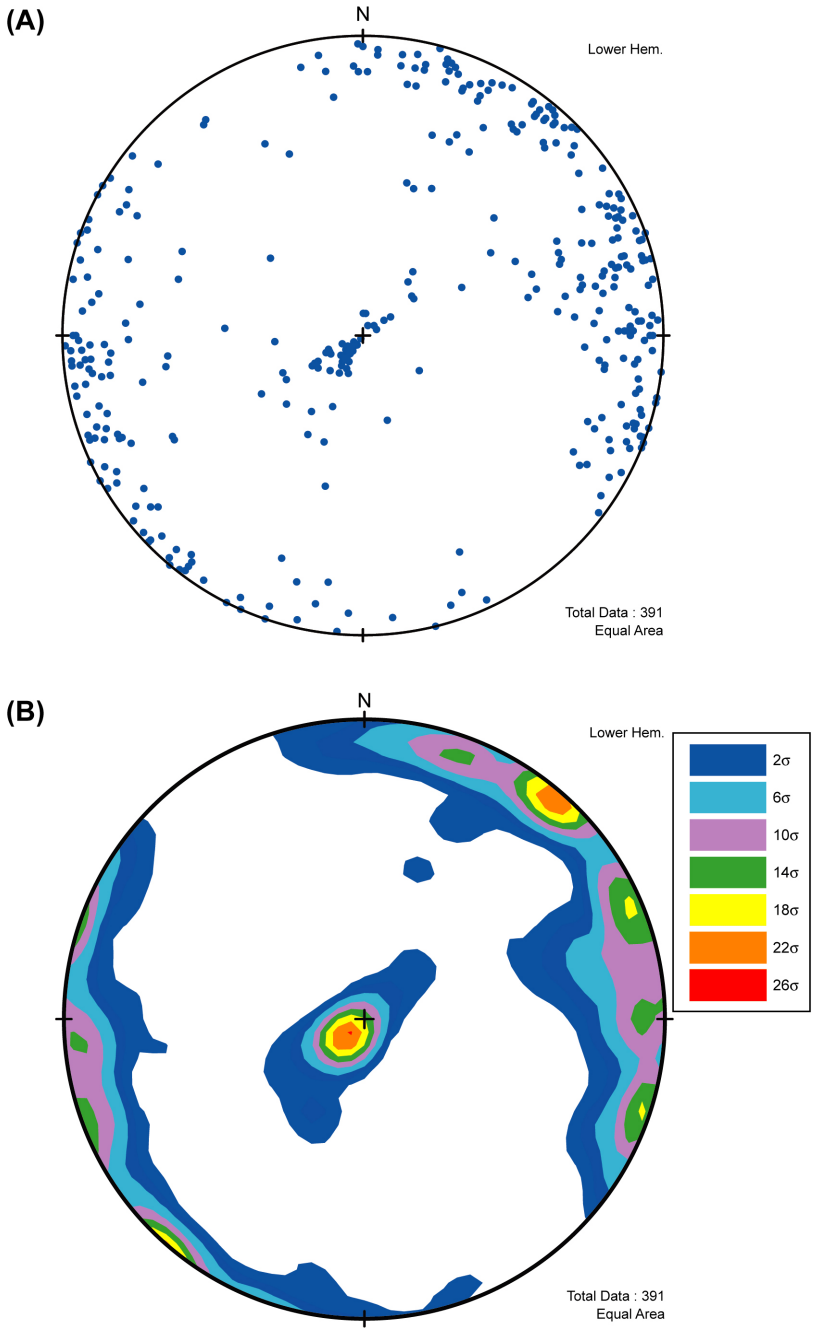

Figure 3-8. Orientation Summary for Small-Scale Fractures from the Topopah Spring Tuff Middle Nonlithophysal Zone Recorded by Detailed Line Survey in the ECRB Cross-Drift. (A) Equal-Area Stereonet Plot of Poles to Fracture Planes. (B) Contours of Poles to Fracture Planes Calculated with the Kamb Method (Kamb, 1959).

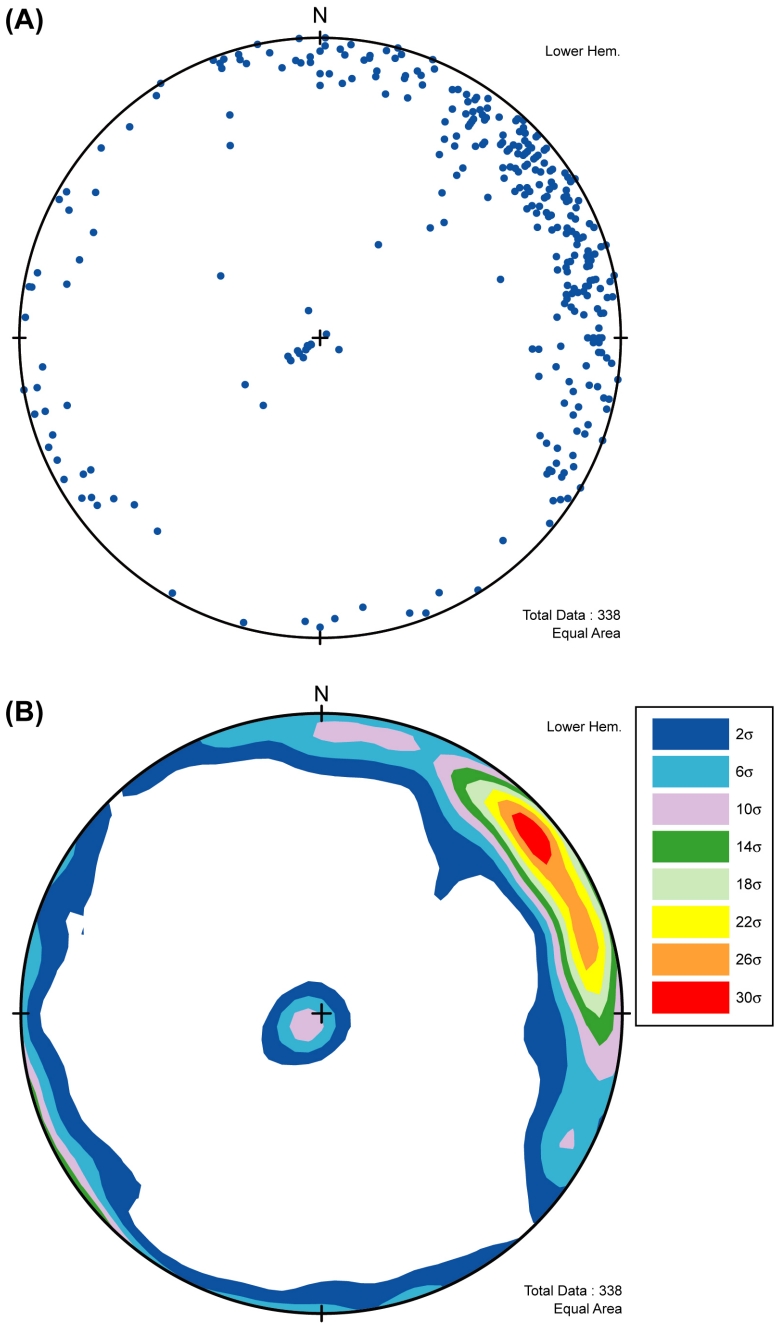

Figure 3-9. Orientation Summary for Fractures from the Topopah Spring Tuff Lower Lithophysal Zone Recorded by Detailed Line Survey in the ESF and the ECRB Cross-Drift. (A) Equal-Area Stereonet Plot of Poles to Fracture Planes. (B) Contours of Poles to Fracture Planes Calculated with the Kamb Method (Kamb, 1959).

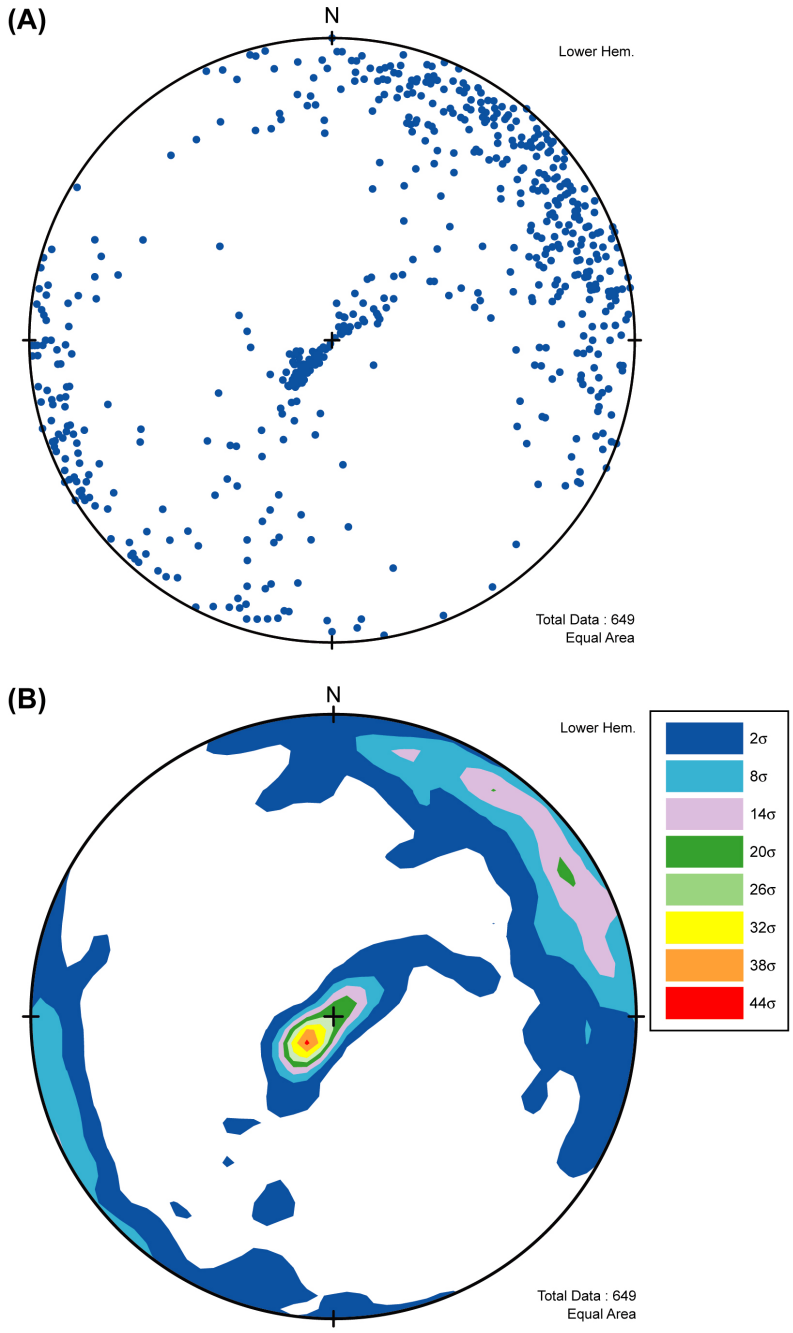

Figure 3-10. Orientation Summary for Small-Scale Fractures from the Topopah Spring Tuff Lower Lithophysal Zone Recorded by Detailed Line Survey in the ECRB Cross-Drift. (A) Equal-Area Stereonet Plot of Poles to Fracture Planes. (B) Contours of Poles to Fracture Planes Calculated with the Kamb Method (Kamb, 1959).

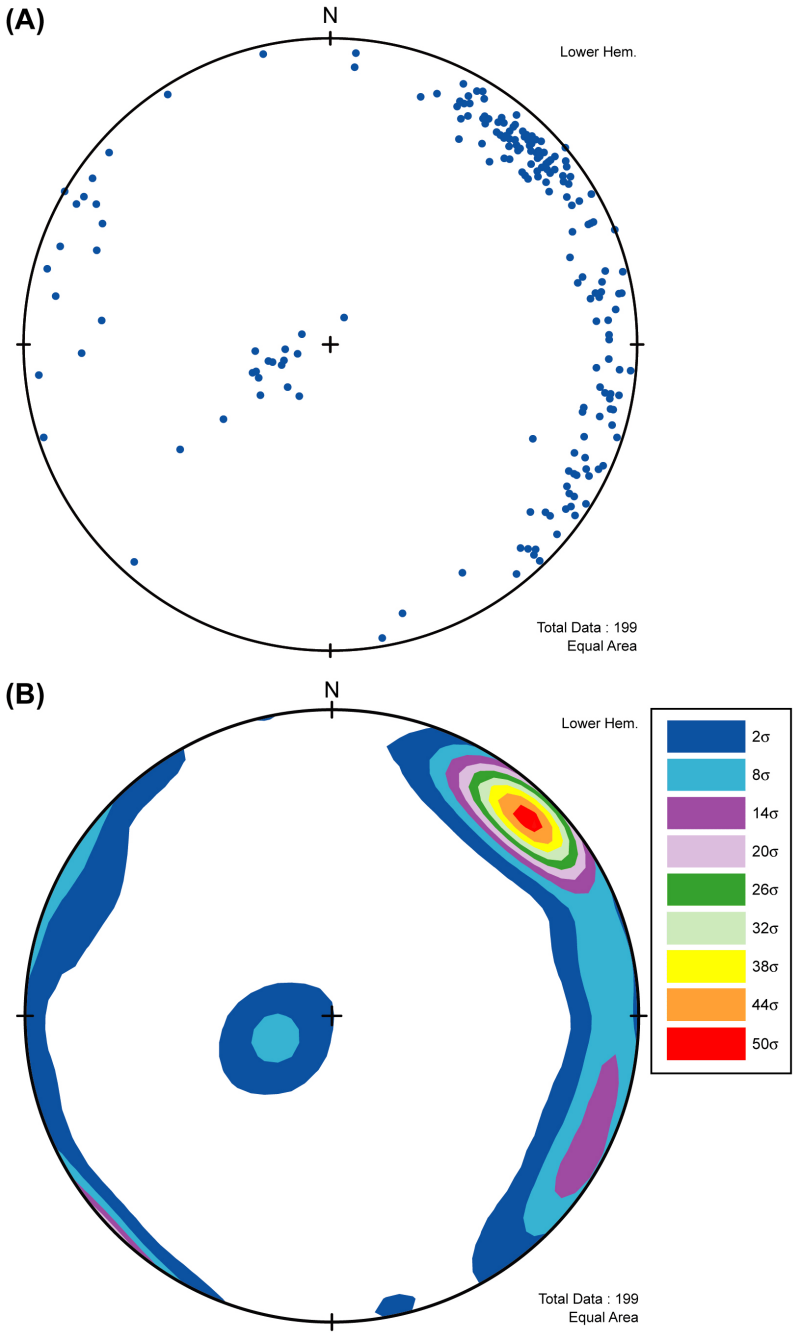

Figure 3-11. Orientation Summary for Fractures from the Topopah Spring Tuff Lower Nonlithophysal Zone Recorded by Detailed Line Survey in the ECRB Cross-Drift. (A) Equal-Area Stereonet Plot of Poles to Fracture Planes. (B) Contours of Poles to Fracture Planes Calculated with the Kamb Method (Kamb, 1959).

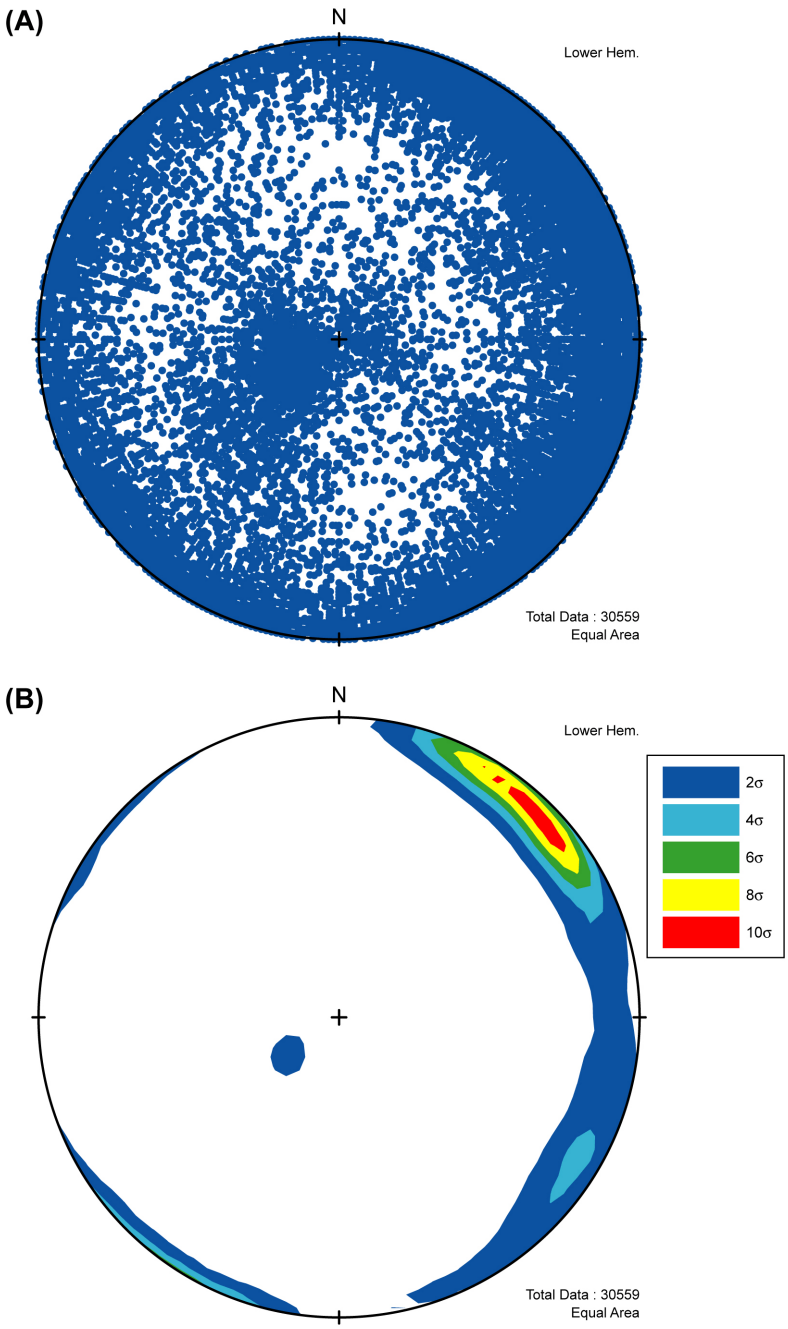

Figure 3-12. Orientation Summary for All Fractures Recorded by Full-Periphery Geologic Mapping in the ESF. (A) Equal-Area Stereonet Plot of Poles to Fracture Planes. (B) Contours of Poles to Fracture Planes Calculated with 1% Area Method.

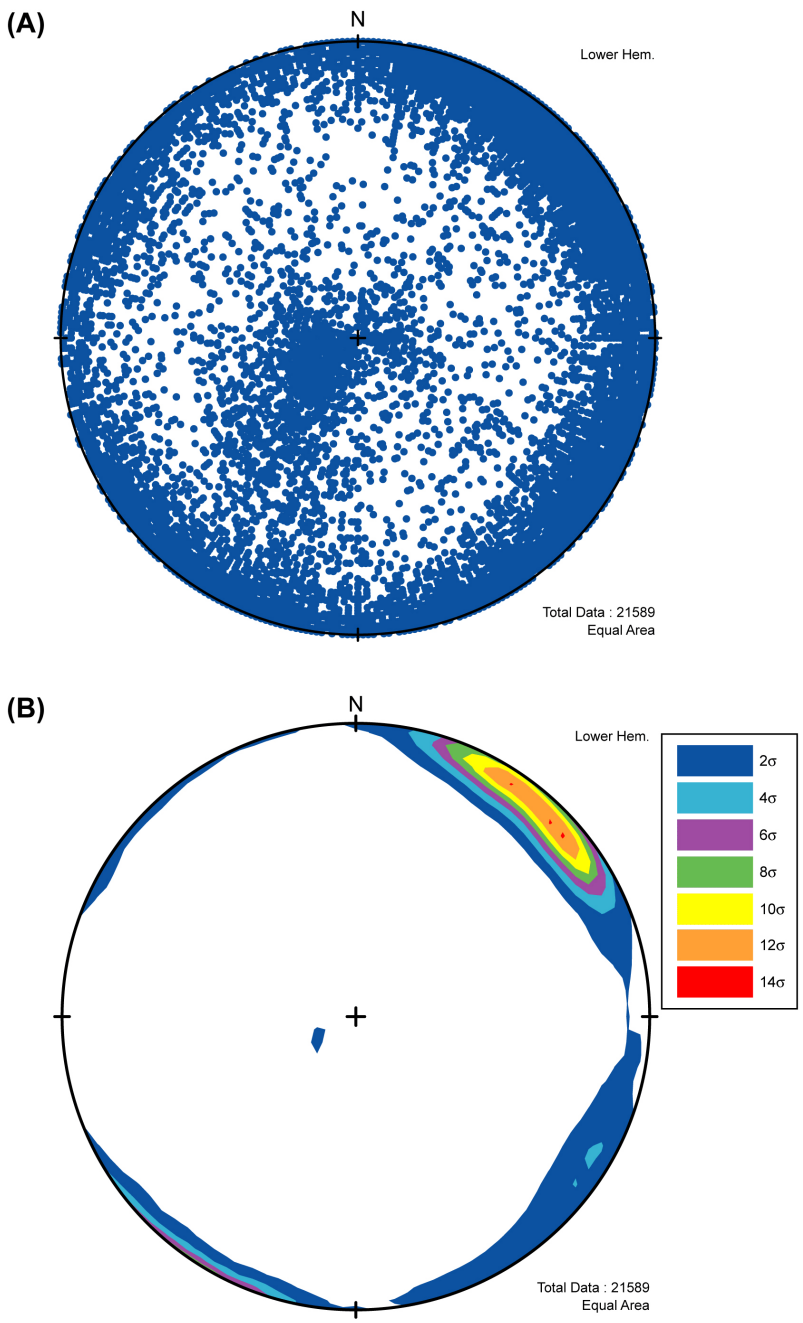

Figure 3-13. Orientation Summary for Fractures Recorded by Full-Periphery Geologic Mapping in the ESF from the Topopah Spring Tuff Upper Lithophysal, Middle Nonlithophysal, and Lower Lithophysal Zones. (A) Equal-Area Stereonet Plot of Poles to Fracture Planes. (B) Contours of Poles to Fracture Planes Calculated with 1% Area Method.

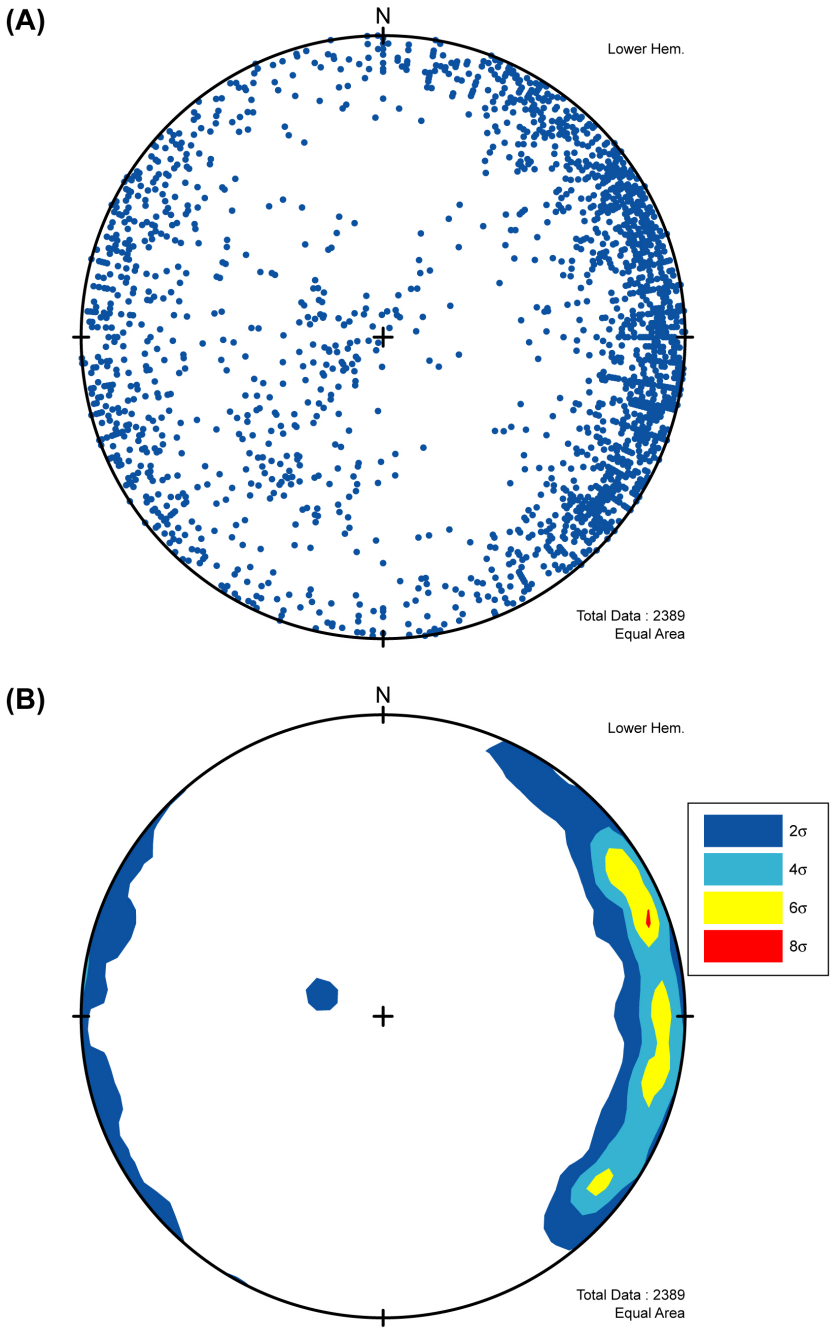

Figure 3-14. Orientation Summary for Fractures Recorded by Full-Periphery Geologic Mapping in the ESF from the Topopah Spring Tuff Upper Lithophysal Zone. (A) Equal-Area Stereonet Plot of Poles to Fracture Planes. (B) Contours of Poles to Fracture Planes Calculated with 1% Area Method.

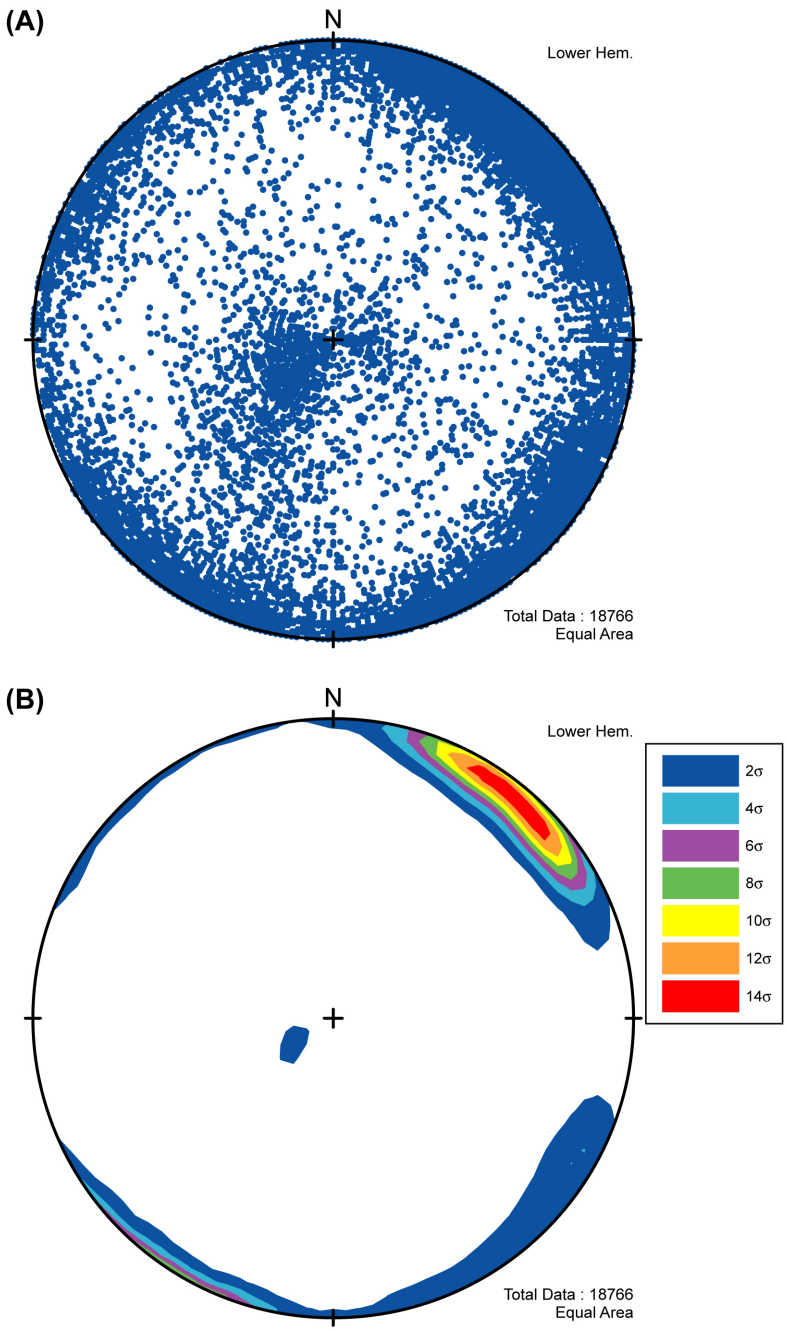

Figure 3-15. Orientation Summary for Fractures Recorded by Full-Periphery Geologic Mapping in the ESF from the Topopah Spring Tuff Middle Nonlithophysal Zone. (A) Equal-Area Stereonet Plot of Poles to Fracture Planes. (B) Contours of Poles to Fracture Planes Calculated with 1% Area Method.

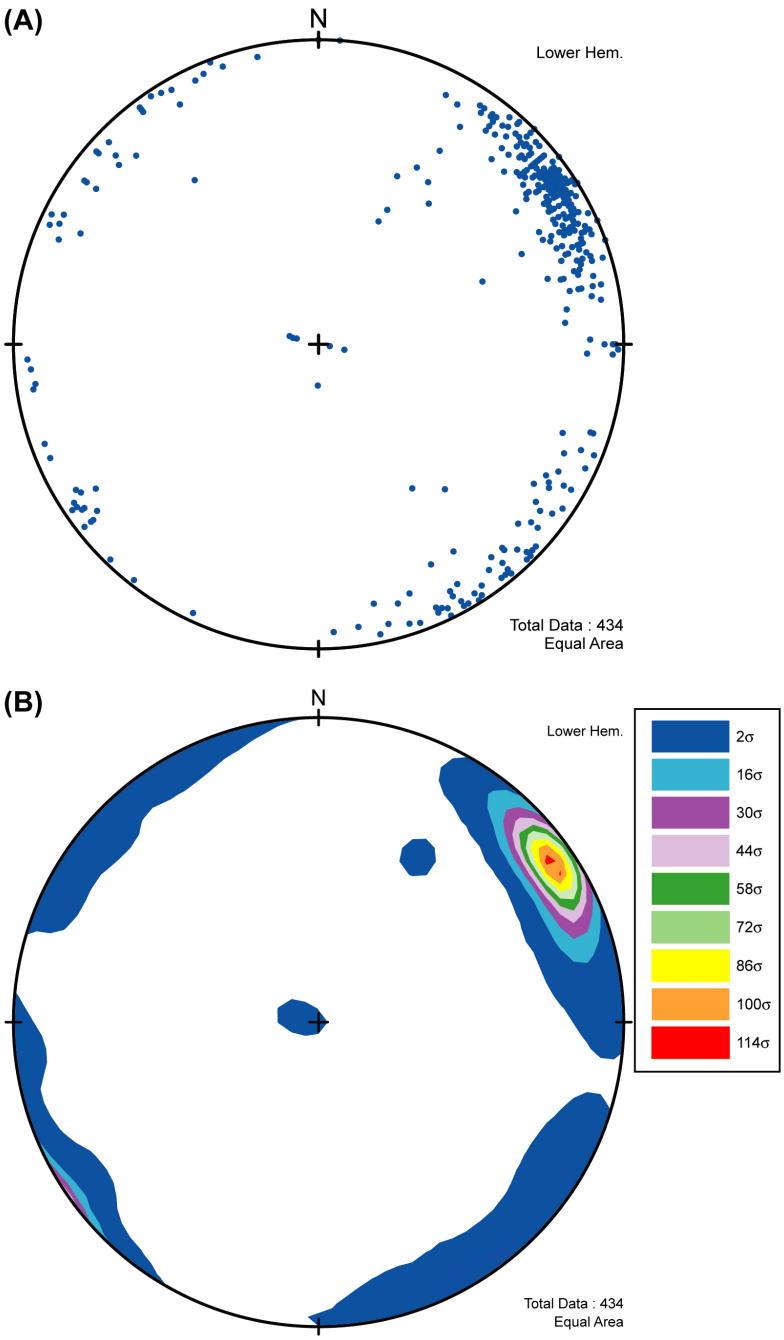

Figure 3-16. Orientation Summary for Fractures Recorded by Full-Periphery Geologic Mapping in the ESF from the Topopah Spring Tuff Lower Lithophysal Zone. (A) Equal-Area Stereonet Plot of Poles to Fracture Planes. (B) Contours of Poles to Fracture Planes Calculated with the Kamb Method (Kamb, 1959).

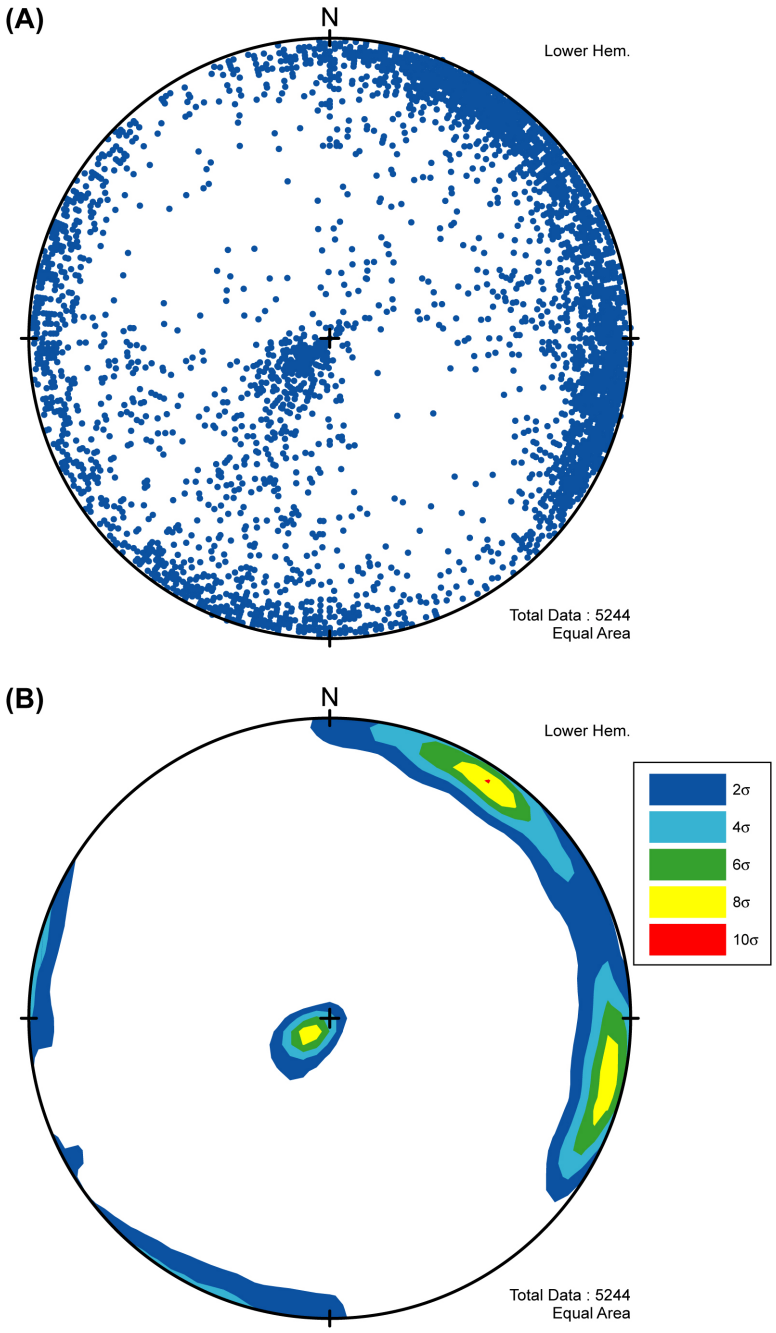

Figure 3-17. Orientation Summary for Fractures Recorded by Full-Periphery Geologic Mapping in the ECRB Cross-Drift. (A) Equal-Area Stereonet Plot of Poles to Fracture Planes. (B) Contours of Poles to Fracture Planes Calculated with 1% Area Method.

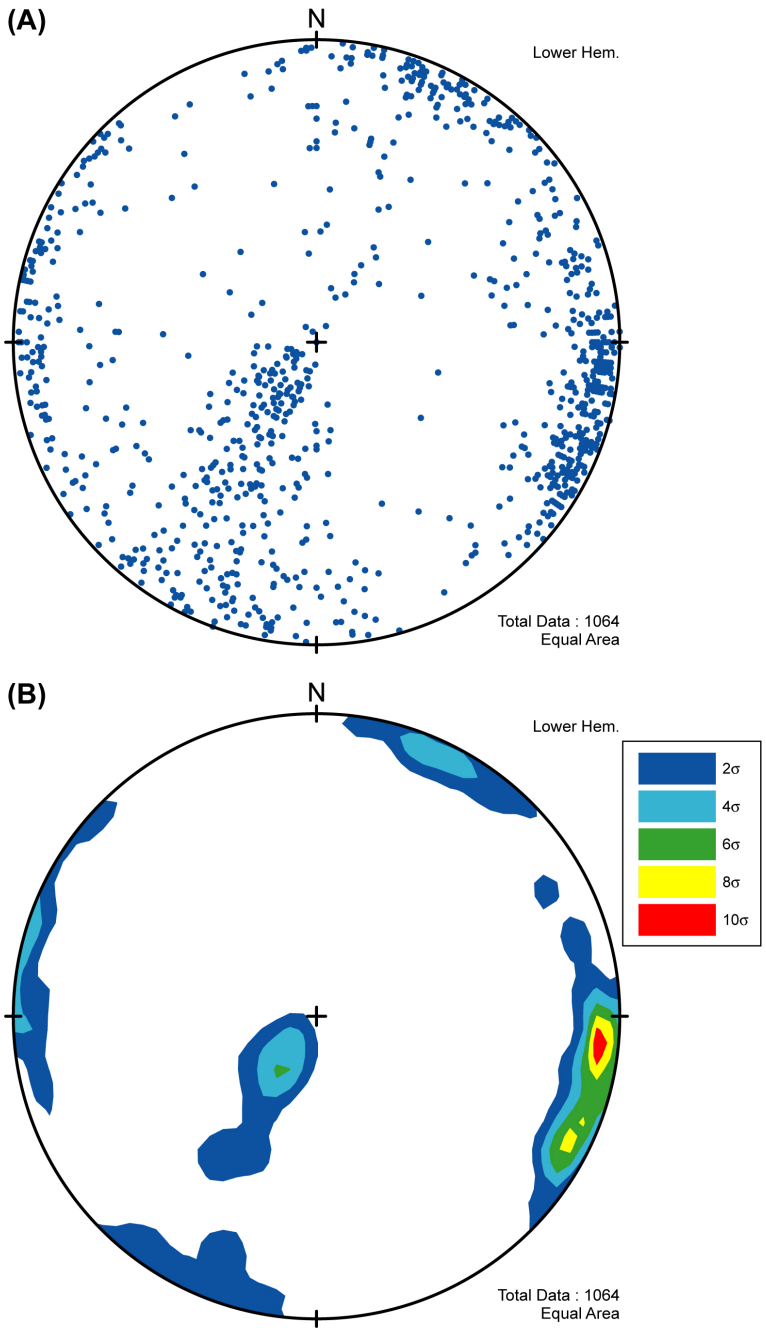

Figure 3-18. Orientation Summary for Fractures from the Topopah Spring Tuff Upper Lithophysal Zone Recorded by Full-Periphery Geologic Mapping in the ECRB Cross-Drift. (A) Equal-Area Stereonet Plot of Poles to Fracture Planes. (B) Contours of Poles to Fracture Planes Calculated with 1% Area Method.

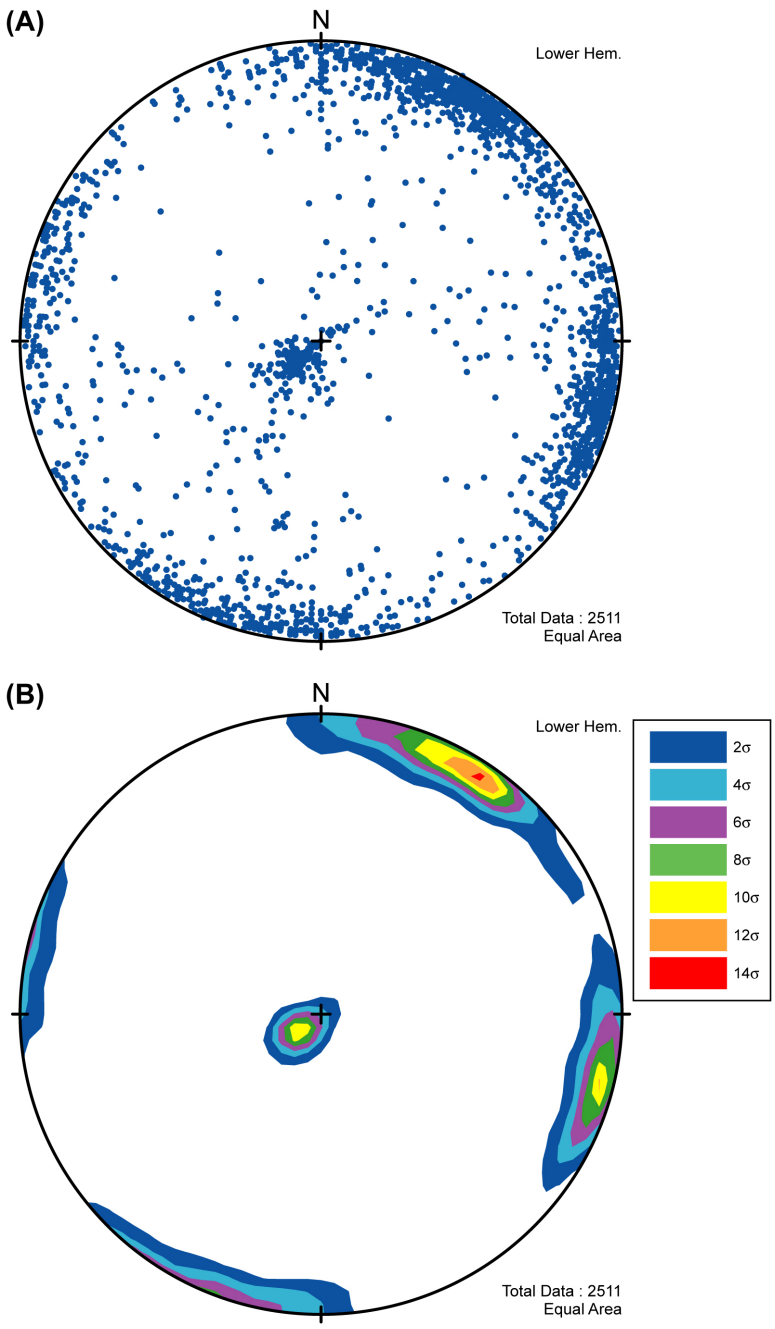

Figure 3-19. Orientation Summary for Fractures from the Topopah Spring Tuff Middle Nonlithophysal Zone Recorded by Full-Periphery Geologic Mapping in the ECRB Cross-Drift. (A) Equal-Area Stereonet Plot of Poles to Fracture Planes. (B) Contours of Poles to Fracture Planes Calculated with 1% Area Method.

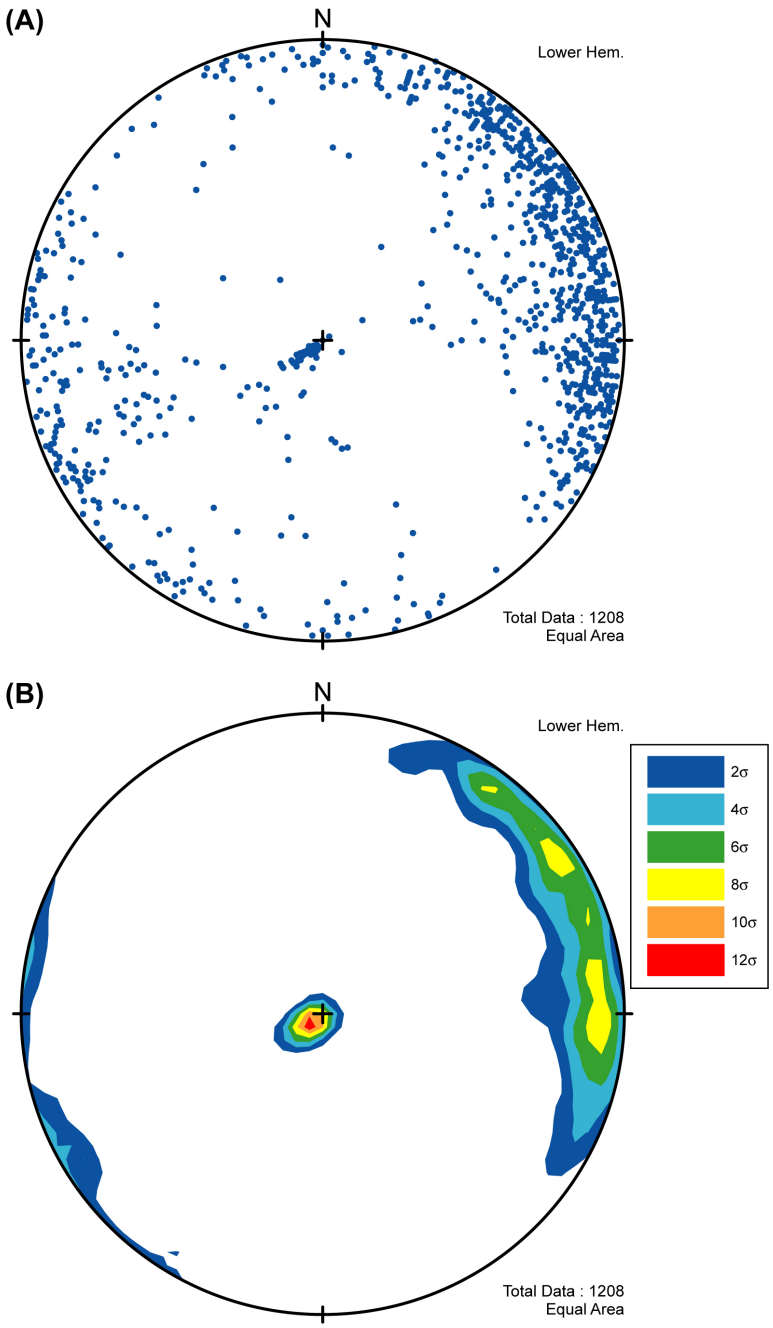

Figure 3-20. Orientation Summary for Fractures from the Topopah Spring Tuff Lower Lithophysal Zone Recorded by Full-Periphery Geologic Mapping in the ECRB Cross-Drift. (A) Equal-Area Stereonet Plot of Poles to Fracture Planes. (B) Contours of Poles to Fracture Planes Calculated with 1% Area Method.

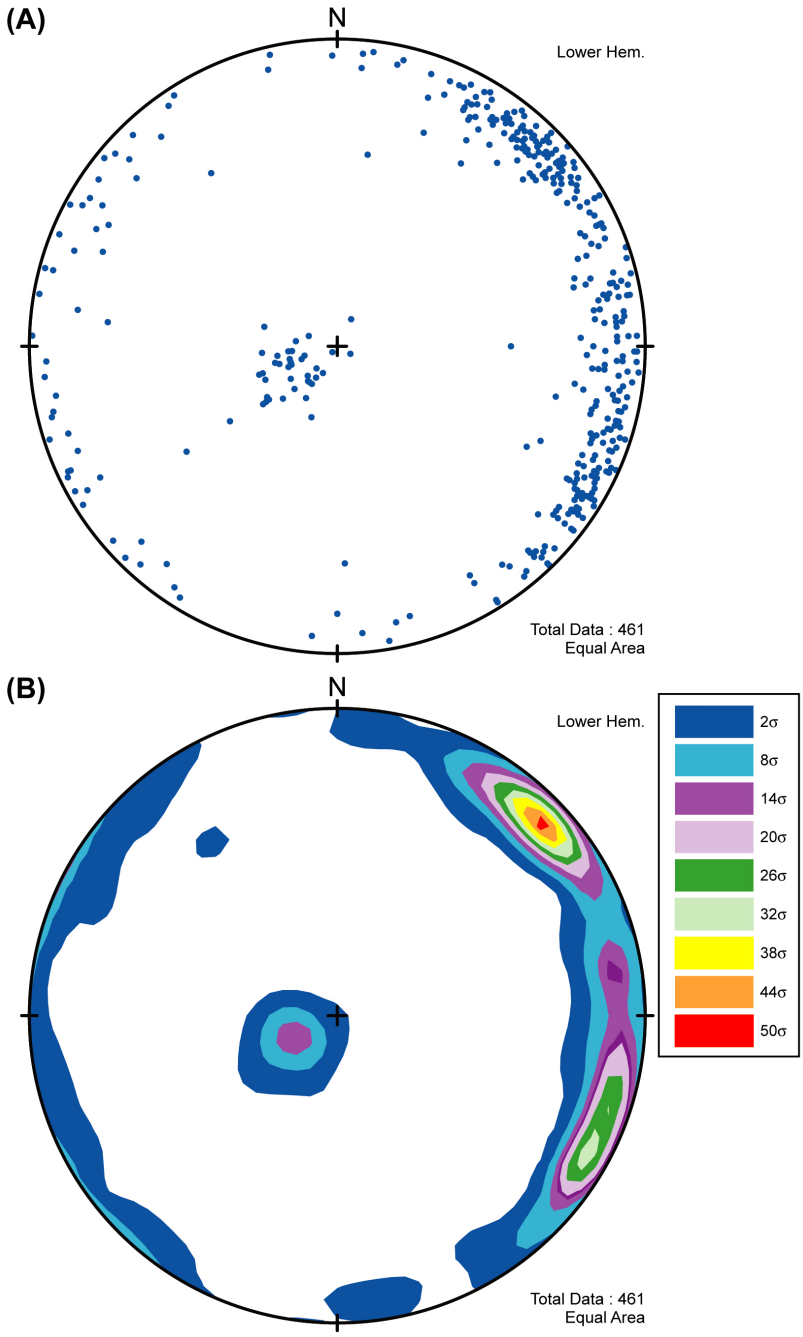

Figure 3-21. Orientation Summary for Fractures from the Topopah Spring Tuff Lower Nonlithophysal Zone Recorded by Full-Periphery Geologic Mapping in the ECRB Cross-Drift. (A) Equal-Area Stereonet Plot of Poles to Fracture Planes. (B) Contours of Poles to Fracture Planes Calculated with the Kamb Method (Kamb, 1959).

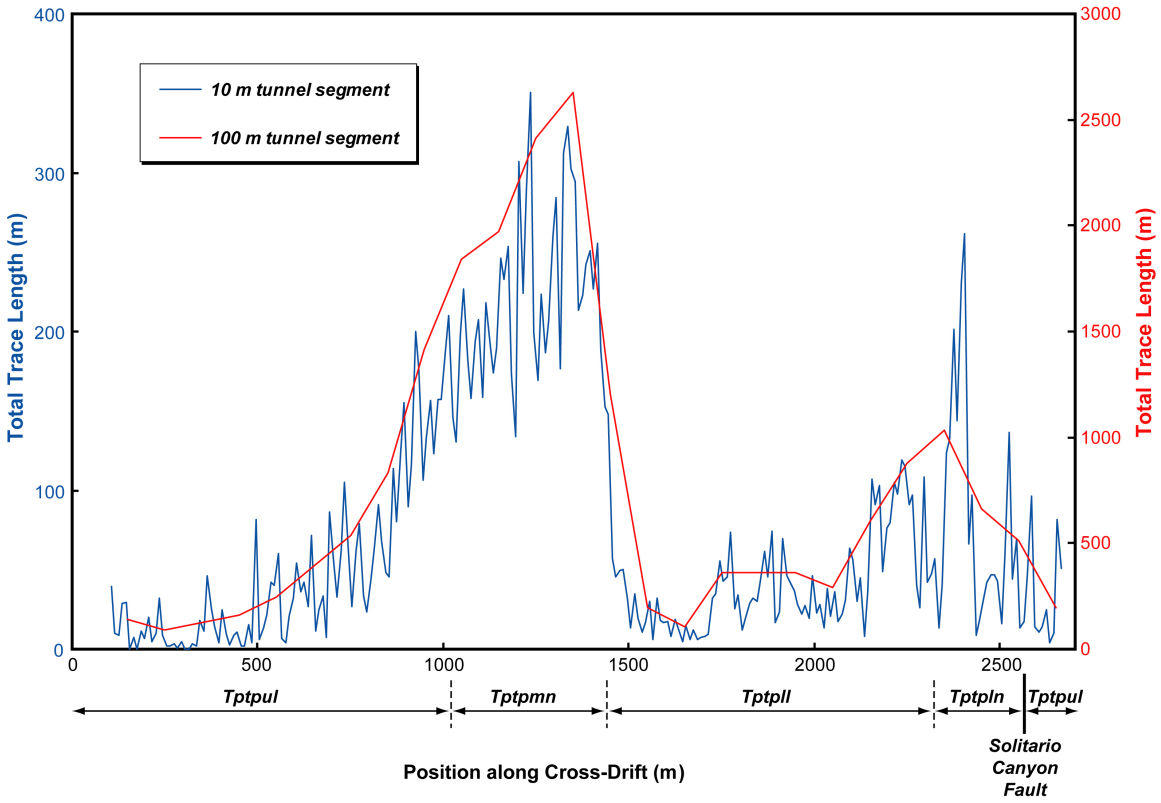

Figure 3-22. Fracture Trace Length Summary. Total Trace Length for 10 m [33 ft] and 100 m [328 ft] Segments of the ECRB Cross-Drift as Determined from Full-Periphery Geologic Mapping Data. Abbreviations for the Topopah Spring Tuff Zones: *Tptpul* = Upper Lithophysal; *Tptpmn* = Middle Nonlithophysal; *Tptpll* = Lower Lithophysal; *Tptpln* = Lower Nonlithophysal.

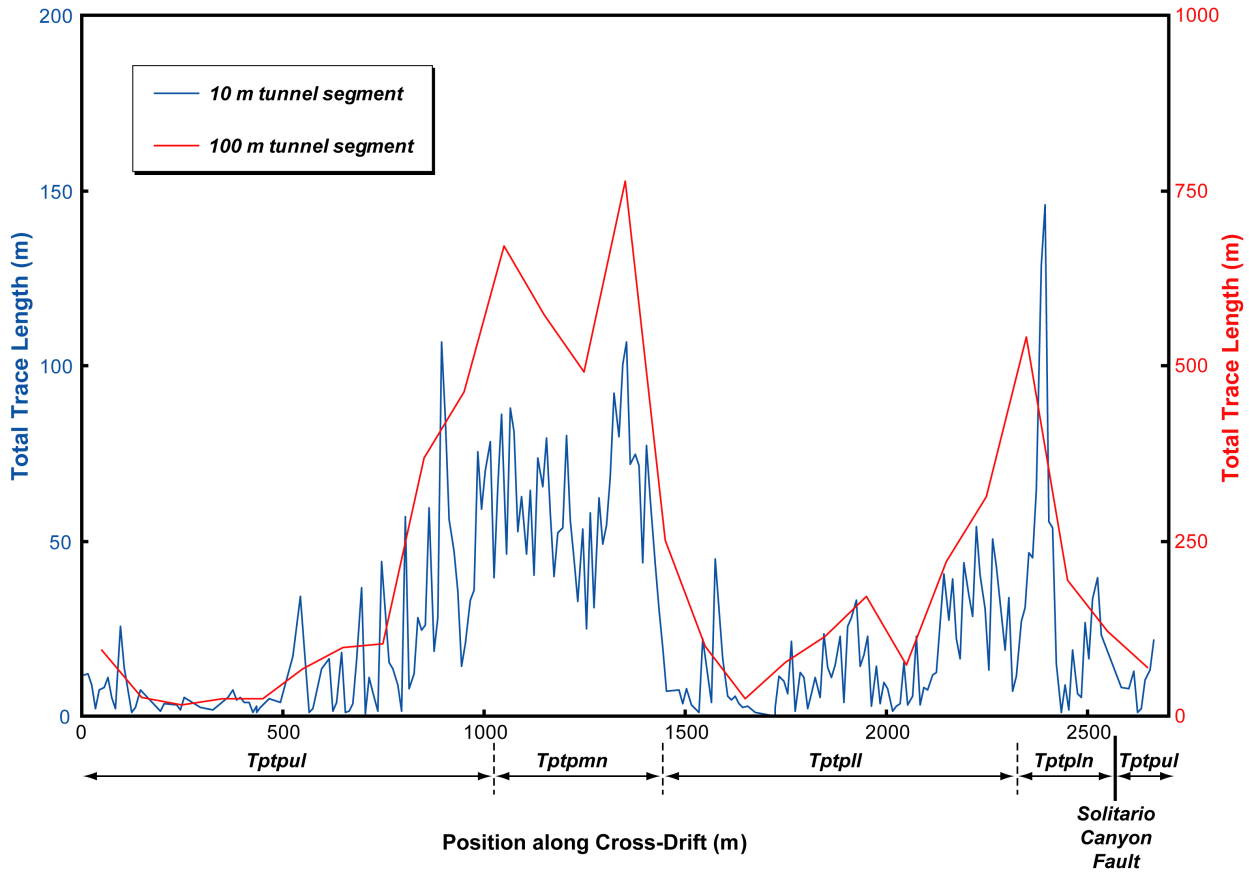

Figure 3-23. Fracture Trace Length Summary. Total Trace Length for 10 m [33 ft] and 100 m [328 ft] Segments of the ECRB Cross-Drift as Determined from Detailed Line Survey Data. Abbreviations Are the Same as Shown in Figure 3-22.

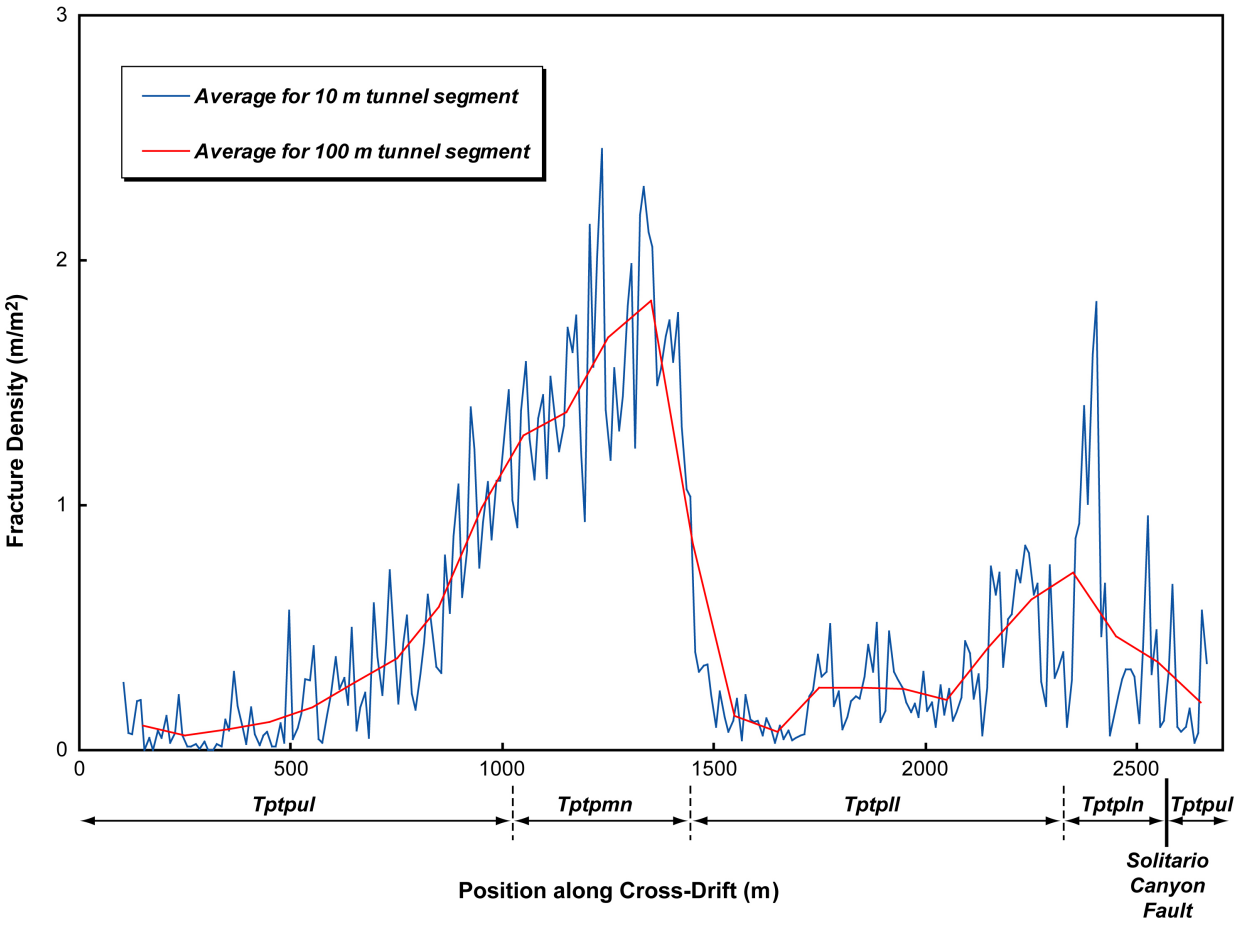

Figure 3-24. Fracture Density Summary. Total Trace Length Per Unit Area (Or P_{21}) Averaged Over 10 m [33 ft] and 100 m [328 ft] Segments of the ECRB Cross-Drift as Determined from Full-Periphery Geologic Mapping Data. Abbreviations Are the Same as Shown in Figure 3-22.

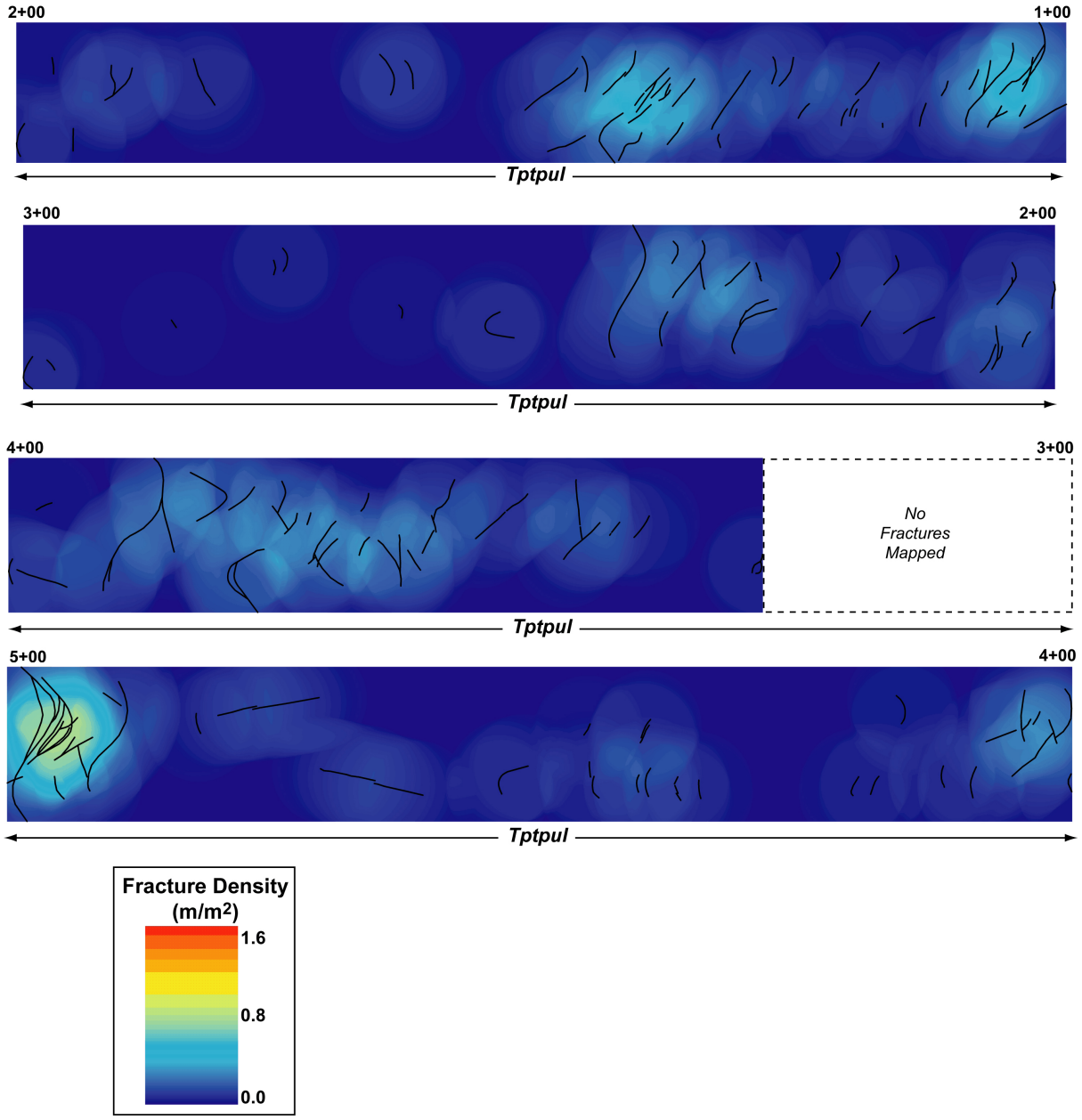

Figure 3-25. Fracture Density Contours Superimposed over Fracture Traces from Full-Periphery Geologic Mapping in the ECRB Cross-Drift for Stations 1+00 to 5+00. Fracture Density Is Calculated as Total Trace Length Per Unit Area (Or P_{21}) Within ArcGIS Based on a 5-m [16-ft]-Diameter Search Radius. Abbreviations Are the Same as Shown in Figure 3-22.

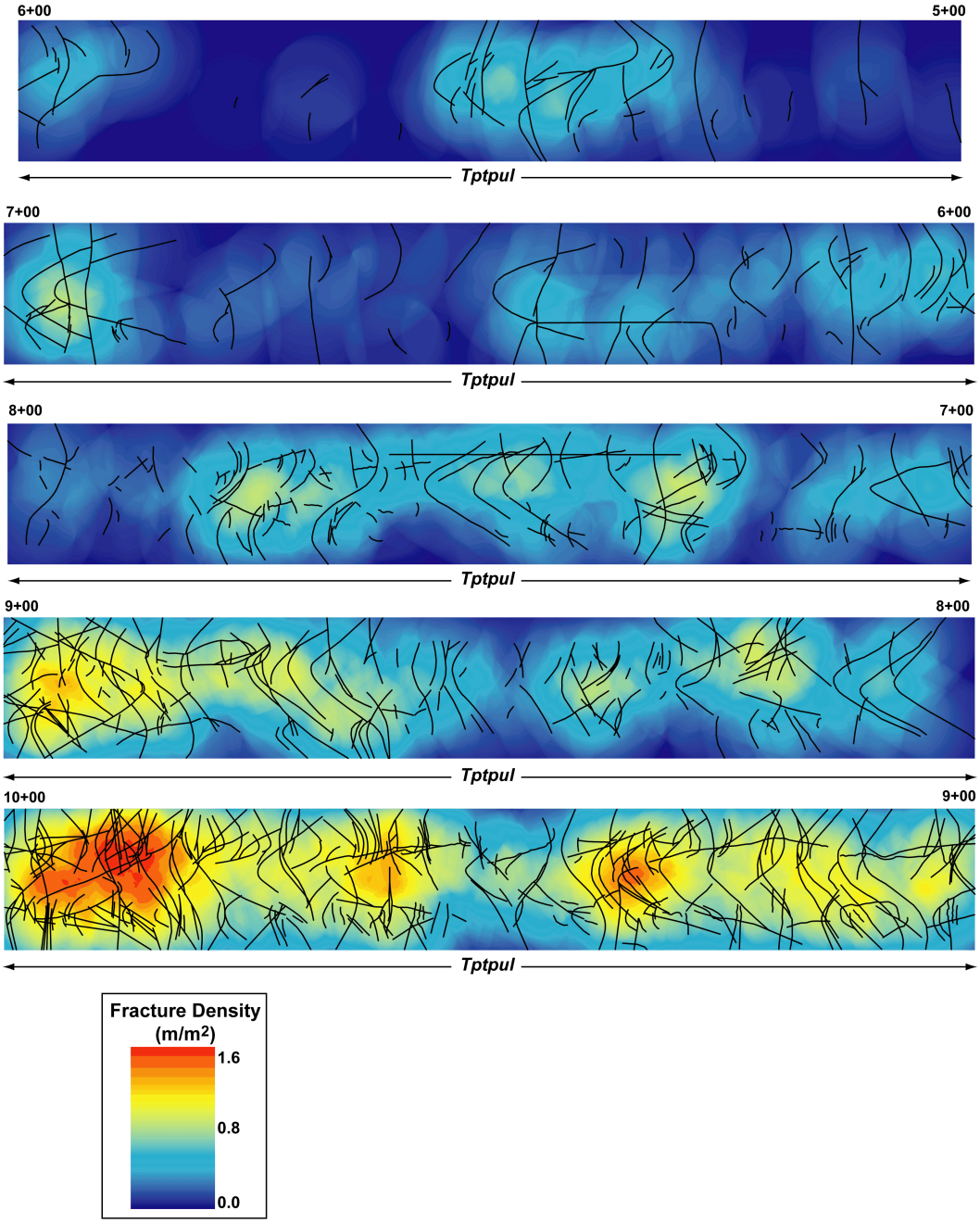

Figure 3-26. Fracture Density Contours Superimposed over Fracture Traces from Full-Periphery Geologic Mapping in the ECRB Cross-Drift for Stations 5+00 to 10+00. Fracture Density Is Calculated as Total Trace Length Per Unit Area (Or P_{21}) Within ArcGIS Based on a 5-m [16-ft]-Diameter Search Radius. Abbreviations Are the Same as Shown in Figure 3-22.

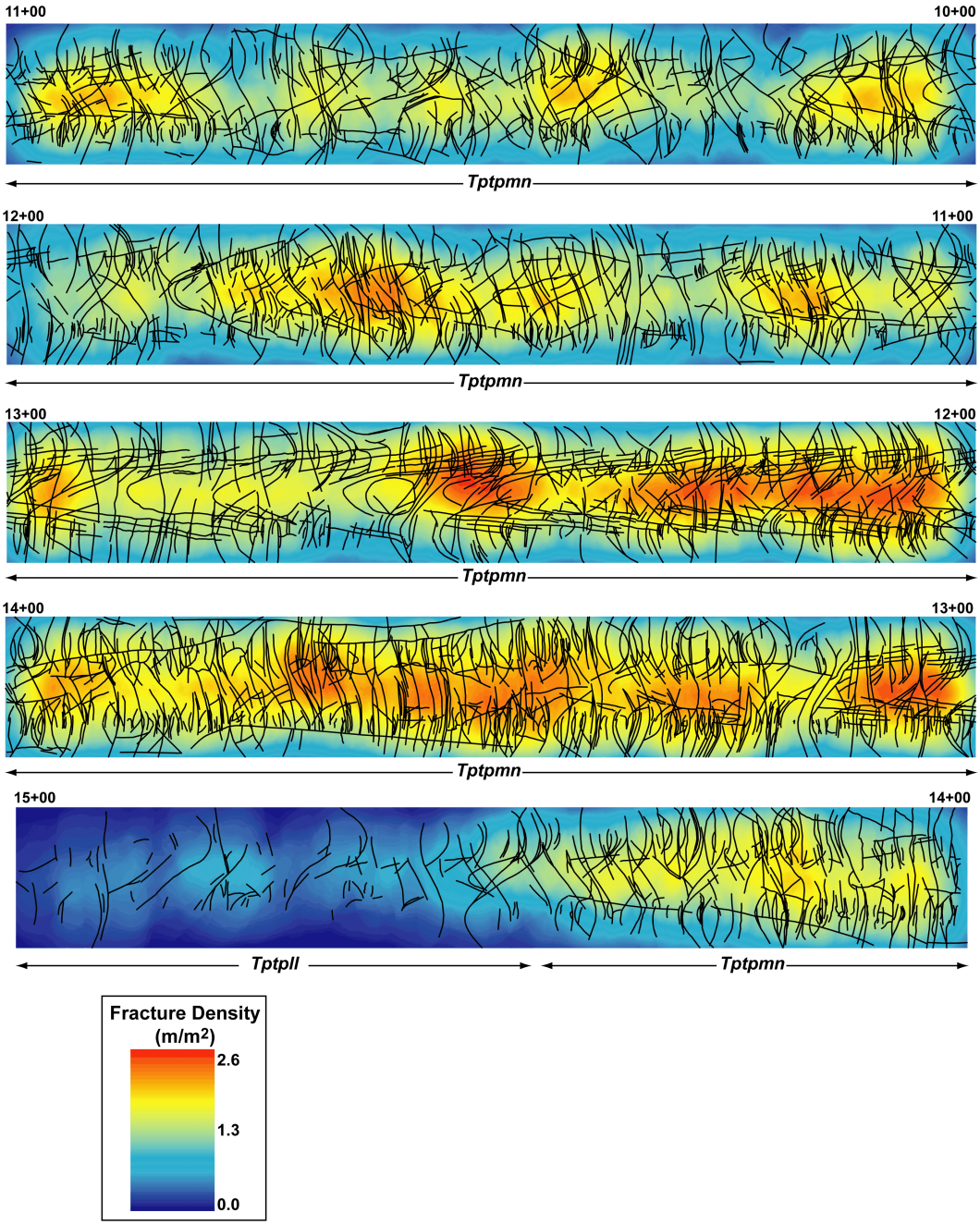

Figure 3-27. Fracture Density Contours Superimposed Over Fracture Traces from Full-Periphery Geologic Mapping in the ECRB Cross-Drift for Stations 10+00 to 15+00. Fracture Density Is Calculated as Total Trace Length Per Unit Area (Or P_{21}) Within ArcGIS Based On a 5-m [16-ft]-Diameter Search Radius. Abbreviations Are the Same as Shown in Figure 3-22.

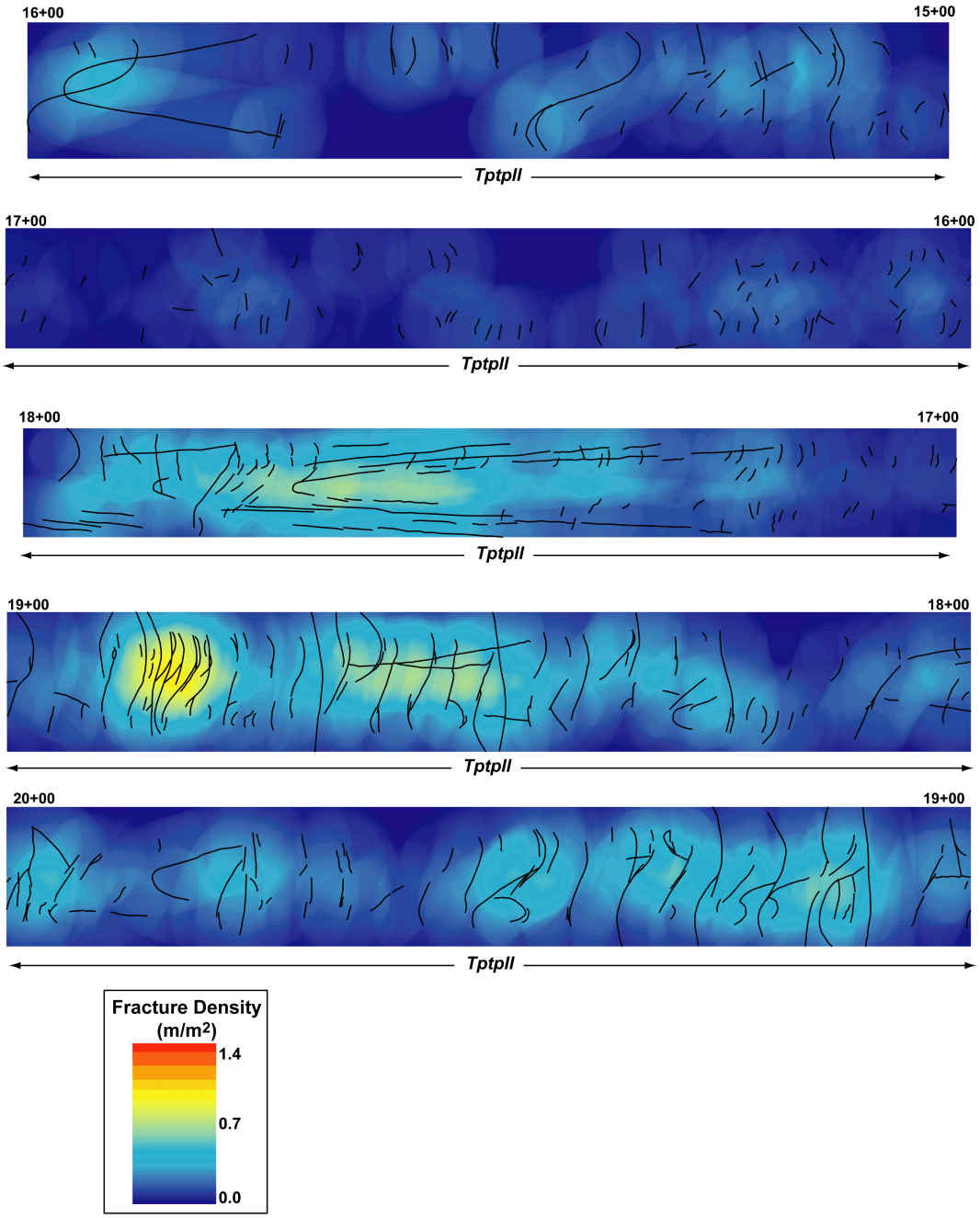

Figure 3-28. Fracture Density Contours Superimposed Over Fracture Traces from Full-Periphery Geologic Mapping in the ECRB Cross-Drift for Stations 15+00 to 20+00. Fracture Density Is Calculated as Total Trace Length Per Unit Area (Or P_{21}) Within ArcGIS Based On a 5-m [16-ft]-Diameter Search Radius. Abbreviations Are the Same as Shown in Figure 3-22.

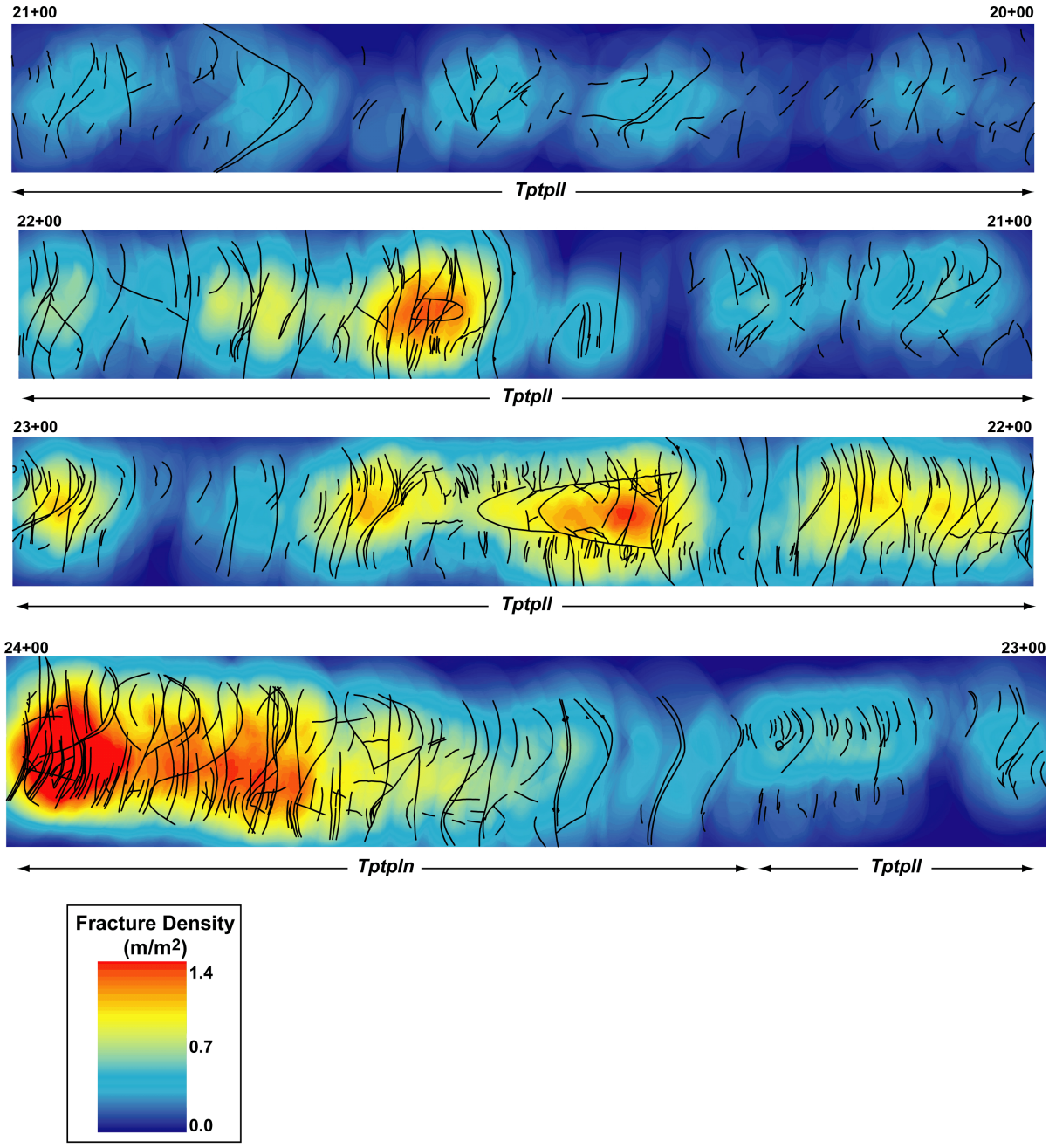

Figure 3-29. Fracture Density Contours Superimposed Over Fracture Traces from Full-Periphery Geologic Mapping in the ECRB Cross-Drift for Stations 20+00 to 24+00. Fracture Density Is Calculated as Total Trace Length Per Unit Area (Or P_{21}) Within ArcGIS Based On a 5-m [16-ft]-Diameter Search Radius. Abbreviations Are the Same as Shown in Figure 3-22.

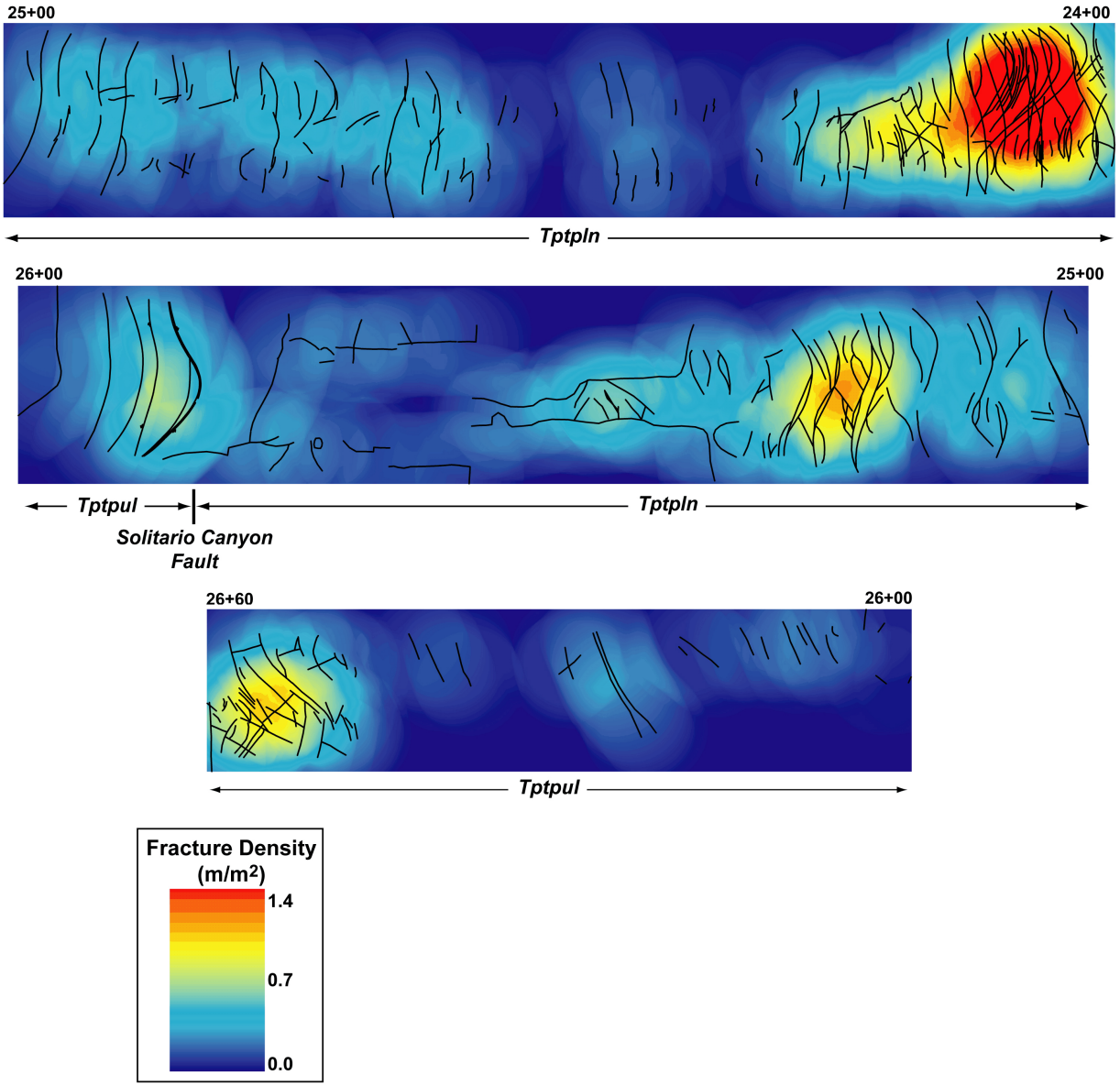

Figure 3-30. Fracture Density Contours Superimposed Over Fracture Traces from Full-Periphery Geologic Mapping in the ECRB Cross-Drift for Stations 24+00 to 26+60. Fracture Density Is Calculated as Total Trace Length Per Unit Area (Or P_{21}) Within ArcGIS Based On a 5-m [16-ft]-Diameter Search Radius. Abbreviations Are the Same as Shown in Figure 3-22.

4 GENERATION AND ANALYSIS OF SYNTHETIC FRACTURE POPULATIONS

Synthetic fracture populations were generated with the commercial software program FracMan (Golder Associates, Inc., 2002, 1998) as part of drift degradation analyses (Bechtel SAIC Company, LLC, 2004b). The synthetic fractures are based upon fracture characteristics derived from the detailed line survey data collected at Yucca Mountain. The primary use for the synthetic fractures is as input for numerical geomechanical analyses of the effects of thermal-and seismic-loading on rockfall and drift stability. As part of this study of the subsurface fracture data from Yucca Mountain, FracMan analyses were conducted for the Middle Nonlithophysal and Lower Lithophysal zones based on the input values that were used by DOE (Bechtel SAIC Company, LLC, 2004b; see Figures 6-18 and B–3). Because the generation of synthetic fractures in FracMan is a stochastic process, two tests were performed with different seed numbers for each zone.

4.1 FracMan Analyses for the Middle Nonlithophysal Zone

For the Middle Nonlithophysal zone, DOE generated synthetic fractures that represent seven different sets (Figure 4-1): (i) two northwest-striking subvertical sets—one for long fractures (set S1l) and one for short fractures (set S1s), (ii) two northeast-striking subvertical sets—one for long fractures (set S2l) and one for short fractures (set S2s), (iii) two northwest-striking sets that dip moderately to the northeast—one for long fractures (set S3l) and one for short fractures (set S3s), and (iv) one subhorizontal set (set VPP). The rationale for generating both long and short fractures was that early formed fractures would be longer than later fractures (Bechtel SAIC Company, LLC, 2004b).

For analysis, synthetic fractures were generated within a 100 m × 100 m × 100 m [328 ft × 328 ft × 328 ft] cube using the DOE input parameters (Figure 4-1). The fracture populations generated for both test cases are characterized by three statistically distinctive fracture sets (Tables 4-1 and 4-2; Figures 4-1 thru 4-3). The northwest-striking, steeply southwest-dipping sets (i.e., sets 1 and 5) are most abundant, but the northeast-striking, steeply northwest-dipping sets (i.e., sets 2 and 6) are also present. The northwest-striking sets (i.e., sets 3 and 7) dip moderately (i.e., ~45°) to the northeast. This third set is somewhat surprising because it is not represented in the natural fracture populations recorded from the Topopah Spring Middle Nonlithophysal zone (c.f., Figures 3-5 and 3-7). Although the FracMan input data contain a subhorizontal set (i.e., set 4) and FracMan generates fractures with this orientation (representing 11 percent of the total population), the overall synthetic fracture population does not contain a statistically significant component of subhorizontal fractures.

The size of synthetic fractures in the FracMan simulations is controlled by the power law distribution specified in the input file for the fracture radius. An exponent of 3.5 was selected by DOE (Bechtel SAIC Company, LLC, 2004b) for all fracture sets, and the size equivalent radius was assigned a value of 1 for all sets. The subhorizontal fractures were left unbounded (i.e., distribution was not truncated). The short subvertical and intermediate-dip fractures (i.e., sets 1, 2, and 3) were produced with a minimum radius of 1 m [3.3 ft] and a maximum of 8 m [26.2 ft]. The long fractures (i.e., sets 5, 6, and 7) had a minimum of 4 m [13.1 ft] and a maximum of 50 m [164.1 ft]. Fracture radius distributions from the resulting synthetic fracture populations are characterized by a large positive skew (Figures 4-4 and 4-5). Fracture sets 1

through 4 for both test cases have mean radii of approximately 1.6 m [5.6 ft] and median radii of approximately 1.3 m [4.3 ft] (Tables 4-1 and 4-2). The long fracture sets (i.e., sets 5, 6, and 7) have mean radii of >6 m [>20 ft] and median radii of >5 m [>16 ft].

To extract linear fracture intensity (i.e., the number of fractures per unit length), nine simulated 1-m-diameter [3.3-ft-diameter] and 100-m [328-ft]-long boreholes were sampled through each cube of synthetic fractures. The synthetic boreholes were defined to be horizontal with a trend of 071° so as to be parallel to the planned emplacement drift orientation. This method is advantageous because FracMan provides the linear fracture intensity as a direct output when using the borehole sampling strategy and this measure can be compared to intensity values derived from the detailed line surveys. The average linear intensity based on all fracture sets is 1.42 m^{-1} [0.43 ft^{-1}] for test 1 and 1.46 m^{-1} [0.44 ft^{-1}] for test 2. Intensity values for individual fracture sets are smaller (as expected) and quite variable (Tables 4-1 and 4-2). The range for test 1 is 0.04 to 0.38 m^{-1} [0.01 to 0.12 ft^{-1}], and the range for test 2 is 0.06 to 0.36 m^{-1} [0.02 to 0.11 ft^{-1}].

Table 4-1. Summary of Fracman®-Generated Synthetic Fracture Data for the Topopah Spring Tuff Middle Nonlithophysal Zone (Test 1). Linear Fracture Intensity Is the Number of Fractures Per Unit Length Determined from Borehole Sampling of the Synthetic Fracture Population. Areal Fracture Intensity Is the Total Fracture Trace Length Per Unit Area Determined from Tunnel Sampling of the Synthetic Fracture Population. An Expanded Data Table That Include Standard Deviations for Fracture Radius is Included in Appendix Table B–1.

Set	Number and Percentage	Mean Orientation (Strike/Dip)	Fisher Dispersion Coefficient*	Fracture Radius, m [ft]		Linear Fracture Intensity, m^{-1} [ft^{-1}]	Areal Fracture Intensity, m/m^2 [ft/ft^2]
				Mean	Median		
All	99285, 100%	*n.a.*	*n.a.*	*n.a.*	*n.a.*	1.42 [0.43]	1.29 [0.39]
1	40062, 40%	123°/84°	10.408	1.60 [5.25]	1.32 [4.33]	0.36 [0.11]	0.37 [0.11]
2	31964, 32%	217°/86°	7.649	1.60 [5.25]	1.31 [4.30]	0.18 [0.05]	0.24 [0.07]
3	10532, 11%	299°/43°	27.525	1.60 [5.25]	1.32 [4.33]	0.04 [0.01]	0.08 [0.02]
4	13146, 13%	298°/47°	5.097	1.65 [5.41]	1.31 [4.30]	0.08 [0.02]	0.10 [0.03]
5	1152, 1%	123°/84°	9.984	6.76 [22.18]	5.40 [17.72]	0.38 [0.12]	0.20 [0.06]
6	1304, 1%	217°/87°	9.005	6.77 [22.21]	5.32 [17.45]	0.24 [0.07]	0.19 [0.06]
7	1125, 1%	324°/07°	25.953	6.52 [21.39]	5.25 [17.23]	0.13 [0.04]	0.11 [0.03]

*The Fisher dispersion coefficient (also referred to as the concentration parameter) is a measure of the degree to which spherical data are concentrated around the mean (Fisher, N.I, T. Lewis, and B.J.J. Embleton. *Statistical Analysis of Spherical Data*. Cambridge, United Kingdom: Cambridge University Press. 1993; Mardia, K.V. *Statistics of Directional Data*. New York, New York: Academic Press. 1972; Fisher, R.A. "Dispersion On a Sphere." Proceedings of the Royal Society of London. Vol. A217. pp. 295–305. 1953). Larger values of the Fisher dispersion coefficient indicate tighter clustering (i.e., less dispersion).

Table 4-2. Summary of Fracman®-Generated Synthetic Fracture Data for the Topopah Spring Tuff Middle Nonlithophysal Zone (Test 2). Linear Fracture Intensity Is the Number of Fractures Per Unit Length Determined from Borehole Sampling of the Synthetic Fracture Population. Areal Fracture Intensity Is the Total Fracture Trace Length Per Unit Area Determined from Tunnel Sampling of the Synthetic Fracture Population. An Expanded Data Table That Includes Standard Deviations for Fracture Radius is Included in Appendix Table B–2.

Set	Number and Percentage	Mean Orientation (Strike/Dip)	Fisher Dispersion Coefficient*	Fracture Radius, m [ft]		Linear Fracture Intensity, m^{-1} [ft^{-1}]	Areal Fracture Intensity, m/m^2 [ft/ft^2]
				Mean	Median		
All	99213, 100%	*n.a.*	*n.a.*	*n.a.*	*n.a.*	1.46 [0.44]	1.35 [0.41]
1	40248, 41%	124°/84°	10.705	1.60 [5.25]	1.32 [4.33]	0.36 [0.11]	0.34 [0.10]
2	31691, 32%	217°/86°	7.868	1.61 [5.28]	1.32 [4.33]	0.20 [0.06]	0.26 [0.08]
3	10701, 11%	299°/43°	27.767	1.60 [5.25]	1.32 [4.33]	0.06 [0.02]	0.06 [0.02]
4	12556, 13%	331°/08°	5.048	1.67 [5.48]	1.32 [4.33]	0.07 [0.02]	0.11 [0.03]
5	1466, 1%	123°/84°	10.278	6.52 [21.39]	5.38 [17.65]	0.34 [0.10]	0.22 [0.07]
6	1431, 1%	217°/87°	7.568	6.60 [21.65]	5.31 [17.42]	0.31 [0.09]	0.22 [0.07]
7	1120, 1%	300°/43°	28.403	6.49 [21.29]	5.31 [17.42]	0.12 [0.04]	0.13 [0.04]

*The Fisher dispersion coefficient (also referred to as the concentration parameter) is a measure of the degree to which spherical data are concentrated around the mean (Fisher, N.I, T. Lewis, and B.J.J. Embleton. *Statistical Analysis of Spherical Data*. Cambridge, United Kingdom: Cambridge University Press. 1993; Mardia, K.V. *Statistics of Directional Data*. New York, New York: Academic Press. 1972; Fisher, R.A. "Dispersion On a Sphere." Proceedings of the Royal Society of London. Vol. A217. pp. 295–305. 1953). Larger values of the Fisher dispersion coefficient indicate tighter clustering (i.e., less dispersion).

Five synthetic tunnels were simulated in each cube of synthetic fractures to extract areal fracture intensity (i.e., trace length per unit area) data. The constructed tunnels were 90 m [295 ft] long and 5.3 m [17.4 ft] in diameter. Each tunnel was constructed by assembling seven trace planes into an octagon-like shape (minus the floor). This configuration provides an approximation of the full-periphery geologic maps, including the data gap beneath the tunnel invert where fractures from the lowermost portions of the ESF and the ECRB Cross-Drift were not mapped. The average areal intensity based on all fracture sets is 1.29 m/m^2 [0.39 ft/ft^2] for test 1 and 1.35 m/m^2 [0.41 ft/ft^2] for test 2. Areal intensity values, like linear intensity values, are quite variable between the different fracture sets. The range for test 1 is 0.08 to 0.37 m/m^2 [0.02 to 0.11 ft/ft^2], and the range for test 2 is 0.06 to 0.34 m/m^2 [0.02 to 0.10 ft/ft^2].

4.2 FracMan Analyses for the Lower Lithophysal Zone

For the Lower Lithophysal zone, DOE generated synthetic fractures that represented six different sets (Figure 4-6): (i) one subhorizontal set (set 1), (ii) two northwest-striking subvertical sets—one for long fractures (set 2) and one for short fractures (set 4), (iii) two north-south-striking subvertical sets—one for long fractures (set 3) and one for short fractures (set 5), and (iv) one east-west-striking set that dips steeply to the south (set 6).

Synthetic fractures were generated for the Lower Lithophysal zone within a [328 ft × 328 ft × 328 ft] cube using the DOE input parameters (Figure 4-6). The fracture populations generated for both test cases are characterized by four fracture sets (Tables 4-3 and 4-4; Figures 4-7 and 4-8). The northwest-striking, steeply southwest-dipping sets (i.e., sets 2 and 4) are the most statistically significant. The north-south-striking subvertical sets (i.e., sets 3 and 5) are clearly developed. The remaining two sets are present but less strongly developed.

Again, DOE (Bechtel SAIC Company, LLC, 2004b) selected a power law distribution for controlling fracture radius. An unbounded distribution with an exponent of 3.1 was selected by DOE for the Lower Lithophysal zone, but the size equivalent radius was varied from set to set. Fracture sets 1 through 3 have size equivalent radii that range from 1.3 to 1.8 m [4.3 to 5.9 ft]. Fracture sets 4 through 6 specify a size equivalent radius of 0.6 m [2.0 ft]. Fracture radius distributions from the resulting synthetic fracture populations are characterized by a large positive skew (Figures 4-9 and 4-10). The subhorizontal fractures (set 1) for both test cases have mean radii of 2.34 m [7.68 ft] and median radii of 1.81 m [5.94 ft] (Tables 4-3 and 4-4). Fracture set 2 has a mean and median of 3.63 m [11.91 ft] and 2.51 m [8.24 ft], respectively, for both test cases. The set 3 fractures have mean radii that range from 2.97 to 3.64 m [9.74 to 11.94 ft] and median radii that range from 2.10 to 2.18 m [6.89 to 7.15 ft]. The three short fracture sets (i.e., sets 4, 5, and 6) all have mean radii of approximately 1.1 to 1.2 m [3.6 to 3.9 ft] and median values of 0.8 to 0.9 m [2.6 to 3.0 ft].

As with the Middle Nonlithophysal zone, nine simulated 1-m [3.3-ft] -diameter and 100-m [328- ft] -long boreholes were sampled through each cube of Lower Lithophysal synthetic fractures to extract linear fracture intensity. The boreholes were defined to be horizontal with a trend of 071°. The average linear intensity based on all fracture sets is 0.278 m^{-1} [0.085 ft^{-1}] for test 1 and 0.323 m^{-1} [0.098 ft^{-1}] for test 2. Intensity values for individual fracture sets are smaller and variable (Tables 4-3 and 4-4). The range for test 1 is 0.0 to 0.168 m^{-1} [0.0 to 0.051 ft^{-1}], and the range for test 2 is 0.010 to 0.168 m^{-1} [0.003 to 0.051 ft^{-1}].

Five synthetic tunnels were also sampled through each cube of Lower Lithophysal synthetic fractures. The simulated tunnels were 90 m [295 ft] long and 5.3 m [17.4 ft] in diameter. Each tunnel was constructed by assembling seven trace planes into an octagon-like shape (minus the floor). This configuration provides an approximation of the full-periphery geologic maps, including the data gap beneath the tunnel invert where fractures from the lowermost portions of the ESF and the ECRB Cross-Drift were not mapped. The average areal intensity based on all fracture sets is 0.144 m/m^2 [0.044 ft/ft^2] for test 1 and 0.139 m/m^2 [0.042 ft/ft^2] for test 2. Areal intensity values are widely variable between the different fracture sets. The range for test 1 is 0.002 to 0.067 m/m^2 [0.001 to 0.020 ft/ft^2], and the range for test 2 is 0.001 to 0.067 m/m^2 [0.0003 to 0.020 ft/ft^2].

Table 4-3. Summary of Fracman®-Generated Synthetic Fracture Data for the Topopah Spring Tuff Lower Lithophysal Zone (Test 1). Linear Fracture Intensity Is the Number of Fractures Per Unit Length Determined from Borehole Sampling of the Synthetic Fracture Population. Areal Fracture Intensity Is the Total Fracture Trace Length Per Unit Area Determined from Tunnel Sampling of the Synthetic Fracture Population. An Expanded Data Table That Includes Standard Deviations for Fracture Radius is Included in Appendix Table B–3.

Set	Number and Percentage	Mean Orientation (Strike/Dip)	Fisher Dispersion Coefficient*	Fracture Radius, m [ft]		Linear Fracture Intensity, m^{-1} [ft^{-1}]	Areal Fracture Intensity, m/m^2 [ft/ft^2]
				Mean	Median		
All	8143, 100%	*n.a.*	*n.a.*	*n.a.*	*n.a.*	0.278 [0.085]	0.144 [0.044]
1	798, 10%	328°/14°	72.950	2.34 [7.68]	1.81 [5.94]	0.007 [0.002]	0.015 [0.005]
2	836, 10%	130°/80°	69.294	3.63 [11.91]	2.51 [8.24]	0.168 [0.051]	0.067 [0.020]
3	482, 6%	166°/80°	63.442	2.97 [9.74]	2.18 [7.15]	0.061 [0.019]	0.021 [0.006]
4	4728, 58%	130°/80°	99.104	1.13 [3.71]	0.83 [2.72]	0.036 [0.011]	0.034 [0.010]
5	908, 11%	170°/80°	100.840	1.20 [3.94]	0.85 [2.79]	0.007 [0.002]	0.005 [0.002]
6	391, 5%	098°/85°	102.250	1.05 [3.45]	0.84 [2.76]	0.000 [0.000]	0.002 [0.001]

*The Fisher dispersion coefficient (also referred to as the concentration parameter) is a measure of the degree to which spherical data are concentrated around the mean (Fisher, N.I, T. Lewis, and B.J.J. Embleton. *Statistical Analysis of Spherical Data*. Cambridge, United Kingdom: Cambridge University Press. 1993; Mardia, K.V. *Statistics of Directional Data*. New York, New York: Academic Press. 1972; Fisher, R.A. "Dispersion On a Sphere." Proceedings of the Royal Society of London. Vol. A217. pp. 295–305. 1953). Larger values of the Fisher dispersion coefficient indicate tighter clustering (i.e., less dispersion).

Table 4-4. Summary of Fracman®-Generated Synthetic Fracture Data for the Topopah Spring Tuff Lower Lithophysal Zone (Test 2). Linear Fracture Intensity Is the Number of Fractures Per Unit Length Determined from Borehole Sampling of the Synthetic Fracture Population. Areal Fracture Intensity Is the Total Fracture Trace Length Per Unit Area Determined from Tunnel Sampling of the Synthetic Fracture Population. An Expanded Data Table That Includes Standard Deviations for Fracture Radius is Included in Appendix Table B–4.

Set	Number and Percentage	Mean Orientation (Strike/Dip)	Fisher Dispersion Coefficient*	Fracture Radius, m [ft]		Linear Fracture Intensity, m^{-1} [ft^{-1}]	Areal Fracture Intensity, m/m^2 [ft/ft^2]
				Mean	Median		
All	8481, 100%	*n.a.*	*n.a.*	*n.a.*	*n.a.*	0.323 [0.098]	0.139 [0.042]
1	798, 10%	328°/14°	72.950	2.34 [7.68]	1.81 [5.94]	0.007 [0.002]	0.015 [0.005]
2	836, 10%	130°/80°	69.294	3.63 [11.91]	2.51 [8.24]	0.168 [0.051]	0.067 [0.020]
3	243, 3%	167°/80°	68.625	3.64 [11.94]	2.10 [6.89]	0.101 [0.031]	0.020 [0.006]
4	5549, 65%	130°/80°	100.160	1.15 [3.77]	0.83 [2.72]	0.038 [0.012]	0.029 [0.009]
5	873, 10%	171°/80°	99.334	1.22 [4.00]	0.83 [2.72]	0.010 [0.003]	0.007 [0.002]
6	182, 2%	098°/85°	104.130	1.18 [3.87]	0.86 [2.82]	0.010 [0.003]	0.001 [0.0003]

*The Fisher dispersion coefficient (also referred to as the concentration parameter) is a measure of the degree to which spherical data are concentrated around the mean (Fisher, N.I, T. Lewis, and B.J.J. Embleton. *Statistical Analysis of Spherical Data*. Cambridge, United Kingdom: Cambridge University Press. 1993; Mardia, K.V. *Statistics of Directional Data*. New York, New York: Academic Press. 1972; Fisher, R.A. "Dispersion On a Sphere." Proceedings of the Royal Society of London. Vol. A217. pp. 295–305. 1953). Larger values of the Fisher dispersion coefficient indicate tighter clustering (i.e., less dispersion).

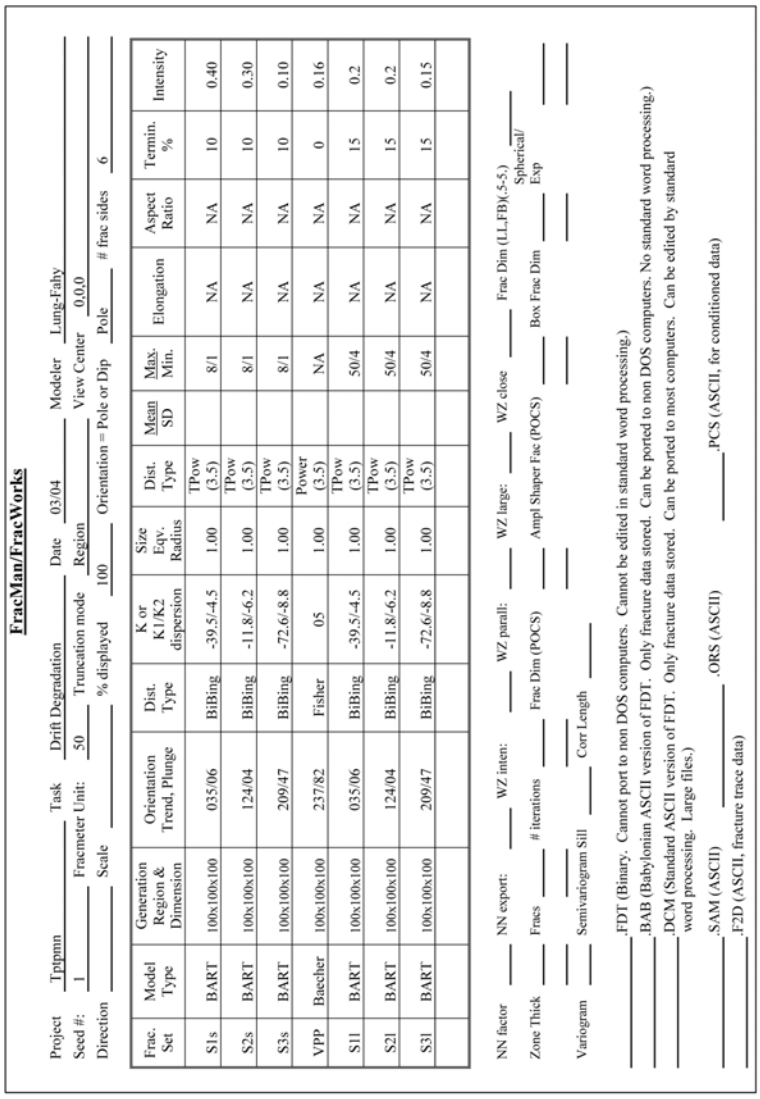

FracMan/FracWorks

Project _____ Task _____ Drift Degradation _____ Date 03/04 _____ Modeler _____ Lung-Fahy

Seed #: 1 Fracmeter Unit: 50 Truncation mode Region View Center 0,0,0

Direction _____ Scale _____ % displayed 100 Orientation = Pole or Dip Pole # frac sides 6

Frac. Set	Model Type	Generation Region & Dimension	Orientation Trend, Plunge	Dist. Type	K or K1/K2 dispersion	Size Eqv. Radius	Dist. Type	Mean SD	Max. Min.	Elongation	Aspect Ratio	Termin. %	Intensity
S1s	BART	100x100x100	035/06	BiBing	-39.5/-4.5	1.00	TPow (3.5)		8/1	NA	NA	10	0.40
S2s	BART	100x100x100	124/04	BiBing	-11.8/-6.2	1.00	TPow (3.5)		8/1	NA	NA	10	0.30
S3s	BART	100x100x100	209/47	BiBing	-72.6/-8.8	1.00	TPow (3.5)		8/1	NA	NA	10	0.10
VPP	Baecher	100x100x100	237/82	Fisher	05	1.00	Power (3.5)		NA	NA	NA	0	0.16
S1l	BART	100x100x100	035/06	BiBing	-39.5/-4.5	1.00	TPow (3.5)		50/4	NA	NA	15	0.2
S2l	BART	100x100x100	124/04	BiBing	-11.8/-6.2	1.00	TPow (3.5)		50/4	NA	NA	15	0.2
S3l	BART	100x100x100	209/47	BiBing	-72.6/-8.8	1.00	TPow (3.5)		50/4	NA	NA	15	0.15

NN factor ____ NN export: ____ WZ inten: ____ WZ parall: ____ WZ large: ____ WZ close ____ Frac Dim (LLFB)(.5-5.) ____

Zone Thick ____ Fracs ____ # iterations ____ Frac Dim (POCS) ____ Ampl Shaper Fac (POCS) ____ Box Frac Dim ____ Spherical/ Exp ____

Variogram ____ ____ Semivariogram Sill ____ Corr Length ____ ____ ____ ____

_____.FDT (Binary;. Cannot port to non DOS computers. Cannot be edited in standard word processing.)

_____.BAB (Babylonian ASCII version of FDT. Only fracture data stored. Can be ported to non DOS computers. No standard word processing.)

_____.DCM (Standard ASCII version of FDT. Only fracture data stored. Can be ported to most computers. Can be edited by standard word processing. Large files.)

_____.SAM (ASCII) _____.ORS (ASCII) _____.PCS (ASCII, for conditioned data)

_____.F2D (ASCII, fracture trace data)

NOTE: See Figure 6-17 for detailed line survey source DTNs. The parameter, "K or K1/K2 dispersion" is determined using CLUSTRAN (with the exception of VPP, or vapor-phase parting, which is determined visually by comparing simulated stereonets to observed stereonets). The parameter, "Size Eqv. Radius" is the mean radius (m). The power law distribution is used for the parameter, "Dist. Type." The power law is selected because the fracture process generally follows power law physics, such that the number of fractures greater than a given length (x) is proportional to 1/x raised to the power law exponent. The parameter, "Intensity" is selected to maintain the proportion of fractures in each set.

Figure 6-18. FracMan Input Sheet for the Tptpmn

Figure 4-1. Summary of Fracman® Input Values for the Topopah Spring Tuff Middle Nonlithophysal Zone from Bechtel SAIC Company, LLC (2004b).

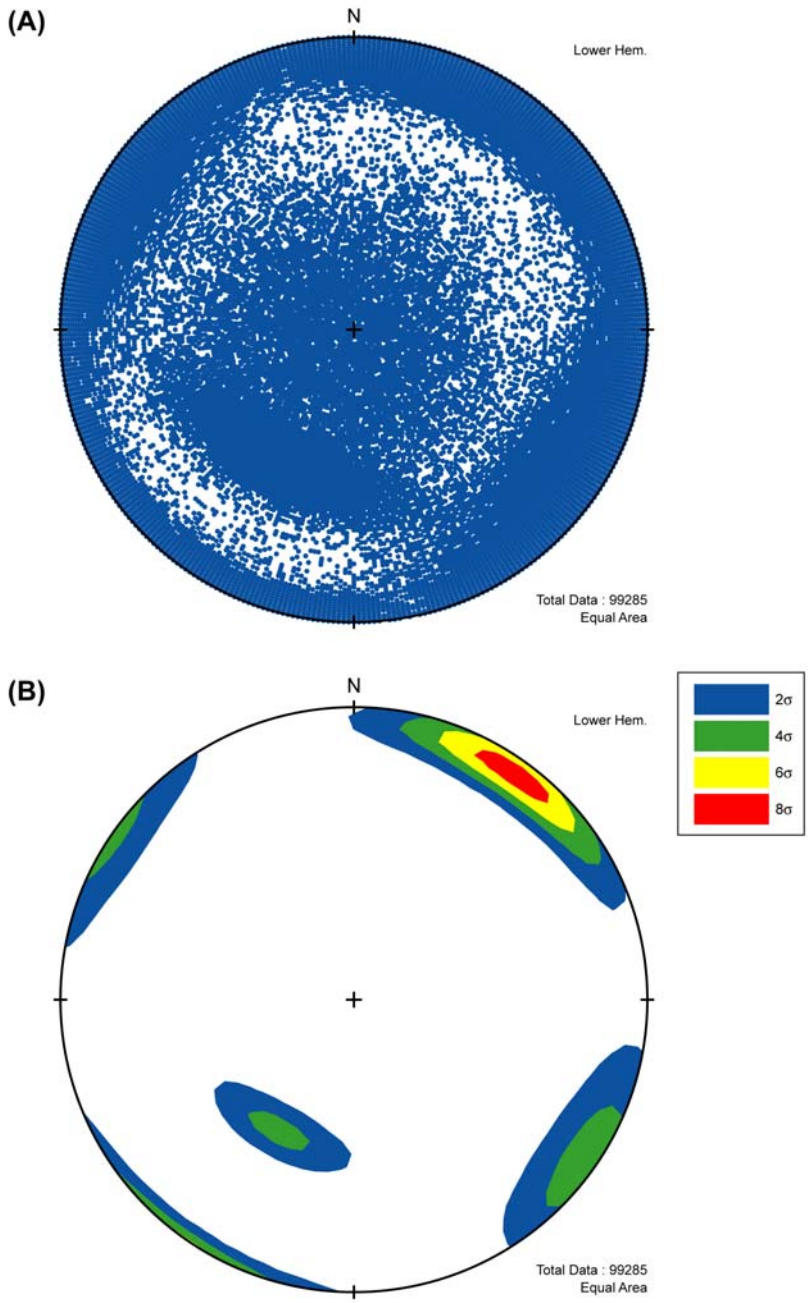

Figure 4-2. Orientation Summary for Synthetic Fractures Generated for the Middle Nonlithophysal Zone (Test 1). (A) Equal-Area Stereonet Plot of Poles to Fracture Planes. (B) Contours of Poles to Fracture Planes Calculated With 1% Area Method.

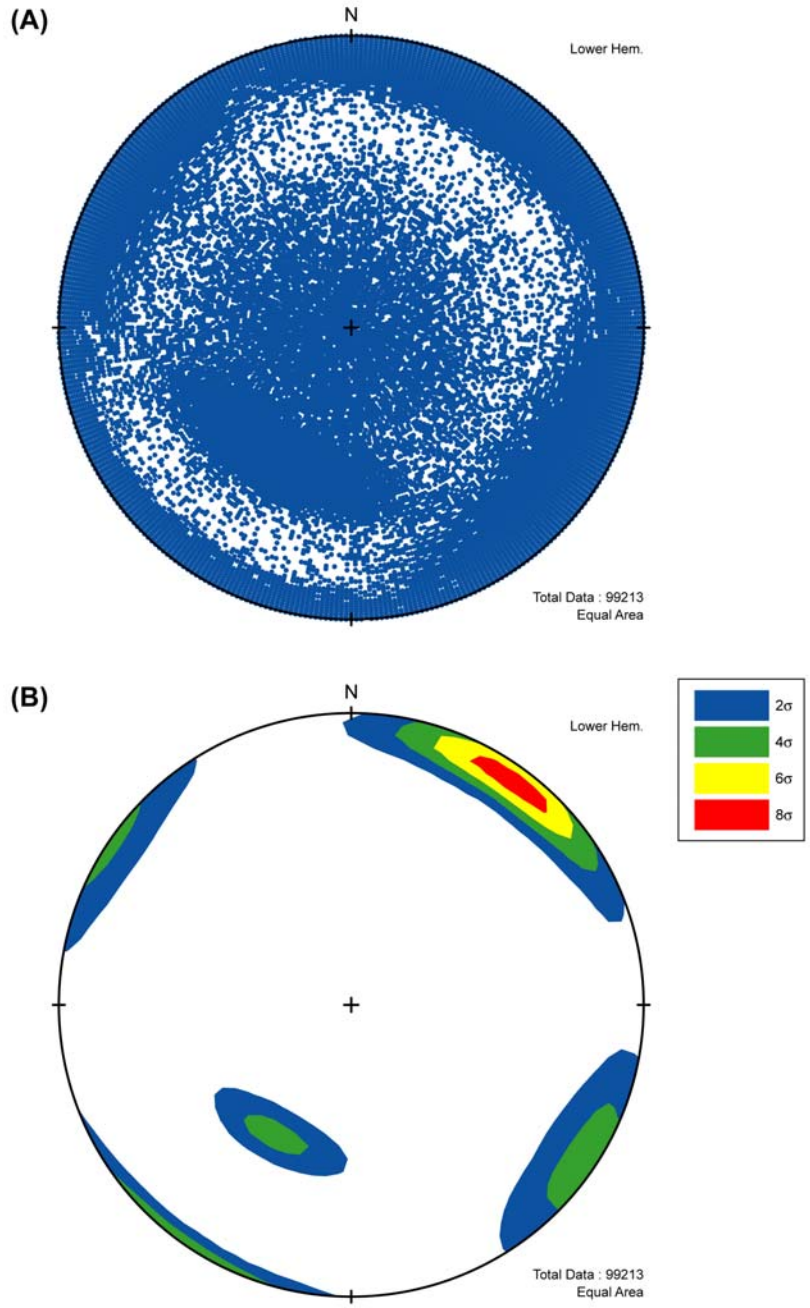

Figure 4-3. Orientation Summary for Synthetic Fractures Generated for the Middle Nonlithophysal Zone (Test 2). (A) Equal-Area Stereonet Plot of Poles to Fracture Planes. (B) Contours of Poles to Fracture Planes Calculated With 1% Area Method.

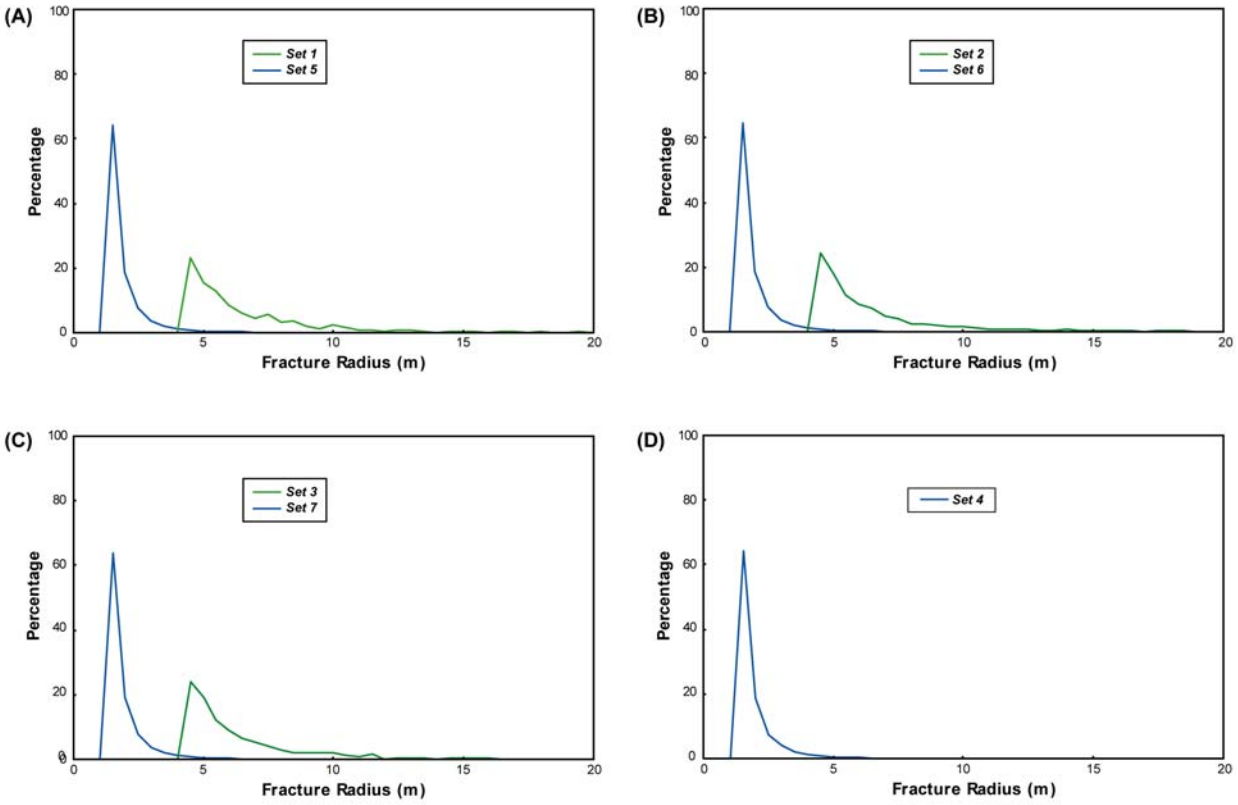

Figure 4-4. Summary of Synthetic Fracture Radius Distributions for the Middle Nonlithophysal Zone (Test 1). (A) Set 1 and 5 Fractures Are Northwest-Striking and Subvertical. (B) Set 2 and 6 Fractures Are Northeast-Striking and Subvertical. (C) Set 3 and 7 Fractures Are Northwest-Striking with an Intermediate Dip to the Northeast. (D) Set 4 Fractures Are Subhorizontal.

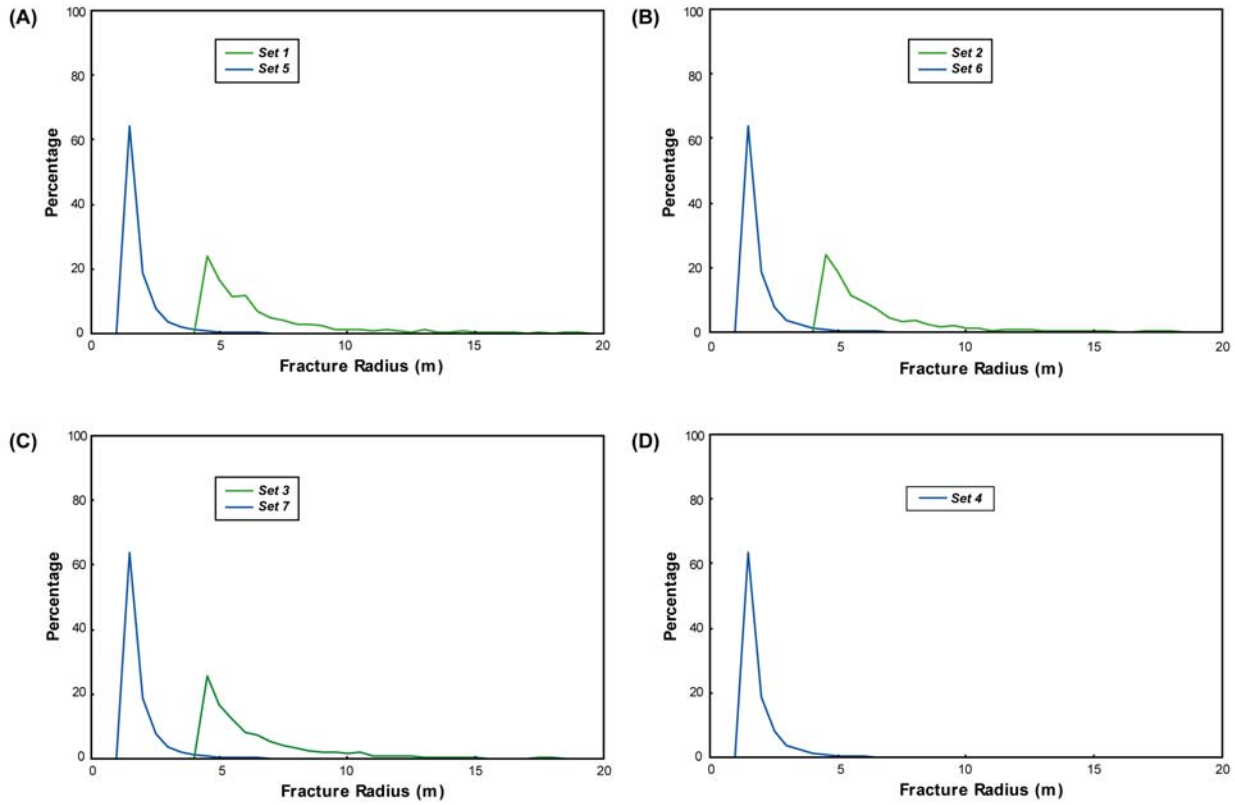

Figure 4-5. Summary of Synthetic Fracture Radius Distributions for the Middle Nonlithophysal Zone (Test 2). (A) Set 1 and 5 Fractures Are Northwest-Striking and Subvertical. (B) Set 2 and 6 Fractures Are Northeast-Striking and Subvertical. (C) Set 3 and 7 Fractures Are Northwest-Striking With an Intermediate Dip to the Northeast. (D) Set 4 Fractures Are Subhorizontal.

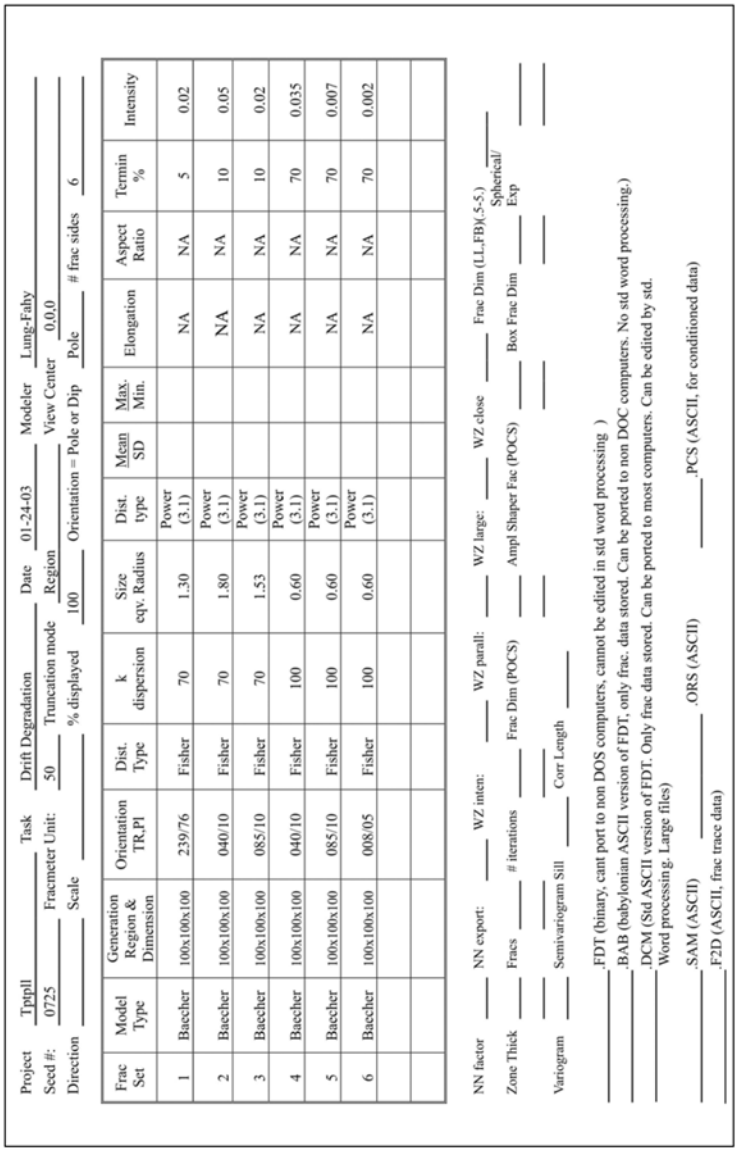

Project Tptpll Task
Seed #: 0725 Fracmeter Unit:
Direction Scale

Drift Degradation Date 01-24-03 Modeler Lung-Fahy
50 Truncation mode Region View Center 0,0,0
% displayed 100 Orientation = Pole or Dip Pole # frac sides 6

Frac Set	Model Type	Generation Region & Dimension	Orientation TR,PI	Dist. Type	k dispersion	Size eqv. Radius	Dist. type	Mean SD	Max. Min.	Elongation	Aspect Ratio	Termin %	Intensity
1	Baecher	100x100x100	239/76	Fisher	70	1.30	Power (3.1)			NA	NA	5	0.02
2	Baecher	100x100x100	040/10	Fisher	70	1.80	Power (3.1)			NA	NA	10	0.05
3	Baecher	100x100x100	085/10	Fisher	70	1.53	Power (3.1)			NA	NA	10	0.02
4	Baecher	100x100x100	040/10	Fisher	100	0.60	Power (3.1)			NA	NA	70	0.035
5	Baecher	100x100x100	085/10	Fisher	100	0.60	Power (3.1)			NA	NA	70	0.007
6	Baecher	100x100x100	008/05	Fisher	100	0.60	Power (3.1)			NA	NA	70	0.002

NN factor ____ NN export: ____ WZ inten: ____ WZ parall: ____ WZ large: ____ WZ close ____ Frac Dim (LL,FB)(.5-5.)
Zone Thick ____ Fracs ____ # iterations ____ Frac Dim (POCS) ____ Ampl Shaper Fac (POCS) ____ Box Frac Dim ____ Spherical/ Exp
Variogram ____ Semivariogram Sill ____ Corr Length ____

____.FDT (binary, cant port to non DOS computers, cannot be edited in std word processing)
____.BAB (babylonian ASCII version of FDT, only frac. data stored. Can be ported to non DOC computers. No std word processing.)
____.DCM (Std ASCII version of FDT. Only frac data stored. Can be ported to most computers. Can be edited by std.
____Word processing g. Large files)
____.SAM (ASCII) ____.ORS (ASCII) ____.PCS (ASCII, for conditioned data)
____.F2D (ASCII, frac trace data)

Source: DTN: GS990408314224.001 [DIRS 108396]; GS990408314224.002 [DIRS 105625].

NOTE: The parameter, "k dispersion" is determined visually by comparing simulated stereonets to observed stereonets. The parameter, "size eqv. radius" is the mean radius (m). The power law distribution is used for the parameter, "dist. type." The power law is selected because the fracture process generally follows power law physics, such that the number of fractures greater than a given length (x) is proportional to 1/x raised to the power law exponent. The parameter, "intensity" is selected to maintain the proportion of fractures in each set.

Figure B-3. FracMan Input Sheet for the Tptpll

Figure 4-6. Summary of Fracman® Input Values for the Topopah Spring Tuff Lower Lithophysal Zone from Bechtel SAIC Company, LLC (2004b).

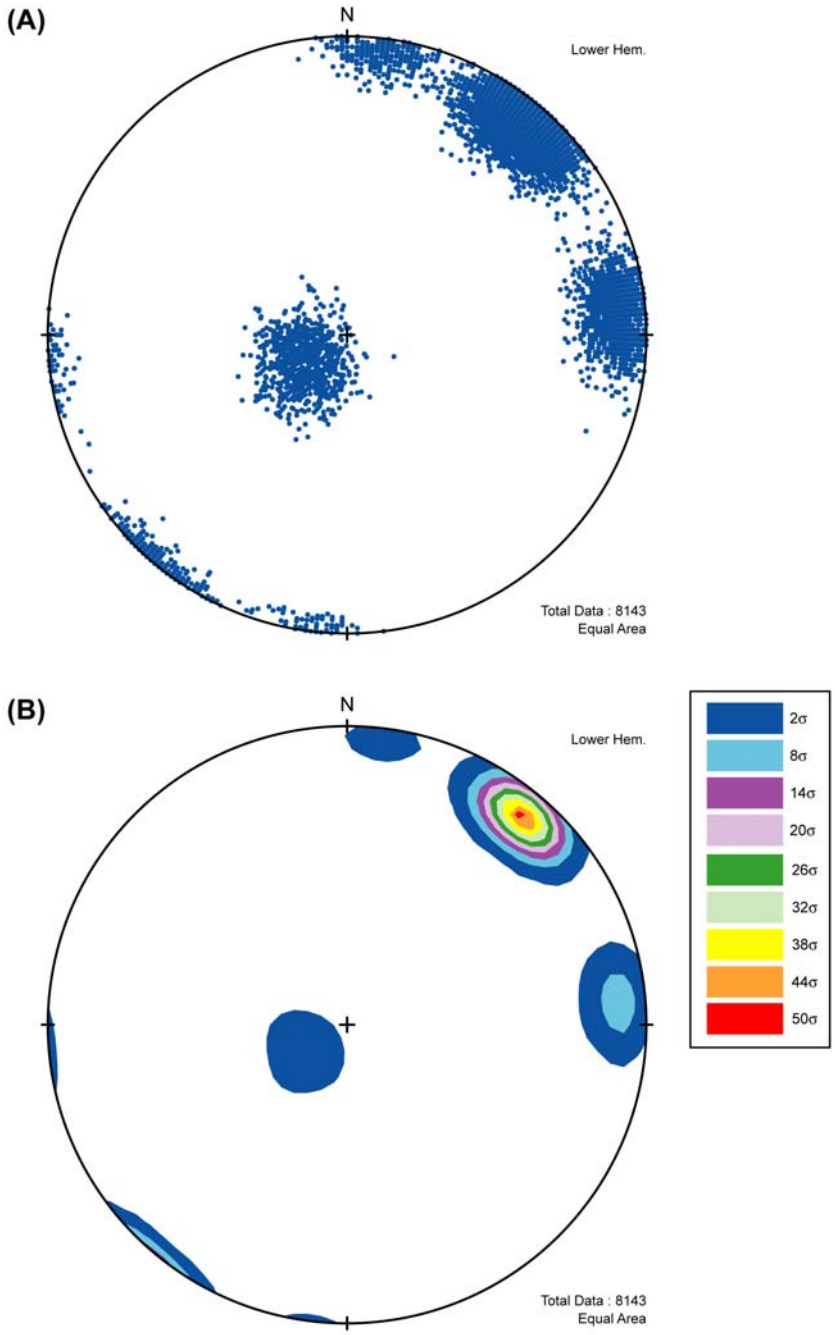

Figure 4-7. Orientation Summary for Synthetic Fractures Generated for the Lower Lithophysal Zone (Test 1). (A) Equal-Area Stereonet Plot of Poles to Fracture Planes. (B) Contours of Poles to Fracture Planes Calculated With 1% Area Method.

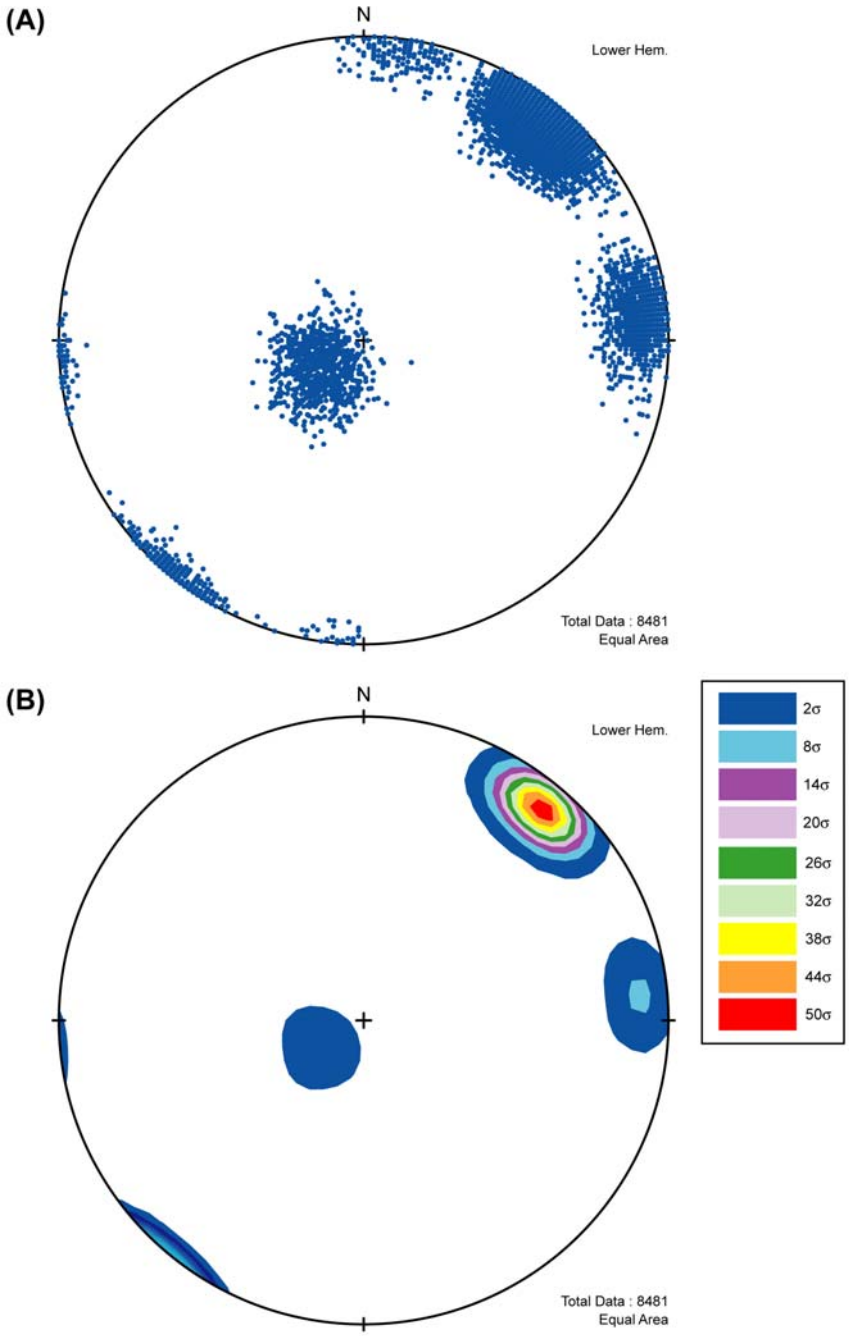

Figure 4-8. Orientation Summary for Synthetic Fractures Generated for the Lower Lithophysal Zone (Test 2). (A) Equal-Area Stereonet Plot of Poles to Fracture Planes. (B) Contours of Poles to Fracture Planes Calculated With 1% Area Method.

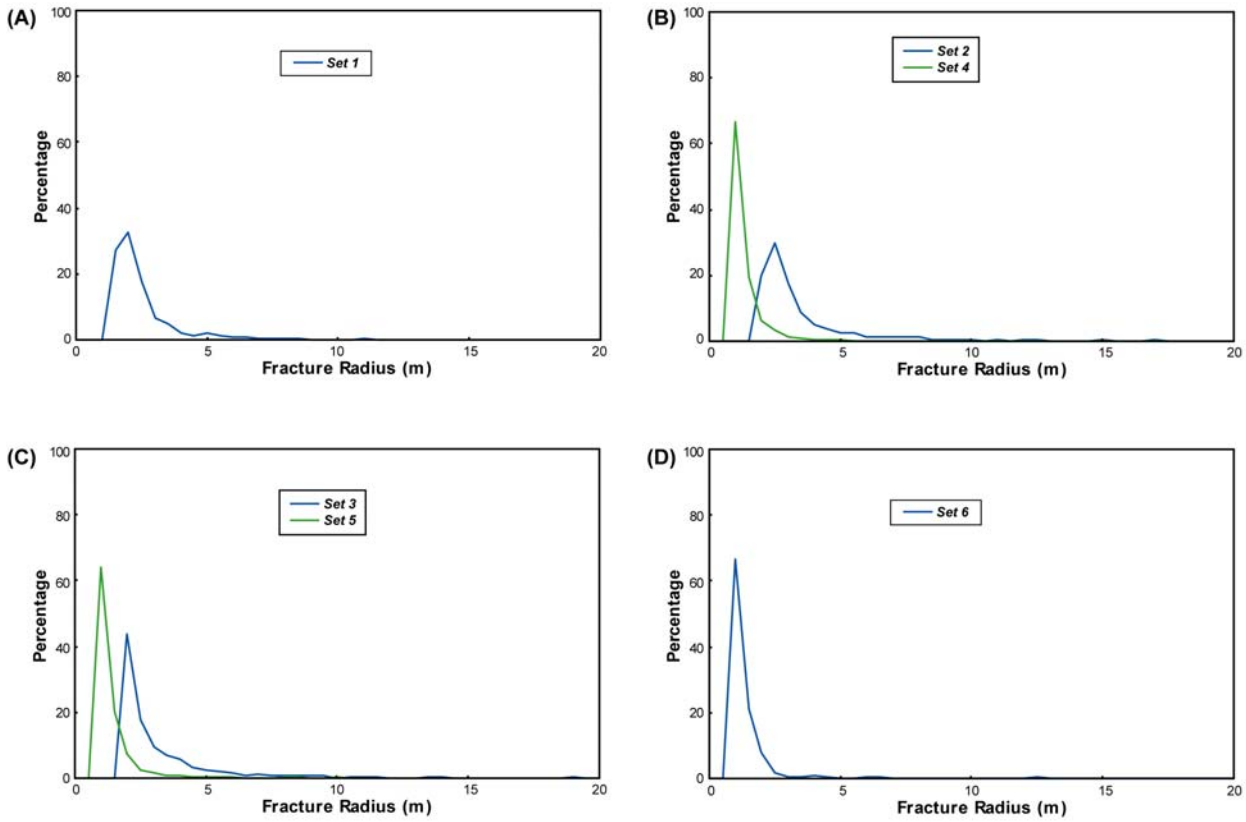

Figure 4-9. Summary of Synthetic Fracture Radius Distributions for the Lower Lithophysal Zone (Test 1). (A) Set 1 Fractures Are Subhorizontal. (B) The Fractures In Sets 2 and 4 Are Northwest-Striking and Steeply Southwest Dipping. (C) The Fractures In Sets 3 and 5 Are North-South-Striking and Steeply West Dipping. (D) Set 6 Fractures Are East-West-Striking and Steeply South Dipping.

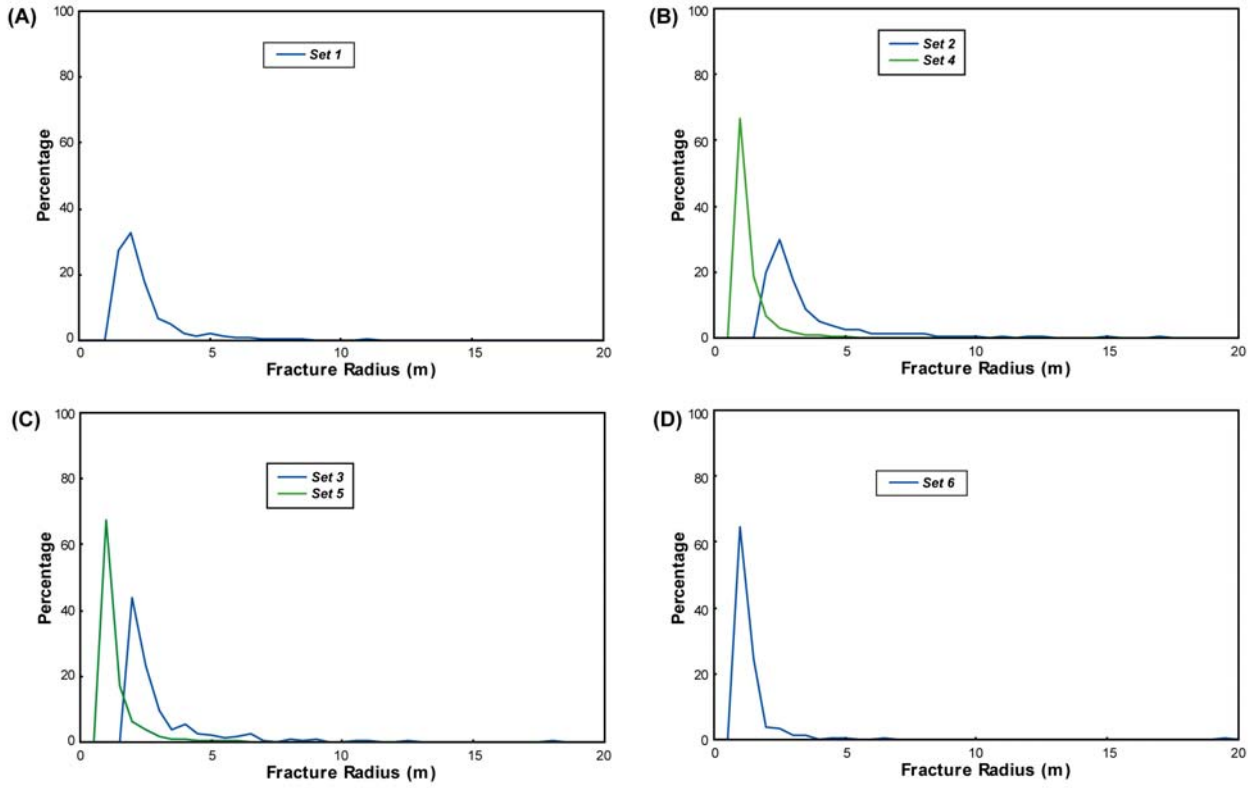

Figure 4-10. Summary of Synthetic Fracture Radius Distributions for the Lower Lithophysal Zone (Test 2). (A) Set 1 Fractures Are Subhorizontal. (B) The Fractures In Sets 2 and 4 Are Northwest-Striking and Steeply Southwest Dipping. (C) The Fractures In Sets 3 and 5 Are North-South-Striking and Steeply West Dipping. (D) Set 6 Fractures Are East-West-Striking and Steeply South Dipping.

5 SUMMARY

This report provides an up-to-date synthesis of the subsurface fracture data collected by detailed line survey and full-periphery geologic mapping of the Topopah Spring Tuff Upper Lithophysal, Middle Nonlithophysal, Lower Lithophysal, and Lower Nonlithophysal zones in the ESF and the ECRB Cross-Drift at Yucca Mountain, Nevada. The first goal of this report is to summarize the data collected by DOE and its contractors and to provide a synthesis that staff can refer to during review of a license application. This synthesis is considered necessary because fractures are direct contributors to most geotechnical processes for the stability of underground openings, including rock fall. Also, fractures influence related processes such as thermal stress accommodation, and in-drift heat transfer. Near-surface infiltration, seepage, flow, and radionuclide transport in the unsaturated zone are additional processes where fractures influence drift- and mountain-scale processes. Furthermore, deficiencies associated with previous fracture syntheses (e.g., Nieder-Westermann, 2000) have been documented (Smart, 2005; Ferrill, et al., 2000).

The second goal of this report is to provide a rigorous analysis of those fracture characteristics that are expected to be most important to features, events, or processes of a license application. In particular, this report focuses on (i) delineating primary fracture sets on the basis of lithostratigraphy and orientation; (ii) fracture spacing, and one-dimensional (i.e., linear) and two-dimensional (i.e., areal) measures of fracture intensity; and (iii) fracture size (i.e., trace length) distributions. An additional focus is on extraction of fracture information from the full-periphery geologic maps that were produced from the ECRB Cross-Drift. The nature of the full-periphery maps only permits extraction of information on fracture orientation, fracture trace length distributions, and areal fracture intensity.

The final goal of this report is an initial analysis of synthetic fracture populations that DOE generated with FracMan for the Topopah Spring Tuff Middle Nonlithophysal and Lower Lithophysal zones. DOE used the synthetic fracture populations for drift degradation analyses (Bechtel SAIC Company, LLC, 2004a,b). The DOE analyses were replicated so that independent data would be available during license review.

A number of general conclusions can be drawn regarding the fracture data collected by detailed line survey and full-periphery geologic mapping in the ESF and the ECRB Cross-Drift at Yucca Mountain:

- Definitive cooling joints and vapor phase partings are present in all four Topopah Spring Tuff zones, but they are not abundant and represent only 5–11 percent of all recorded fractures (Figure 3-1).

- Fractures with measurable displacement are also present, but account for only 3–4 percent of the total population (Figures 3-2, 3-3). These fractures are predominantly subvertical with either a northwest-southeast or northeast-southwest strike.

Table 5-1. Comparison of Fracture Orientation, Spacing, and Trace Length Data as Determined in This Report and as Reported by U.S. Department of Energy (DOE). For Consistency of Comparison, Data From This Report are From Detailed Line Surveys of Fractures With Trace Lengths >1 m [3.3 ft].

		This Report			DOE		
Zone	Set	Orientation (Strike/Dip)	Median Spacing, m [ft]	Median Trace Length, m [ft]	Orientation (Strike/Dip)	Median Spacing, m [ft]	Median Trace Length, m [ft]
Upper Lithophysal*	1	116°/85°	0.75 [2.46]	1.44 [4.72]	121°/83°	2.29 [7.51]	2.08 [6.82]
	2	181°/85°	0.65 [2.13]	1.30 [4.66]	186°/82°	2.20 [7.23]	2.13 [6.99]
	3	320°/19°	1.29 [4.23]	4.31 [14.14]	320°/19°	1.54 [5.05]	4.10 [13.45]
Middle Nonlithophysal†	1	126°/84°	0.19 [0.62]	1.70 [5.58]	120°/84°	0.48 [1.57]	3.30 [10.83]
	2	227°/86°	0.46 [1.51]	1.35 [4.43]	215°/88°	1.08 [3.54]	2.80 [9.19]
	3	326°/08°	0.52 [1.71]	1.54 [5.05]	329°/14°	2.46 [8.07]	3.50 [11.48]
Lower Lithophysal‡	1	158°/81°	1.39 [4.56]	1.88 [6.19]	145°/82°	1.57 [5.15]	2.11 [6.92]
	2	087°/85°	6.17 [20.24]	1.63 [5.35]	180°/79°	3.18 [10.43]	1.70 [5.58]
	3	329°/05°	1.39 [4.56]	3.42 [11.22]	315°/05°	0.57 [1.87]	3.42 [11.22]
Lower Nonlithophysal§	1	134°/80°	0.73 [2.40]	2.25 [7.38]	136°/79°	0.74 [2.43]	2.30 [7.55]
	2	209°/85°	0.70 [2.30]	1.66 [5.45]	209°/82°	1.36 [4.46]	1.89 [6.20]
	3	337°/15°	1.59 [5.22]	1.31 [4.30]	330°/13°	1.64 [5.38]	1.27 [4.17]

*Data from this report (Tables 3-1, A–1). DOE data reported in Nieder-Westermann, G.H. "Fracture Geometry Analysis for the Stratigraphic Units of the Repository Host Horizon." ANL–EBS–GE–000006. Rev. 00. Las Vegas, Nevada: CRWMS M&O. 2000.
†Data from this report (Tables 3-2, A–2). DOE data reported in Bechtel SAIC Company, LLC. "Drift Degradation Analysis." ANL–EBS–MD–000027. Rev. 3. Las Vegas, Nevada: Bechtel SAIC Company, LLC. 2004.
‡Data from this report (Tables 3-6, A–6). DOE data reported in Nieder-Westermann, G.H. "Fracture Geometry Analysis for the Stratigraphic Units of the Repository Host Horizon." ANL–EBS–GE–000006. Rev. 00. Las Vegas, Nevada: CRWMS M&O. 2000.
§Data from this report (Tables 3-8, A–8). DOE data reported in Nieder-Westermann, G.H. "Fracture Geometry Analysis for the Stratigraphic Units of the Repository Host Horizon." ANL–EBS–GE–000006. Rev. 00. Las Vegas, Nevada: CRWMS M&O. 2000.

Table 5-2. Summary of Orientation, Spacing, and Trace Length Data Based On Measurements of Small-Scale Fractures {i.e., < 1 m [3.3 ft]}.				
Zone	**Set**	**Orientation (Strike/Dip)**	**Median Spacing, m [ft]**	**Median Trace Length, m [ft]**
Middle Nonlithophysal*	1	179°/89°	0.04 [0.13]	0.15 [0.49]
	2	118°/86°	0.07 [0.23]	0.30 [0.98]
	3	312°/05°	0.12 [0.39]	0.31 [1.02]
Lower Lithophysal†	1	134°/82°	0.03 [0.10]	0.17 [0.56]
	2	079°/82°	0.12 [0.39]	0.14 [0.50]
	3	313°/04°	0.06 [0.20]	0.19 [0.62]
*Data from this report (Tables 3-5, A–5). †Data from this report (Tables 3-7, A–7).				

- Regardless of lithostratigraphic interval, distinctive orientation-based fracture sets are present (i.e., the distribution of fractures is not random). This observation holds for analyses of long fractures {i.e., trace lengths >1 m [3.3 ft]} (Table 5-1) and short fractures {i.e., trace lengths <1 m [3.3 ft]} (Table 5-2). In general, the fracture set orientations determined in this report are similar to those previously reported by DOE (e.g., Bechtel SAIC Company, LLC,2004b; Nieder-Westermann, 2000).

- Raw fracture data suggest that the most abundant fractures throughout the Middle Nonlithophysal, Lower Lithophysal, and Lower Nonlithophysal zones belong to a northwest-striking subvertical set. This apparent dominance of northwest-striking subvertical fractures in the overall measurement population reflects in part the orientation bias introduced by the ESF and ECRB Cross-Drift tunnels. A shallowly dipping or subhorizontal fracture set is also present. In addition, one or more additional steeply dipping fracture sets are observed.

- In general, fracture spacing in nonlithophysal zones is smaller than in lithophysal zones when determined for fractures with trace lengths of >1 meter [3.3. feet] (Table 5-1). Fracture spacing for small-scale fractures {i.e., trace lengths <1 meter [3.3 feet]} does not show a clear correlation to presence or absence of lithophysae (Table 5-2).

- The analyses show that fracture spacing varies as a function of fracture orientation even after corrections for orientation-induced bias are applied (Table 5-1). For example, the spacing of northwest-striking subvertical fractures in the Middle Nonlithophysal zone is approximately one-half that for the other fracture sets in this interval. Fracture spacing also varies as a function of trace length (i.e., spacing based on short fractures is less than spacing based on long fractures for any lithostratigraphic zone).

- Average orientations differ between long (Table 5-1) and short (Table 5-2) fractures for the same lithostratigraphic zone.

- Subhorizontal fractures have a higher intensity (i.e., smaller spacing) than indicated in some previous DOE reports (e.g., Bechtel SAIC Company, LLC,2004b) because the directional sampling bias in the detailed line survey data introduced by the tunnel orientation has been partially corrected in this report (Table 5-1).

- FracMan synthetic fracture populations generated for the Middle Nonlithophysal zone (using DOE input parameters) contain the prominent northwest-striking subvertical set along with a northeast-striking subvertical set. A northwest-striking, moderately northeast-dipping set that is present in the synthetic population does not appear to be represented by an equivalent or corresponding set of fractures in the natural fracture population. The subhorizontal fracture set is not well developed in the synthetic fracture population.

- FracMan synthetic fracture populations generated for the Lower Lithophysal zone (using DOE input parameters) also contain the prominent northwest-striking subvertical set. Both north-south-striking subvertical and subhorizontal fracture sets are well represented in the synthetic fracture populations.

6 REFERENCES

Ahola, M.P., R. Chen, H. Karimi, S. Hsiung, and A.H. Chowdhury. "A Parametric Study of Drift Stability in Jointed Rock Mass. Phase I: Discrete Element Thermal-Mechanical Analysis of Unbackfilled Drifts." CNWRA 96-009. San Antonio, Texas: CNWRA. 1996.

Albin, A.L., W.L. Singleton, T.C. Moyer, A.C. Lee, R.C. Lung, G.L.W. Eatman, and D.L. Barr. "Geology of the Main Drift—Station 28+00 to 55+00, Exploratory Studies Facility, Yucca Mountain Project, Yucca Mountain, Nevada." DOE Report DTN GS970208314224.005, Milestone Report SPG42AM3. Denver, Colorado: Bureau of Reclamation and U.S. Geological Survey. 1997.

Barr, D.L., T.C. Moyer, W.L. Singleton, A.L. Albin, R.C. Lung, A.C. Lee, S.C. Beason, and G.L.W. Eatman. "Geology of the North Ramp—Station 4+00 to 28+00, Exploratory Studies Facility, Yucca Mountain Project, Yucca Mountain, Nevada." DOE Report DTN GS960908314224.020. Denver, Colorado: Bureau of Reclamation and U.S. Geological Survey. 1996.

Barton, C.C., E. Larsen, W.R. Page, and T.M. Howard. "Characterizing Fractured Rock for Fluid-Flow, Geomechanical, and Paleostress Modeling." Denver, Colorado: U.S. Geological Survey Open-File Report 93–269. 1993.

Beason, S.C., G.A. Turlington, R.C. Lung, G.L.W. Eatman, D. Ryter, and D.L. Barr. "Geology of the North Ramp—Station 0+60 to 4+00, Exploratory Studies Facility, Yucca Mountain Project, Yucca Mountain, Nevada." Denver, Colorado: Bureau of Reclamation and U.S. Geological Survey. 1996.

Bechtel SAIC Company, LLC. "Technical Basis Document No. 4: Mechanical Degradation and Seismic Effects." Rev. 1. Las Vegas, Nevada: Bechtel SAIC Company, LLC. 2004a.

_____. "Drift Degradation Analysis." ANL–EBS–MD–000027. Rev. 3. Las Vegas, Nevada: Bechtel SAIC Company, LLC. 2004b.

_____. "Technical Basis Document No. 1: Climate and Infiltration." Rev. 1. Las Vegas, Nevada: Bechtel SAIC Company, LLC. 2004c.

_____. "Technical Basis Document No. 3: Water Seeping Into Drifts." Rev. 2. Las Vegas, Nevada: Bechtel SAIC Company, LLC. 2003.

_____. "Geologic Framework Model (GFM2000)." Rev. 01. Las Vegas, Nevada: Bechtel SAIC Company, LLC. 2002.

Board, M. "Resolution Strategy for Geomechanically-Related Repository Design and Thermal-Mechanical Effects (RDTME)." Las Vegas, Nevada: Bechtel SAIC Company, LLC. 2003.

Brechtel, C.E., M. Lin, E. Martin, and D.S. Kessel. "Geotechnical Characterization of the North Ramp of the Exploratory Studies Facility." SAND95–0488/1 and 2 (two volumes). Albuquerque, New Mexico: Sandia National Laboratories. 1995.

Buesch, D.C. and R.W. Spengler. "Detailed Correlation of Lithostratigraphic and Borehole Geophysical Log Data for Identifying Contacts at Yucca Mountain." High-Level Radioactive Waste Management, Proceedings of the Eighth International Conference, Las Vegas, Nevada, May 11–14, 1998. pp. 248–251. La Grange Park, Illinois: American Nuclear Society. 1998.

Buesch, D.C., R.W. Spengler, T.C. Moyer, and J.K. Geslin. "Proposed Stratigraphic Nomenclature and Macroscopic Identification of Lithostratigraphic Units of the Paintbrush Group Exposed at Yucca Mountain, Nevada." Denver, Colorado: U.S. Geological Survey Open-File Report 94-469. 1996a.

Buesch, D.C., J.E. Nelson, R.P. Dickerson, R.M. Drake, II, R.W. Spengler, J.K. Geslin, T.C. Moyer, and C.A. San Juan. "Distribution of Lithostratigraphic Units Within the Central Block of Yucca Mountain, Nevada: A Three-Dimensional Computer-Based Model, Version YMP.R2.0." Denver, Colorado: U.S. Geological Survey Open-File Report 95-124. 1996b.

Chen, R. "Drift Stability and Ground Support Performance Under Thermal and Dynamic Load in Fractured Rock Mass at Yucca Mountain, Nevada." CNWRA 2000-04. San Antonio, Texas: CNWRA. 2000.

CRWMS M&O. "Yucca Mountain Site Description." TDR–CRW–GS–000001. Rev. 01. ICN 01. Las Vegas, Nevada: CRWMS M&O. 2000.

_____. "Determination of Available Volume for Repository Siting." BCA000000–01717–0200–00007. Rev. 00. Las Vegas, Nevada: CRWMS M&O. 1997.

Davis, J.C. *Statistics and Data Analysis in Geology*. Second Edition. New York, New York: John Wiley and Sons, Inc. 1986.

Day, W.C., R.P. Dickerson, C.J. Potter, D.S. Sweetkind, C.A. San Juan, R.M. Drake II, and C.J. Fridrich. "Bedrock Geologic Map of the Yucca Mountain Area, Nye County, Nevada." U.S. Geological Survey Geologic Investigations Series I-2627. Denver, Colorado: U.S. Geological Survey. 1998.

Dershowitz, W.S. and H.H. Herda. "Interpretation of Fracture Spacing and Intensity." *Rock Mechanics: Proceedings of the 32nd U.S. Rock Mechanics Symposium*. J.R. Tillerson and W.R. Wawersik, eds. Rotterdam, The Netherlands: A.A. Balkema. pp. 757–766. 1992.

Eatman, G.L.W., W.L. Singleton, T.C. Moyer, D.L. Barr, A.L. Albin, R.C. Lung, and S.C Beason. "Geology of the South Ramp–Station 55+00 to 78+77, Exploratory Studies Facility, Yucca Mountain Project, Yucca Mountain, Nevada." Denver, Colorado: Bureau of Reclamation and U.S. Geological Survey. 1997.

Fedors, R.W., J.R. Winterle, W.A. Illman, C.L. Dinwiddie, and D.L. Hughson. "Unsaturated Zone Flow at Yucca Mountain, Nevada: Effects of Fracture Heterogeneity and Flow in the Nonwelded Paintbrush Tuff Unit." San Antonio, Texas: CNWRA. 2002.

Ferrill, D.A., W. Dunne, S. Hsiung, and A. Morris. "Review of AMR Entitled Fracture Geometry Analysis for the Stratigraphic Units of the Repository Host Horizon." San Antonio, Texas: CNWRA. 2000.

Fisher, N.I., T. Lewis, and B.J.J. Embleton. *Statistical Analysis of Spherical Data*. Cambridge, United Kingdom: Cambridge University Press. 1993.

Fisher, R.A. "Dispersion On a Sphere." Proceedings of the Royal Society of London. Vol. A217. pp. 295–305. 1953.

Geslin, J.K. and T.C. Moyer. "Summary of Lithologic Logging of New and Existing Boreholes at Yucca Mountain, Nevada, March 1994 to June 1994." U.S. Geological Survey Open-File Report 94-451. 1995.

Geslin, J.K., T.C. Moyer, and D.C. Buesch. "Summary of Lithologic Logging of New and Existing Boreholes at Yucca Mountain, Nevada, August 1993 to February 1994." U.S. Geological Survey Open-File Report 94-342. 1995.

Golder Associates, Inc. "FracWorksXP Module User Documentation." Seattle, Washington: Golder Associates, Inc. 2002.

_____. "FracMan Interactive Discrete Feature Data Analysis, Geometric Modeling, and Exploration Simulation User Documentation, Version 2.6." Seattle, Washington: Golder Associates, Inc. 1998.

Gute, G.D., G. Ofoegbu, F. Thomassy, S. Hsiung, G. Adams, A. Ghosh, B. Dasgupta, A.H. Chowdhury, and S. Mohanty. "MECHFAIL: A Total-System Performance Assessment Code Module for Evaluating Engineered Barrier Performance Under Mechanical Loading Conditions." CNWRA 2003-06. San Antonio, Texas: CNWRA. 2003.

Hinds, J., G.S. Bodvarsson, and G.H. Nieder-Westermann. "Conceptual Evaluation of the Potential Role of Fractures in Unsaturated Processes at Yucca Mountain." *Journal of Contaminant Hydrology*. Vol. 62 and 63. pp. 111–132. 2003.

International Society for Rock Mechanics. "Suggested Methods for the Quantitative Description of Discontinuities in Rock Masses." Commission on Standardization of Laboratory and Field Tests. *International Journal of Rock Mechanics, Mining Science, & Geomechanics Abstracts*. Vol. 15. pp. 183–197. 1978.

Kamb, W.B. "Petrofabric Observations from Blue Glacier, Washington, In Relation to Theory and Experiment." *Journal of Geophysical Research*. Vol. 64. pp. 1891–1909. 1959.

Kicker, D.C., E.R. Martin, C.E. Brechtel, C.A. Stone, and D.S. Kessel. "Geotechnical Characterization for the Main Drift of the Exploratory Studies Facility." SAND95–2183. Albuquerque, New Mexico: Sandia National Laboratories. 1997.

Knopf, E.B. and E. Ingerson. "Structural Petrology." *Geological Society of America Memoir 6*. 1938.

Liu, H.H., C. Doughty, and G.S. Bodvarsson. "An Active Fracture Model for Unsaturated Flow and Transport in Fractured Rocks." *Water Resources Research*. Vol. 34. No. 10. pp. 2,633–2,646. 1998.

Manepally, C., A. Sun, R. Fedors, and D. Farrell. "Drift-Scale Thermohydrological Process Modeling—In-Drift Heat Transfer and Drift Degradation." CNWRA 2004-05. San Antonio, Texas: CNWRA. 2004.

Mardia, K.V. *Statistics of Directional Data*. New York, New York: Academic Press. 1972.

Mongano, G.S., W.L. Singleton, T.C. Moyer, S.C. Beason, G.L.W. Eatman, A.L. Albin, and R.C. Lung. "Geology of the ECRB Cross-Drift—Exploratory Studies Facility, Yucca Mountain Project, Yucca Mountain, Nevada." SPG42GM3. Denver, Colorado: U.S. Geological Survey. 1999.

Moyer, T.C., J.K. Geslin, and D.C. Buesch. "Summary of Lithologic Logging of New and Existing Boreholes at Yucca Mountain, Nevada, July 1994 to November 1994." U.S. Geological Survey Open-File Report 95-102. 1995.

Nelson, R.A. *Geological Analysis of Naturally Fractured Reservoirs*. Second Edition. Houston, Texas: Gulf Professional Publishing. 2001.

Nieder-Westermann, G.H. "Fracture Geometry Analysis for the Stratigraphic Units of the Repository Host Horizon." ANL–EBS–GE–000006. Rev. 00. Las Vegas, Nevada: CRWMS M&O. 2000.

Ofoegbu, G. "Thermal-Mechanical Effects on Long-Term Hydrological Properties at the Proposed Yucca Mountain Nuclear Waste Repository." CNWRA 2000-03. San Antonio, Texas: CNWRA. 2000.

Pearcy, E.C. "Fracture Transport of Uranium at the Nopal I Natural Analog Site." CNWRA 94-011. San Antonio, Texas: CNWRA. 1994.

Pearcy, E.C., J.D. Prikryl, and B.W. Leslie. "Uranium Transport Through Fractured Silicic Tuff and Relative Retention in Areas With Distinct Fracture Characteristics." *Applied Geochemistry*. Vol. 10. pp. 685–704. 1995.

Potter, C.J., W.C. Day, D.S. Sweetkind, and R.P. Dickerson. "Structural Geology of the Proposed Site Area for a High-Level Radioactive Waste Repository, Yucca Mountain, Nevada." Geological Society of America Bulletin. Vol. 116, No. 7/8. pp. 858–879. 2004.

Priest, S.D. *Discontinuity Analysis for Rock Engineering*. New York, New York: Chapman and Hall, Inc. 1993.

Priest, S.D. and J.A. Hudson. "Estimation of Discontinuity Spacing and Trace Length Using Scanline Surveys." *International Journal of Rock Mechanics, Mining Science, & Geomechanics Abstracts*. Vol. 18. 183–197. 1981.

Smart, K.J. "Review by the Office of Nuclear Material Safety and Safeguards of the Department of Energy's Responses to Key Technical Issue Agreements SDS.3.03 for a Potential Geologic Repository at Yucca Mountain, Nevada, Project No. WM-011." San Antonio, Texas: CNWRA. 2005.

Sweetkind, D.S. and S.C. Williams-Stroud. "Characteristics of Fractures at Yucca Mountain, Nevada." Milestone Report 3GGF205M. Denver, Colorado: U.S. Geological Survey. 1996.

Sweetkind, D.S., E.R. Verbeek, F.R. Singer, F.M. Byers, Jr., and L.G. Martin. "Surface Fracture Network at Pavement P2001, Fran Ridge, Near Yucca Mountain, Nye County, Nevada." Denver, Colorado: U.S. Geological Survey. 1995a.

Sweetkind, D.S., E.R. Verbeek, J.K. Geslin, and T.C. Moyer. "Fracture Character of the Paintbrush Tuff Nonwelded Hydrologic Unit, Yucca Mountain, Nevada." Denver, Colorado: U.S. Geological Survey. 1995b.

Terzaghi, R.D. "Sources of Error in Joint Surveys." *Geotechnique*. Vol. 15. pp. 287–304. 1965.

Throckmorton, C.K. and E.R. Verbeek. "Joint Networks in the Tiva Canyon and Topopah Spring Tuffs of the Paintbrush Group, Southwestern Nevada." U.S. Geological Survey Open-File Report 95-2. 1995.

Turner, F.J. and L.E. Weiss. *Structural Analysis of Metamorphic Tectonites*. New York, New York: McGraw-Hill Book Company, Inc. 1963.

U.S. Bureau of Reclamation and U.S. Geological Survey. "Underground Geologic Mapping." Technical Procedure YMP–USGS–GP–32, R1. Denver, Colorado: U.S. Bureau of Reclamation and U.S. Geological Survey. 1997.

Witte, R.S. *Statistics*. 2nd Edition. New York, New York: Holt, Rinehart, and Winston. 1985.

7 SOURCE DATA, LISTED BY DATA TRACKING NUMBER

GS971108314224.020. Revision 1 of Detailed Line Survey Data, Station 0+60 to Station 4+00, North Ramp Starter Tunnel, Exploratory Studies Facility. Submittal date: 12/03/1997.

GS971108314224.021. Revision 1 of Detailed Line Survey Data, Station 4+00 to Station 8+00, North Ramp, Exploratory Studies Facility. Submittal date: 12/3/97.

GS971108314224.022. Revision 1 of Detailed Line Survey Data, Station 8+00 to Station 10+00, North Ramp, Exploratory Studies Facility. Submittal date: 12/3/97.

GS971108314224.023. Revision 1 of Detailed Line Survey Data, Station 10+00 to Station 18+00, North Ramp, Exploratory Studies Facility. Submittal date: 12/3/97.

GS971108314224.024. Revision 1 of Detailed Line Survey Data, Station 18+00 to Station 26+00, North Ramp, Exploratory Studies Facility. Submittal date: 12/3/97.

GS971108314224.025. Revision 1 of Detailed Line Survey Data, Station 26+00 to Station 30+00, North Ramp, Exploratory Studies Facility. Submittal date: 12/3/97.

GS960708314224.008. Provisional Results: Geotechnical Data for Station 30+00 to Station 35+00, Main Drift of the ESF. Submittal date: 08/05/1996.

GS000608314224.004. Fracture Type data from the Main Drift of the ESF, and Yucca Mountain Project Detailed Line Survey-Data collected from Station 35+00 to 40+00, 01/05/1996 to 02/02/1996.

GS960708314224.010. Provisional results: Geotechnical Data for Station 40+00 to Station 45+00, Main Drift of the ESF. Submittal date: 08/05/1996.

GS971108314224.026. Revision 1 of Detailed Line Survey Data, Station 45+00 to Station 50+00, Main Drift, Exploratory Studies Facility. Submittal date: 12/03/1997.

GS960908314224.014. Fracture Type data from the ESF North Ramp, and Yucca Mountain Project Detailed Line Survey-Data Collected from Station 50+00 to 55+00. 05/06/1996 to 06/05/1996.

GS971108314224.028. Fracture Type data (Revision 1 of Detailed Line Survey data) South Ramp, ESF, collected from stations 55+00.18 to 59+99.95, 06/04/1996 to 07/02/1996.

GS970208314224.003. Geotechnical Data for Station 60+00 to Station 65+00, South Ramp of the ESF. Submittal date: 12/12/1997.

GS970808314224.008. Provisional Results: Geotechnical Data for Station 65+00 to Station 70+00, South Ramp of the ESF. Submittal date: 08/18/1997.

GS970808314224.010. Provisional Results: Geotechnical Data for Station 70+00 to Station 75+00, South Ramp of the ESF. Submittal date: 08/25/1997.

GS970808314224.012. Provisional Results: Geotechnical Data for Station 75+00 to Station 78+77, South Ramp of the ESF. Submittal date: 08/25/1997.

GS990408314224.001. Detailed Line Survey Data for Stations 00+00.89 to 14+95.18, ECRB Cross-Drift. Submittal Date: 09/09/1999.

GS990408314224.002. Detailed Line Survey Data for Stations 15+00.85 TO 26+63.8, ECRB Cross-Drift. Submittal Date: 09/09/1999.

GS990408314224.003. Full-Periphery Geologic Maps for Station -0+10 TO 10+00, ECRB Cross-Drift. Submittal Date: 09/09/1999.

GS990408314224.004. Full-Periphery Geologic Maps for Station 10+00 TO 15+00, ECRB Cross-Drift. Submittal Date: 09/09/1999.

GS990408314224.005. Full-Periphery Geologic Maps for Station 15+00 TO 20+00, ECRB Cross-Drift. Submittal Date: 09/09/1999.

GS990408314224.006. Full-Periphery Geologic Maps for Station 20+00 TO 26+81, ECRB Cross-Drift. Submittal Date: 09/09/1999.

GS990908314224.009. Detailed line survey data for horizontal and vertical traverses, ECRB. Submittal Date: 09/16/1999.

MO9904MWDFPG16.000. Fracture Attitude data for full periphery geotechnical mapping of strike and dip data entry correction analysis, 10/07/1998 to 03/19/1999.

APPENDIX A

Table A–1. Expanded Summary of Fracture Data From the Topopah Spring Tuff Upper Lithophysal Zone Based on Detailed Line Surveys in the Enhanced Characterization of the Repository Block (ECRB) Cross-Drift and the Exploratory Studies Facility (ESF). This Data Set Was Collected With a Lower Trace Length Cut-Off of 1 m [3.3 ft] {i.e., Sampled Fractures with Trace Lengths >1 m [3.3 ft]}. True Spacing Reflects Correction of Orientation Bias Using a Truncated Terzaghi Approach.* Median Intensity Is the Inverse of Median Fracture Spacing (Equivalent to Number of Fractures Per Unit Length of Scanline).

Set	Number and Percentage	Mean Orientation (Strike/Dip)	Fisher Dispersion Coefficient†	Total Trace Length, m [ft]			TrueSpacing, m [ft]			Median Linear Fracture Intensity, m^{-1} [ft^{-1}]
				Mean	Standard Deviation	Median	Mean	Standard Deviation	Median	
All	1758, 100%	*n.a.*	*n.a.*	2.56 [8.40]	3.59 [11.78]	1.42 [4.66]	*n.a.*	*n.a.*	*n.a.*	*n.a.*
1	538, 31%	116°/85°	7.462	2.09 [6.86]	2.17 [7.12]	1.44 [4.72]	2.82 [9.25]	8.80 [28.87]	0.75 [2.46]	1.34 [0.41]
2	1024, 58%	181°/85°	1.945	2.29 [7.51]	3.25 [10.66]	1.30 [4.66]	1.73 [5.68]	3.55 [11.65]	0.65 [2.13]	1.53 [0.47]
3	95, 5%	320°/19°	9.436	5.73 [18.80]	6.18 [20.28]	4.31 [14.14]	3.98 [13.06]	6.59 [21.62]	1.29 [4.23]	0.77 [0.23]
Random	101, 6%	*n.a.*	*n.a.*	4.87 [15.98]	6.42 [21.06]	2.10 [6.89]	*n.a.*	*n.a.*	*n.a.*	*n.a.*

*Terzaghi, R.D. "Sources of Error in Joint Surveys." *Geotechnique*. Vol. 15. pp. 287–304. 1965.

†The Fisher dispersion coefficient (also referred to as the concentration parameter) is a measure of the degree to which spherical data are concentrated around the mean (Fisher, N.I, T. Lewis, and B.J.J. Embleton. *Statistical Analysis of Spherical Data*. Cambridge, United Kingdom: Cambridge University Press. 1993; Mardia, K.V. *Statistics of Directional Data*. New York, New York: Academic Press. 1972; Fisher, R.A. "Dispersion On a Sphere." Proceedings of the Royal Society of London. Vol. A217. pp. 295–305. 1953). Larger values of the Fisher dispersion coefficient indicate tighter clustering (i.e., less dispersion).

Table A–2. Expanded Summary of Fracture Data From the Topopah Spring Tuff Middle Nonlithophysal Zone (Including Intensely Fractured Zone) Based on Detailed Line Surveys in the Exploratory Studies Facility (ESF) and the Enhanced Characterization of the Repository Block (ECRB) Cross-Drift. This Data Set Was Collected With a Lower Trace Length Cut-Off of 1 m [3.3 ft]. True Spacing Reflects Correction of Orientation Bias Using a Truncated Terzaghi Approach.* Median Intensity Is the Inverse of Median Fracture Spacing (Equivalent to Number of Fractures Per Unit Length of Scanline).

Set	Number & Percentage	Mean Orientation (Strike/Dip)	Fisher Dispersion Coefficient†	Total Trace Length, m [ft]			True Spacing, m [ft]			Median Linear Fracture Intensity, m^{-1} [ft^{-1}]
				Mean	Standard Deviation	Median	Mean	Standard Deviation	Median	
All	13493, 100%	*n.a.*	*n.a.*	2.12 [6.96]	2.26 [7.42]	1.58 [5.18]	*n.a.*	*n.a.*	*n.a.*	*n.a.*
1	8919, 66%	126°/84°	17.670	2.18 [7.15]	1.96 [6.43]	1.70 [5.58]	0.42 [1.39]	4.01 [13.16]	0.19 [0.62]	5.20 [1.58]
2	2973, 22%	227°/86°	5.329	1.90 [6.23]	2.62 [8.60]	1.35 [4.43]	0.92 [3.02]	1.50 [4.92]	0.46 [1.51]	2.19 [0.67]
3	679, 5%	326°/08°	27.225	2.47 [8.10]	3.40 [11.16]	1.54 [5.05]	1.19 [3.90]	2.23 [7.32]	0.52 [1.71]	1.92 [0.59]
Random	922, 7%	*n.a.*	*n.a.*	2.02 [6.63]	2.65 [8.69]	1.27 [4.17]	*n.a.*	*n.a.*	*n.a.*	*n.a.*

*Terzaghi, R.D. "Sources of Error in Joint Surveys." *Geotechnique*. Vol. 15. pp. 287–304. 1965.

†The Fisher dispersion coefficient (also referred to as the concentration parameter) is a measure of the degree to which spherical data are concentrated around the mean (Fisher, N.I, T. Lewis, and B.J.J. Embleton. *Statistical Analysis of Spherical Data*. Cambridge, United Kingdom: Cambridge University Press. 1993; Mardia, K.V. *Statistics of Directional Data*. New York, New York: Academic Press. 1972; Fisher, R.A. "Dispersion On a Sphere." Proceedings of the Royal Society of London. Vol. A217. pp. 295–305. 1953). Larger values of the Fisher dispersion coefficient indicate tighter clustering (i.e., less dispersion).

Table A–3. Expanded Summary of Fracture Data from the Intensely Fractured Zone in the Topopah Spring Tuff Middle Nonlithophysal Zone Based on Detailed Line Surveys in the Exploratory Studies Facility (ESF). This Data Set Was Collected With a Lower Trace Length Cut-Off of 1 m [3.3 ft]. True Spacing Reflects Correction of Orientation Bias Using a Truncated Terzaghi Approach.* Median Intensity Is the Inverse of Median Fracture Spacing (Equivalent to Number of Fractures Per Unit Length of Scanline).

Set	Number and Percentage	Mean Orientation (Strike/Dip)	Fisher Dispersion Coefficient†	Total Trace Length, m [ft]			True Spacing, m [ft]			Median Linear Fracture Intensity, m^{-1} [ft^{-1}]
				Mean	Standard Deviation	Median	Mean	Standard Deviation	Median	
All	4566, 100%	*n.a.*	*n.a.*	2.18 [7.15]	1.59 [5.22]	1.80 [5.91]	*n.a.*	*n.a.*	*n.a.*	*n.a.*
1	3875, 85%	129°/84°	29.093	2.23 [7.32]	1.60 [5.25]	1.85 [6.07]	0.20 [0.66]	0.25 [0.82]	0.12 [0.39]	8.27 [2.52]
2	525, 11%	231°/87°	7.943	2.04 [6.69]	1.63 [5.35]	1.57 [5.15]	1.34 [4.40]	1.77 [5.81]	0.74 [2.43]	1.35 [0.41]
3	54, 1%	340°/07°	20.711	1.21 [3.97]	1.10 [3.61]	0.96 [3.15]	2.08 [6.82]	5.19 [17.03]	0.43 [1.41]	2.32 [0.71]
Random	112, 2%	*n.a.*	*n.a.*	1.73 [5.68]	1.26 [4.13]	1.37 [4.49]	*n.a.*	*n.a.*	*n.a.*	*n.a.*

*Terzaghi, R.D. "Sources of Error in Joint Surveys." *Geotechnique*. Vol. 15. pp. 287–304. 1965.

†The Fisher dispersion coefficient (also referred to as the concentration parameter) is a measure of the degree to which spherical data are concentrated around the mean (Fisher, N.I, T. Lewis, and B.J.J. Embleton. *Statistical Analysis of Spherical Data*. Cambridge, United Kingdom: Cambridge University Press. 1993; Mardia, K.V. *Statistics of Directional Data*. New York, New York: Academic Press. 1972; Fisher, R.A. "Dispersion On a Sphere." Proceedings of the Royal Society of London. Vol. A217. pp. 295–305. 1953). Larger values of the Fisher dispersion coefficient indicate tighter clustering (i.e., less dispersion).

Table A–4. Expanded Summary of Fracture Data from the Topopah Spring Tuff Middle Nonlithophysal Zone (Excluding Intensely Fractured Zone) Based on Detailed Line Surveys in the Exploratory Studies Facility (ESF) and the Enhanced Characterization of the Repository Block (ECRB) Cross-Drift. This Data Set Was Collected with a Lower Trace Length Cut-Off of 1 m [3.3 ft]. True Spacing Reflects Correction of Orientation Bias Using a Truncated Terzaghi Approach.* Median Intensity Is the Inverse of Median Fracture Spacing (Equivalent to Number of Fractures Per Unit Length of Scanline).

Set	Number and Percentage	Mean Orientation (Strike/Dip)	Fisher Dispersion Coefficient†	Total Trace Length, m [ft]			True Spacing, m [ft]			Median Linear Fracture Intensity, m^{-1} [ft^{-1}]
				Mean	Standard Deviation	Median	Mean	Standard Deviation	Median	
All	8927, 100%	*n.a.*	*n.a.*	2.09 [6.86]	2.54 [8.33]	1.43 [4.69]	*n.a.*	*n.a.*	*n.a.*	*n.a.*
1	5044, 57%	124°/85°	13.814	2.14 [7.02]	2.19 [7.19]	1.52 [4.99]	0.59 [1.94]	5.12 [16.80]	0.28 [0.92]	3.54 [1.08]
2	2448, 27%	226°/86°	4.994	1.87 [6.14]	2.79 [9.15]	1.30 [4.27]	0.84 [2.76]	1.46 [4.79]	0.41 [1.35]	2.41 [0.73]
3	625, 7%	326°/08°	27.979	2.58 [8.46]	3.50 [11.48]	1.61 [5.28]	1.09 [3.58]	1.60 [5.25]	0.53 [1.74]	1.89 [0.58]
Random	810, 9%	*n.a.*	*n.a.*	2.07 [6.79]	2.79 [9.15]	1.27 [4.17]	*n.a.*	*n.a.*	*n.a.*	*n.a.*

*Terzaghi, R.D. "Sources of Error in Joint Surveys." *Geotechnique*. Vol. 15. pp. 287–304. 1965.

†The Fisher dispersion coefficient (also referred to as the concentration parameter) is a measure of the degree to which spherical data are concentrated around the mean (Fisher, N.I, T. Lewis, and B.J.J. Embleton. *Statistical Analysis of Spherical Data*. Cambridge, United Kingdom: Cambridge University Press. 1993; Mardia, K.V. *Statistics of Directional Data*. New York, New York: Academic Press. 1972; Fisher, R.A. "Dispersion On a Sphere." Proceedings of the Royal Society of London. Vol. A217. pp. 295–305. 1953). Larger values of the Fisher dispersion coefficient indicate tighter clustering (i.e., less dispersion).

Table A–5. Expanded Summary of Small-Scale Fracture Data from the Topopah Spring Tuff Middle Nonlithophysal Zone Based on Two 6-m [20-ft] Horizontal and Six 2-m [7-ft] Vertical Scanlines in the Enhanced Characterization of the Repository Block (ECRB) Cross-Drift. This Data Set Was Collected With an Upper Trace Length Cut-Off of 1 m [3.3 ft]. True Spacing Reflects Correction of Orientation Bias Using a Truncated Terzaghi Approach .* Median Intensity Is the Inverse of Median Fracture Spacing (Equivalent to Number of Fractures Per Unit Length of Scanline).

Set	Number and Percentage	Mean Orientation (Strike/Dip)	Fisher Dispersion Coefficient†	Total Trace Length, m [ft]			True Spacing, m [ft]			Median Linear Fracture Intensity, m^{-1} [ft^{-1}]
				Mean	Standard Deviation	Median	Mean	Standard Deviation	Median	
All	391, 100%	*n.a.*	*n.a.*	0.63 [2.07]	1.32 [4.33]	0.20 [0.66]	*n.a.*	*n.a.*	*n.a.*	*n.a.*
1	164, 42%	179°/88°	14.449	0.38 [1.25]	1.22 [4.00]	0.15 [0.49]	0.07 [0.23]	0.10 [0.33]	0.04 [0.13]	26.10 [7.95]
2	118, 30%	118°/86°	15.514	1.06 [3.48]	1.67 [5.48]	0.30 [0.98]	0.11 [0.36]	0.13 [0.43]	0.07 [0.23]	15.31 [4.67]
3	54, 14%	312°/05°	42.197	0.76 [2.49]	1.00 [3.28]	0.31 [1.02]	0.19 [0.62]	0.18 [0.59]	0.12 [0.39]	8.37 [2.55]
Random	55, 14%	*n.a.*	*n.a.*	0.33 [1.08]	0.63 [2.07]	0.17 [0.56]	*n.a.*	*n.a.*	*n.a.*	*n.a.*

*Terzaghi, R.D. "Sources of Error in Joint Surveys." *Geotechnique*. Vol. 15. pp. 287–304. 1965.

†The Fisher dispersion coefficient (also referred to as the concentration parameter) is a measure of the degree to which spherical data are concentrated around the mean (Fisher, N.I, T. Lewis, and B.J.J. Embleton. *Statistical Analysis of Spherical Data*. Cambridge, United Kingdom: Cambridge University Press. 1993; Mardia, K.V. *Statistics of Directional Data*. New York, New York: Academic Press. 1972; Fisher, R.A. "Dispersion On a Sphere." Proceedings of the Royal Society of London. Vol. A217. pp. 295–305. 1953). Larger values of the Fisher dispersion coefficient indicate tighter clustering (i.e., less dispersion).

Table A–6. Expanded Summary of Fracture Data from the Topopah Spring Tuff Lower Lithophysal Zone Based on Detailed Line Surveys in the Exploratory Studies Facility (ESF) and the Enhanced Characterization of the Repository Block (ECRB) Cross-Drift. This Data Set Was Collected With a Lower Trace Length Cut-Off of 1 m [3.3 ft]. True Spacing Reflects Correction of Orientation Bias Using a Truncated Terzaghi Approach.* Median Intensity Is the Inverse of Median Fracture Spacing (Equivalent to Number of Fractures Per Unit Length of Scanline).

Set	Number and Percentage	Mean Orientation (Strike/Dip)	Fisher Dispersion Coefficient†	Total Trace Length, m [ft]			True Spacing, m [ft]			Median Linear Fracture Intensity, m^{-1} [ft^{-1}]
				Mean	Standard Deviation	Median	Mean	Standard Deviation	Median	
All	338, 100%	*n.a.*	*n.a.*	4.04 [13.26]	4.91 [16.11]	1.92 [6.30]	*n.a.*	*n.a.*	*n.a.*	*n.a.*
1	254, 75%	158°/81°	2.606	4.21 [13.81]	4.69 [15.39]	1.88 [6.19]	3.48 [11.42]	6.26 [20.54]	1.39 [4.56]	0.72 [0.22]
2	60, 18%	087°/85°	17.759	2.32 [7.61]	1.93 [6.33]	1.63 [5.35]	9.07 [29.76]	9.12 [29.92]	6.17 [20.24]	0.16 [0.05]
3	19, 6%	329°/05°	53.085	7.36 [24.15]	10.39 [34.09]	3.42 [11.22]	4.59 [15.06]	7.41 [24.31]	1.39 [4.56]	0.72 [0.22]
Random	5, 1%	*n.a.*	*n.a.*	3.16 [10.37]	1.16 [3.81]	3.55 [11.65]	*n.a.*	*n.a.*	*n.a.*	*n.a.*

*Terzaghi, R.D. "Sources of Error in Joint Surveys." *Geotechnique*. Vol. 15. pp. 287–304. 1965.

†The Fisher dispersion coefficient (also referred to as the concentration parameter) is a measure of the degree to which spherical data are concentrated around the mean (Fisher, N.I, T. Lewis, and B.J.J. Embleton. *Statistical Analysis of Spherical Data*. Cambridge, United Kingdom: Cambridge University Press. 1993; Mardia, K.V. *Statistics of Directional Data*. New York, New York: Academic Press. 1972; Fisher, R.A. "Dispersion On a Sphere." Proceedings of the Royal Society of London. Vol. A217. pp. 295–305. 1953). Larger values of the Fisher dispersion coefficient indicate tighter clustering (i.e., less dispersion).

Table A–7. Expanded Summary of Small-Scale Fracture Data from the Topopah Spring Tuff Lower Lithophysal Zone Based on Three 6-m [20-ft] Horizontal and Nine 2-m [7-ft] Vertical Scanlines in the Enhanced Characterization of the Repository Block (ECRB) Cross-Drift. This Data Set Was Collected With an Upper Trace Length Cut-Off of 1 m [3.3 ft]. True Spacing Reflects Correction of Orientation Bias Using a Truncated Terzaghi Approach.* Median Intensity Is the Inverse of Median Fracture Spacing (Equivalent to Number of Fractures Per Unit Length of Scanline).

Set	Number and Percentage	Mean Orientation (Strike/Dip)	Fisher Dispersion Coefficient†	Total Trace Length, m [ft]			True Spacing, m [ft]			Median Linear Fracture Intensity, m^{-1} [ft^{-1}]
				Mean	Standard Deviation	Median	Mean	Standard Deviation	Median	
All	649, 100%	*n.a.*	*n.a.*	0.31 [1.02]	0.98 [3.22]	0.16 [0.52]	*n.a.*	*n.a.*	*n.a.*	*n.a.*
1	421, 65%	134°/82°	3.344	0.25 [0.82]	0.42 [1.38]	0.17 [0.56]	1.08 [3.54]	14.49 [47.54]	0.03 [0.10]	27.56 [8.40]
2	49, 8%	079°/82°	14.633	0.19 [0.62]	0.15 [0.49]	0.14 [0.50]	0.24 [0.79]	0.32 [1.05]	0.12 [0.39]	8.39 [2.56]
3	125, 19%	313°/04°	47.359	0.63 [2.07]	2.07 [6.79]	0.19 [0.62]	0.10 [0.33]	0.14 [0.50]	0.06 [0.20]	16.71 [5.09]
Random	54, 8%	*n.a.*	*n.a.*	0.17 [0.56]	0.17 [0.56]	0.12 [0.39]	*n.a.*	*n.a.*	*n.a.*	*n.a.*

*Terzaghi, R.D. "Sources of Error in Joint Surveys." *Geotechnique*. Vol. 15. pp. 287–304. 1965.

†The Fisher dispersion coefficient (also referred to as the concentration parameter) is a measure of the degree to which spherical data are concentrated around the mean (Fisher, N.I, T. Lewis, and B.J.J. Embleton. *Statistical Analysis of Spherical Data*. Cambridge, United Kingdom: Cambridge University Press. 1993; Mardia, K.V. *Statistics of Directional Data*. New York, New York: Academic Press. 1972; Fisher, R.A. "Dispersion On a Sphere." Proceedings of the Royal Society of London. Vol. A217. pp. 295–305. 1953). Larger values of the Fisher dispersion coefficient indicate tighter clustering (i.e., less dispersion).

Table A–8. Expanded Summary of Fracture Data from the Topopah Spring Tuff Lower Nonlithophysal Zone Based on Detailed Line Surveys in the Enhanced Characterization of the Repository Block (ECRB) Cross-Drift. This Data Set Was Collected With a Lower Trace Length Cut-Off of 1 m [3.3 ft]. True Spacing Reflects Correction of Orientation Bias Using a Truncated Terzaghi Approach.* Median Intensity Is the Inverse of Median Fracture Spacing (Equivalent to Number of Fractures Per Unit Length of Scanline).

Set	Number and Percentage	Mean Orientation (Strike/Dip)	Fisher Dispersion Coefficient†	Total Trace Length, m [ft]			True Spacing, m [ft]			Median Linear Fracture Intensity, m^{-1} [ft^{-1}]
				Mean	Standard Deviation	Median	Mean	Standard Deviation	Median	
All	199, 100%	*n.a.*	*n.a.*	4.04 [13.26]	4.44 [14.57]	1.93 [6.33]	*n.a.*	*n.a.*	*n.a.*	*n.a.*
1	121, 61%	134°/80°	48.804	4.39 [14.40]	4.22 [13.85]	2.25 [7.38]	1.89 [6.20]	3.63 [11.91]	0.73 [2.40]	1.37 [0.42]
2	61, 31%	209°/85°	18.362	4.05 [13.29]	5.20 [17.06]	1.66 [5.45]	1.79 [5.87]	3.58 [11.75]	0.70 [2.30]	1.42 [0.43]
3	16, 8%	337°/15°	67.639	1.55 [5.09]	1.02 [3.35]	1.31 [4.30]	2.75 [9.02]	3.60 [11.81]	1.59 [5.22]	0.63 [0.19]
Random	1, <1%	*n.a.*	*n.a.*	1.85 [6.07]	*n.a.*	1.85 [6.07]	*n.a.*	*n.a.*	*n.a.*	*n.a.*

*Terzaghi, R.D. "Sources of Error in Joint Surveys." *Geotechnique*. Vol. 15. pp. 287–304. 1965.

†The Fisher dispersion coefficient (also referred to as the concentration parameter) is a measure of the degree to which spherical data are concentrated around the mean (Fisher, N.I, T. Lewis, and B.J.J. Embleton. *Statistical Analysis of Spherical Data*. Cambridge, United Kingdom: Cambridge University Press. 1993; Mardia, K.V. *Statistics of Directional Data*. New York, New York: Academic Press. 1972; Fisher, R.A. "Dispersion On a Sphere." Proceedings of the Royal Society of London. Vol. A217. pp. 295–305. 1953). Larger values of the Fisher dispersion coefficient indicate tighter clustering (i.e., less dispersion).

APPENDIX B

Table B–1. Expanded Summary of Fracman®-Generated Synthetic Fracture Data for the Topopah Spring Tuff Middle Nonlithophysal Zone (Test 1). Linear Fracture Intensity Is the Number of Fractures Per Unit Length Determined from Borehole Sampling of the Synthetic Fracture Population. Areal Fracture Intensity Is the Total Fracture Trace Length Per Unit Area Determined From Tunnel Sampling of the Synthetic Fracture Population.

Set	Number and Percentage	Mean Orientation (Strike/Dip)	Fisher Dispersion Coefficient*	Fracture Radius, m [ft]			Linear Fracture Intensity, m^{-1} [ft^{-1}]		Areal Fracture Intensity, m/m^2 [ft/ft^2]	
				Mean	Standard Deviation	Median	Mean	Standard Deviation	Mean	Standard Deviation
All	99285, 100%	*n.a.*	*n.a.*	*n.a.*	*n.a.*	*n.a.*	1.42 [0.43]	0.27 [0.08]	1.29 [0.39]	0.21 [0.06]
1	40062, 40%	123°/84°	10.408	1.60 [5.25]	0.83 [2.72]	1.32 [4.33]	0.36 [0.11]	0.05 [0.02]	0.37 [0.11]	0.10 [0.03]
2	31964, 32%	217°/86°	7.649	1.60 [5.25]	0.82 [2.69]	1.31 [4.30]	0.18 [0.05]	0.06 [0.02]	0.24 [0.07]	0.06 [0.02]
3	10532, 11%	299°/43°	27.525	1.60 [5.25]	0.84 [2.76]	1.32 [4.33]	0.04 [0.01]	0.02 [0.01]	0.08 [0.02]	0.03 [0.01]
4	13146, 13%	298°/47°	5.097	1.65 [5.41]	1.26 [4.13]	1.31 [4.30]	0.08 [0.02]	0.03 [0.01]	0.10 [0.03]	0.05 [0.02]
5	1152, 1%	123°/84°	9.984	6.76 [22.18]	4.22 [13.85]	5.40 [17.72]	0.38 [0.12]	0.13 [0.04]	0.20 [0.06]	0.04 [0.01]
6	1304, 1%	217°/87°	9.005	6.77 [22.21]	4.52 [14.83]	5.32 [17.45]	0.24 [0.07]	0.10 [0.03]	0.19 [0.06]	0.07 [0.02]
7	1125, 1%	324°/07°	25.953	6.52 [21.39]	4.01 [13.16]	5.25 [17.23]	0.13 [0.04]	0.06 [0.02]	0.11 [0.03]	0.03 [0.01]

*The Fisher dispersion coefficient (also referred to as the concentration parameter) is a measure of the degree to which spherical data are concentrated around the mean (Fisher, N.I, T. Lewis, and B.J.J. Embleton. *Statistical Analysis of Spherical Data*. Cambridge, United Kingdom: Cambridge University Press. 1993; Mardia, K.V. *Statistics of Directional Data*. New York, New York: Academic Press. 1972; Fisher, R.A. "Dispersion On a Sphere." Proceedings of the Royal Society of London. Vol. A217. pp. 295–305. 1953). Larger values of the Fisher dispersion coefficient indicate tighter clustering (i.e., less dispersion).

Table B–2. Expanded Summary of Fracman®-Generated Synthetic Fracture Data for the Topopah Spring Tuff Middle Nonlithophysal Zone (Test 2). Linear Fracture Intensity Is the Number of Fractures Per Unit Length Determined From Borehole Sampling of the Synthetic Fracture Population. Areal Fracture Intensity Is the Total Fracture Trace Length Per Unit Area Determined From Tunnel Sampling of the Synthetic Fracture Population.

Set	Number and Percentage	Mean Orientation (Strike/Dip)	Fisher Dispersion Coefficient*	Fracture Radius, m [ft]			Linear Fracture Intensity, m^{-1} [ft^{-1}]		Areal Fracture Intensity, m/m^2 [ft/ft^2]	
				Mean	Standard Deviation	Median	Mean	Standard Deviation	Mean	Standard Deviation
All	99213, 100%	*n.a.*	*n.a.*	*n.a.*	*n.a.*	*n.a.*	1.46 [0.44]	0.20 [0.06]	1.35 [0.41]	0.18 [0.05]
1	40248, 41%	124°/84°	10.705	1.60 [5.25]	0.83 [2.72]	1.32 [4.33]	0.36 [0.11]	0.07 [0.02]	0.34 [0.10]	0.07 [0.02]
2	31691, 32%	217°/86°	7.868	1.61 [5.28]	0.84 [2.76]	1.32 [4.33]	0.20 [0.06]	0.05 [0.02]	0.26 [0.08]	0.07 [0.02]
3	10701, 11%	299°/43°	27.767	1.60 [5.25]	0.82 [2.69]	1.32 [4.33]	0.06 [0.02]	0.03 [0.01]	0.06 [0.02]	0.03 [0.01]
4	12556, 13%	331°/08°	5.048	1.67 [5.48]	1.26 [4.13]	1.32 [4.33]	0.07 [0.02]	0.03 [0.01]	0.11 [0.03]	0.05 [0.02]
5	1466, 1%	123°/84°	10.278	6.52 [21.39]	3.72 [12.21]	5.38 [17.65]	0.34 [0.10]	0.07 [0.02]	0.22 [0.07]	0.06 [0.02]
6	1431, 1%	217°/87°	7.568	6.60 [21.65]	3.94 [12.93]	5.31 [17.42]	0.31 [0.09]	0.08 [0.02]	0.22 [0.07]	0.06 [0.02]
7	1120, 1%	300°/43°	28.403	6.49 [21.29]	3.89 [12.76]	5.31 [17.42]	0.12 [0.04]	0.05 [0.02]	0.13 [0.04]	0.06 [0.02]

*The Fisher dispersion coefficient (also referred to as the concentration parameter) is a measure of the degree to which spherical data are concentrated around the mean (Fisher, N.I, T. Lewis, and B.J.J. Embleton. *Statistical Analysis of Spherical Data*. Cambridge, United Kingdom: Cambridge University Press. 1993; Mardia, K.V. *Statistics of Directional Data*. New York, New York: Academic Press. 1972; Fisher, R.A. "Dispersion On a Sphere." Proceedings of the Royal Society of London. Vol. A217. pp. 295–305. 1953). Larger values of the Fisher dispersion coefficient indicate tighter clustering (i.e., less dispersion).

Table B–3. Expanded Summary of Fracman®-Generated Synthetic Fracture Data for the Topopah Spring Tuff Lower Lithophysal Zone (Test 1). Linear Fracture Intensity Is the Number of Fractures Per Unit Length Determined from Borehole Sampling of the Synthetic Fracture Population. Areal Fracture Intensity Is the Total Fracture Trace Length Per Unit Area Determined From Tunnel Sampling of the Synthetic Fracture Population.

Set	Number and Percentage	Mean Orientation (Strike/Dip)	Fisher Dispersion Coefficient*	Fracture Radius, m [ft]			Linear Fracture Intensity, m^{-1} [ft^{-1}]		Areal Fracture Intensity, m/m^2 [ft/ft^2]	
				Mean	Standard Deviation	Median	Mean	Standard Deviation	Mean	Standard Deviation
All	8143, 100%	*n.a.*	*n.a.*	*n.a.*	*n.a.*	*n.a.*	0.278 [0.085]	0.057 [0.017]	0.144 [0.044]	0.036 [0.011]
1	798, 10%	328°/14°	72.950	2.34 [7.68]	2.08 [6.82]	1.81 [5.94]	0.007 [0.002]	0.007 [0.002]	0.015 [0.005]	0.015 [0.005]
2	836, 10%	130°/80°	69.294	3.63 [11.91]	8.13 [26.67]	2.51 [8.24]	0.168 [0.051]	0.039 [0.012]	0.067 [0.020]	0.031 [0.009]
3	482, 6%	166°/80°	63.442	2.97 [9.74]	2.65 [8.69]	2.18 [7.15]	0.061 [0.019]	0.048 [0.015]	0.021 [0.006]	0.015 [0.005]
4	4728, 58%	130°/80°	99.104	1.13 [3.71]	1.21 [3.97]	0.83 [2.72]	0.036 [0.011]	0.027 [0.008]	0.034 [0.010]	0.016 [0.005]
5	908, 11%	170°/80°	100.840	1.20 [3.94]	1.23 [4.04]	0.85 [2.79]	0.007 [0.002]	0.011 [0.003]	0.005 [0.002]	0.005 [0.002]
6	391, 5%	098°/85°	102.250	1.05 [3.45]	0.83 [2.72]	0.84 [2.76]	0.000 [0.000]	0.000 [0.000]	0.002 [0.001]	0.004 [0.001]

*The Fisher dispersion coefficient (also referred to as the concentration parameter) is a measure of the degree to which spherical data are concentrated around the mean (Fisher, N.I, T. Lewis, and B.J.J. Embleton. *Statistical Analysis of Spherical Data*. Cambridge, United Kingdom: Cambridge University Press. 1993; Mardia, K.V. *Statistics of Directional Data*. New York, New York: Academic Press. 1972; Fisher, R.A. "Dispersion On a Sphere." Proceedings of the Royal Society of London. Vol. A217. pp. 295–305. 1953). Larger values of the Fisher dispersion coefficient indicate tighter clustering (i.e., less dispersion).

Table B–4. Expanded Summary of Fracman®-Generated Synthetic Fracture Data for the Topopah Spring Tuff Lower Lithophysal Zone (Test 2). Linear Fracture Intensity Is the Number of Fractures Per Unit Length Determined from Borehole Sampling of the Synthetic Fracture Population. Areal Fracture Intensity Is the Total Fracture Trace Length Per Unit Area Determined From Tunnel Sampling of the Synthetic Fracture Population.

Set	Number and Percentage	Mean Orientation (Strike/Dip)	Fisher Dispersion Coefficient*	Fracture Radius, m [ft]			Linear Fracture Intensity, m^{-1} [ft^{-1}]		Areal Fracture Intensity, m/m^2 [ft/ft^2]	
				Mean	Standard Deviation	Median	Mean	Standard Deviation	Mean	Standard Deviation
All	8481, 100%	*n.a.*	*n.a.*	*n.a.*	*n.a.*	*n.a.*	0.323 [0.098]	0.068 [0.021]	0.139 [0.042]	0.060 [0.018]
1	798, 10%	328°/14°	72.950	2.34 [7.68]	2.08 [6.82]	1.81 [5.94]	0.007 [0.002]	0.007 [0.002]	0.015 [0.005]	0.015 [0.005]
2	836, 10%	130°/80°	69.294	3.63 [11.91]	8.13 [26.67]	2.51 [8.24]	0.168 [0.051]	0.039 [0.012]	0.067 [0.020]	0.031 [0.009]
3	243, 3%	167°/80°	68.625	3.64 [11.94]	12.36 [40.55]	2.10 [6.89]	0.101 [0.031]	0.015 [0.005]	0.020 [0.006]	0.010 [0.003]
4	5549, 65%	130°/80°	100.160	1.15 [3.77]	1.41 [4.63]	0.83 [2.72]	0.038 [0.012]	0.022 [0.007]	0.029 [0.009]	0.016 [0.005]
5	873, 10%	171°/80°	99.334	1.22 [4.00]	2.68 [8.79]	0.83 [2.72]	0.010 [0.003]	0.017 [0.005]	0.007 [0.002]	0.007 [0.002]
6	182, 2%	098°/85°	104.130	1.18 [3.87]	1.51 [4.95]	0.86 [2.82]	0.010 [0.003]	0.000 [0.000]	0.001 [0.0003]	0.002 [0.001]

*The Fisher dispersion coefficient (also referred to as the concentration parameter) is a measure of the degree to which spherical data are concentrated around the mean (Fisher, N.I, T. Lewis, and B.J.J. Embleton. *Statistical Analysis of Spherical Data*. Cambridge, United Kingdom: Cambridge University Press. 1993; Mardia, K.V. *Statistics of Directional Data*. New York, New York: Academic Press. 1972; Fisher, R.A. "Dispersion On a Sphere." Proceedings of the Royal Society of London. Vol. A217. pp. 295–305. 1953). Larger values of the Fisher dispersion coefficient indicate tighter clustering (i.e., less dispersion).